UNIVERSITY OF CALIFORNIA
SANTA CRUZ

MICROBIAL ECOLOGY, BIOGEOCHEMICAL CYCLING, AND WATER QUALITY DURING MANAGED AQUIFER RECHARGE

A dissertation submitted in partial satisfaction
of the requirements for the degree of

DOCTOR OF PHILOSOPHY

in

MICROBIOLOGY AND ENVIRONMENTAL TOXICOLOGY

by

Nicole M. Schrad
September 2022

The Dissertation of Nicole M. Schrad is approved:

_____
Professor Chad Saltikov, chair

_____
Michael Patnode, Ph.D.

_____
Samantha Ying, Ph.D.

_____
Peter Biehl
Vice Provost and Dean of Graduate Studies

Table of Contents

List of Figures

Chapter 3

Chapter 4

Abstract: Contribution of Microbial Communities to Geochemical Cycling during Managed Aquifer Recharge

by Nicole M. Schrad

Thesis Statement:

Managed aquifer recharge (MAR) is a set of tools and protocols that purposefully collects water to replenish underground aquifers. Types of MAR vary in their capacity to recharge, the price to implement them, and the water quality of infiltrating water. Distributed stormwater collection MAR uses hillslopes and gravity to direct stormwater into collection basins where it then infiltrates back down into the aquifer.

This dissertation uses techniques from microbiology, water analysis, carbon characterization, and metagenomic sequences to elucidate how the design of a distributed stormwater collection MAR basin impacts the microbial community, thus impacting the geochemical cycling and water quality. The addition of a carbon-rich permeable reactive barrier (PRB) layered on top of a collection basin promotes the removal of nitrates from agricultural stormwater. The removal of nitrates, along with most of the geochemical cycling in the subsurface soil, is primarily done by the native microbial community. However, prior to this research, it was unclear how the microbial was being impacted by either infiltration or infiltration with a carbon-rich PRB. There was also little research into how different PRB materials could have different results in both water quality and microbial community composition.

This research's overarching hypothesis was that the addition of a carbon-rich PRB would provide carbon to the native subsurface microbes and power their denitrification. We also hypothesized this carbon shift would provide a trophic benefit to a common consort of microbes and the type of carbon being provided would have different outcomes. This research gives first insights into the soil-microbe-water interactions that occur during MAR and helps provide a framework for a predictive understanding of the carbon and nutrient cycling occurring during MAR infiltration.

We first looked at how the soil and water characteristics influence the microbial communities of three pilot-scale field experiments simulating shallow MAR infiltration. We found there was a common shift towards *Proteobacteria* in sites that had coarser soil profiles (mainly sand) after infiltration, while sites with finer soil profiles (more clay and silt) did not exhibit significant changes in microbial community composition. This soil characteristic trend continued when we compared soil communities below a carbon-rich PRB of woodchips to communities below a plot with no PRB. The finer soil did not show major differences in genera with the addition of a PRB, but the coarse soils had similar increases in bacteria capable of complex carbon degradation and decreases in genera capable of nitrification.

The next question we asked was: how is the PRB influencing the metabolism of the underlying microbial soil community? To answer this, we took the leachate from two PRB materials: almond shells and woodchips and created anaerobic microcosms with soil to mimic fully saturated MAR conditions. We observed the almond shell leachate removed nitrate as quickly as the positive control microcosm

amended with lactate, while woodchip leachate was a little slower but faster than the unamended microcosm. This corresponded to the metagenomic analysis where we saw an increase in denitrifying genes such as *napA* and *nosZ* in the after samples. Overall the division of genes into different subcategories of metabolism remains unchanged, although the assigned taxonomy of the samples varied greatly between pre- and post- incubation.

The final question we asked was: How can we characterize the carbon being leached off the different PRB materials? In order to answer this, we used a biodegradable organic carbon assay, an assimilable organic carbon assay, ultraviolet-visible absorption, and nuclear magnetic resonance to characterize the leachates. Our results show that microbes are able to use the carbon leached off of the almond shells better than the woodchips. The woodchips were composed of more complex carbon which could provide a long-term solution for a MAR basin that is experiencing wet-dry/ oxic/ anoxic cycling.

These results taken together give a greater understanding of how the design of a MAR system is impacting the native communities in the subsurface soil. It also provides the foundation of important predictive factors for future models and analyses of MAR infiltration.

Acknowledgments and Dedication

The text of this dissertation includes reprints of the manuscript submitted to *FEMS Microbiology Ecology* titled “Soil characteristics and redox properties of infiltrating water are determinants of microbial communities at managed aquifer recharge sites”. The co-authors Andrew T. Fisher, and Chad Saltikov listed, directed, and supervised the research which forms the basis for the dissertation. Co-authors Jennifer Pensky, Galen Gorski, and Sarah Beganskas conducted the experiments and collected data that was analyzed in the manuscript.

First, I would like to thank my advisor Chad Saltikov, for letting me join his group and putting up with me. He took in a management consultant with big ideas and little knowledge and let me find my own path to become a scientist. He supports my hobbies and endeavors outside of school, which has allowed me to have a pretty great work-life balance for most of my graduate school. I know I can always count on Chad to cheer me on, even if I fail and I can’t thank him enough for always responding to my slack messages, regardless of the time they were sent. He also is a “word-wizard” and his contributions to my manuscripts and response to the reviewers have taken my passive-voice writing to the next level.

Next, I would like to thank Andrew Fisher. You brought together the collaboration that this thesis is a part of, and I am so appreciative of your support and patience while I determined how the microbiology side was going to contribute to your well-established hydrology projects. Your edits and contributions to my manuscript and the re-writing of my manuscript (both times!) elevated the article to a new level.

I would also like to thank the other members of my committee; Samantha Ying, and Michael Patnode. Sam has always been a wonderful sounding board and I aim to one day be as good of a mentor and cool of a person as ze is. I would also like to thank Michael for always taking the time to meet with me and taking a genuine interest in my project, even though he is building up an amazing new lab. I would also like to thank Vicki Auerbach-Stone for chairing my first qualifying exam, as well as Manel Camps, Karen Otteman, Fitnat Yildiz, Andrew Fisher, and Ed Green for providing constructive criticisms throughout both of my qualifying exams.

I would like to thank Brian Dreyer from the Marine Analytical Lab for his help analyzing dissolved organic carbon and dissolved nitrogen species. I would also like to thank Jack Lee for all of his help using the NMR. I would also like to thank the members of the Salitkov, Fisher, and Ying labs: Kaitlyn Redford for training me and for being my first backpacking partner in Santa Cruz. Sanjin Mehić for always being there to complain about experiments not working, and Esther Muñoz for teaching me how to just go for what you want. I would also like to thank Juliana Mayavanga Nzongo. Shortly after you joined our lab, you found me crying about my qualifying exam. We didn't really know each other but you listened to what I was stressed about and came up with at least three different solutions. This became a common theme throughout our friendships. Thank you for all your help, your support, and your reprimands when I talk too negatively about myself. I would also like to thank Araceli Serrano, Jennifer Pensky, and Galen Gorski for all their guidance and help with the Shimadzu and Lachat.

Thank you to the Beach Hill community. Over the past four years, our house has not only been a place to live but also a source of fun and friendship. Specifically thank you to Colin Dailey, Emma Chiaroni, Manuel Labbe, Scott and Tamara Kleinman, Christina Yang, Tawney Hughes, Curtis Perkins, Matt Conforti, Zack Newland, Lauren Lashmet, Danielle Devincenzi, Chris Garrison, Peter, and Dixie.

I would like to thank Pacific Edge climbing gym for providing me with an amazing community and a way to destress. I would also like to thank Tyler Karow for connecting so many great people from San Francisco and Yosemite and letting me be a part of his community. Specifically, I would like to thank Julia Cheresh, Maddie Ginn, Cheryl He, Adam Martoś, Christa Seidl, and Samantha Spurlin for being the most fun weekend warriors. Spending time in the mountains with all of you was the highlight of the past five years.

I would also like to thank the best group of friends. Thank you to Sarah Allison, Erica Arnold, Jayda Koland, Shea Livingston, Kaylie Russell, and Sarah Sherman. I don't know what I would do without your love and support. You are some of the smartest, funniest, and most wonderful humans, and honestly words can't really encapsulate what you mean to me. Thank you for all the phone calls, ski trips, and dance-floor takeovers.

Thank you to the METX department and the people who made up this community. Specifically, thank you to Sarah Claus, Christina Egami, Myra Finkelstein, Michael Trebino, and Caison Werner for your help during my first time teaching Anatomy. Thank you to my cohort for helping me pass my courses the first

couple of years and to the 4th floor METX hallway for making the building more friendly. Thank you to the best mentoring group: Giovanni Vega, Dominique Banta, and Sydney Smyer.

I would also like to thank my mom and brother. This wouldn't have been possible without your love, advice, and support.

Last but not least, thank you to Mats Allen. Thank you for helping me with my code, taking me on adventures, and not running away when graduate school made me cry. You have been my support and emotional rock the past couple of years, and I am so grateful for you Whether it is an Ironman, a big wall, or a Ph.D. you are always my number one fan and usually you believe I can do something more than I can. Thanks for believing in me and us, even during the tough times.

This thesis is dedicated to all of you who helped me over the past years.

Chapter 1: Thesis overview

Introduction

The main fields of interest in this dissertation are environmental microbial ecology and biogeochemical cycling. This dissertation is particularly focused on how the microbial community in the subsurface soil can transform substances in water infiltrating back into an aquifer. I aim to connect microbial community composition to environmental factors and find trends caused by infiltration and design of a distributed stormwater collection managed aquifer recharge (MAR) basin. The results of this dissertation will hopefully provide insights and recommendations to improve the quality of recharged water using microbes that already exist in the soil.

Current Knowledge

Managed aquifer recharge (MAR) is the collection and purposeful restoration of water back into underground aquifers (Dillon and Arshad, 2016). There are many types of MAR, each with different water inflows, collection capacity, and water quality concerns (Casanova et al., 2016). Few studies have included microbial communities as part of the samples collected from MAR experiments and most of the methods used to sequence the DNA of microbes are not as accurate as next-generation sequencing (Li *et al.*, 2013; Barba *et al.*, 2019). Our collaboration group previously published next-generation 16S rRNA sequences as part of an analysis of in-situ field experiments replicating MAR conditions and found genera of microbes capable of complex carbon degradation and denitrification (Beganskas, et al., 2018; Gorski et al., 2019; Pensky et al., 2022). It is known that adding a carbon-rich permeable reactive barrier (PRB), made out of materials such as reed stalks, biochar,

or woodchips, can improve the degradation of pollutants in the infiltrating water (Qian, Wang, Jin, Liu, Chen, and Paul H Fallgren, 2011; Valhondo et al., 2014; Beganskas, et al., 2018). Microbes drive a lot of the geochemical cycling that occurs in the subsurface soil (Stein *et al.*, 2010), so it is imperative to understand how communities, and consequently water quality, are impacted by the introduction of a MAR system.

Knowledge Gaps

Although MAR is a widely used tool, the impact of the microbial community is not well known. Few studies have analyzed microbial communities at MAR systems and fewer still have used the highly accurate sequencing tools now available. Mapping the geochemical conditions to the most common populations has also not occurred. It is not understood how the PRB impacts the microbial community composition. The carbon leached from different PRB materials has not been characterized in terms of how much carbon is being provided to the biomass.

Hypotheses

The main hypotheses are (i) microbial communities in simulated MAR will be influenced by the geochemical parameters, (ii) the genetic composition of the microbial community will change when exposed to DOC from PRB materials toward carbon degradation and anaerobic respiration, and (iii) carbon from PRB materials that have faster denitrification rates will have a higher percentage of usable carbon.

Research Design

To test our hypotheses, we conducted a variety of experiments to address the knowledge gaps. First, we analyzed large meta-datasets of both microbial and

chemical data from three test locations that stimulated MAR through the subsurface. We used statistical analysis to observe trends in population dynamics that existed at all three locations. We also quantified the number of nitrous oxide reductase genes present in two of the soils. To further study the genetic composition of the microbial community in relation to nitrate removal, we ran shotgun metagenomic sequencing on samples from anaerobic microcosms. To make the microcosms, we soaked PRB materials in water for 24 hours in an anaerobic chamber before filtering and adjusting DOC. This PRB leachate was used for all further studies. We characterized the PRB leachate by performing an assimilable organic carbon assay using two known carbon-degrading strains, a biodegradable organic carbon assay using native soil populations, Ultraviolet-Visualization, Specific Ultraviolet Absorbance, and proton Nuclear Magnetic Resonance.

Purpose of the Study

The purpose of this study was to gain insights into the microbial populations at distributed stormwater collection managed aquifer recharge basins. Microbes are a primary driver of geochemical reactions in the subsurface soil. Geochemical reactions can be positive, such as removing pollutants, or can be negative like releasing heavy metals from the soil. Understanding how the community contributes to and is affected by the infiltrating water will give us insights into ways to improve the designs of MAR systems. One such design is the application of a carbon-rich permeable reactive barrier to drive denitrification. This study observes how different materials impact the genetic makeup of the microbial community. It also aims to characterize how much of the organic carbon leached off of these materials can be used by the microbes.

Overview of Chapters

Chapter 2 provides a review of biogeochemical cycling in managed aquifer recharge. Chapter 3 discusses microbial signatures of managed aquifer recharge. It is a reprint of an article submitted to FEMS Microbiology Ecology. Chapter 4 presents changes to the genes of the microbial community after exposure to PRB leachates. Chapter 4 further analyzes the carbon leached from the PRB material and the changes that occur during incubation with soil microbes. Together this work provides insights into the microbial ecology during aquifer recharge infiltration and provides guidelines for the design of MAR distributed stormwater collection basins. Chapter 5 gives insights into future directions and concludes the major takeaways from this study.

References

Barba, C., Folch, A., Gaju, N., Sanchez-Vila, X., Carrasquilla, M., Grau-Martínez, A., and Martínez-Alonso, M. (2019) Microbial community changes induced by Managed Aquifer Recharge activities: linking hydrogeological and biological processes. Hydrology and Earth System Sciences 23: 139–154.

Beganskas, S., Gorski, G., Weathers, T., Fisher, A.T., Schmidt, C., Saltikov, C., et al. (2018) A horizontal permeable reactive barrier stimulates nitrate removal and shifts microbial ecology during rapid infiltration for managed recharge. Water Research 144: 274–284.

Casanova, J., Devau, N., and Pettenati, M. (2016) Managed Aquifer Recharge: An Overview of Issues and Options. In Integrated Groundwater Management. Cham: Springer International Publishing, pp. 413–434.

Dillon, P. and Arshad, M. (2016) Managed Aquifer Recharge in Integrated Water Resource Management. In Integrated Groundwater Management. Cham: Springer International Publishing, pp. 435–452.

Gorski, G., Fisher, A.T., Beganskas, S., Weir, W.B., Redford, K., Schmidt, C., and Saltikov, C. (2019) Field and Laboratory Studies Linking Hydrologic, Geochemical, and Microbiological Processes and Enhanced Denitrification during Infiltration for Managed Recharge. Environmental Science & Technology 53: 9491–9501.

Li, D., Alidina, M., Ouf, M., Sharp, J.O., Saikaly, P., and Drewes, J.E. (2013) Microbial community evolution during simulated managed aquifer recharge in response to different biodegradable dissolved organic carbon (BDOC) concentrations. Water Research 47: 2421–2430.

Pensky, J., Fisher, A.T., Gorski, G., Schrad, N., Dailey, H., Beganskas, S., and Saltikov, C. (2022) Enhanced cycling of nitrogen and metals during rapid infiltration: Implications for managed recharge. Science of The Total Environment 838: 156439.

Qian, J., Wang, Z., Jin, S., Liu, Y., Chen, T., and Fallgren, P.H. (2011) Nitrate removal from groundwater in columns packed with reed and rice stalks. Environmental Technology 32: 1589–1595.

Stein, H., Kellermann, C., Schmidt, S.I., Brielmann, H., Steube, C., Berkhoff, S.E., et al. (2010) The potential use of fauna and bacteria as ecological indicators for

the assessment of groundwater quality. Journal of Environmental Monitoring 12: 242–254.

Valhondo, C., Carrera, J., Ayora, C., Barbieri, M., Nödler, K., Licha, T., and Huerta, M. (2014) Behavior of nine selected emerging trace organic contaminants in an artificial recharge system supplemented with a reactive barrier. Environmental Science and Pollution Research 21: 11832–11843.

Chapter 2: Introduction to Biogeochemical Cycles during Managed Aquifer Recharge

Introduction

Availability of fresh water is a worldwide concern. Many cities depend on underground aquifers as their primary water source. However, aquifers, especially in Asia and North America, are being depleted of water faster than they are being replenished. It is estimated that 1.7 billion people live in areas with threatened groundwater resources (Gleeson *et al.*, 2012). Groundwater depletion can cause underground caverns and channels to collapse causing sinkholes on the earth's surface (Casanova *et al.*, 2016b). In coastal areas, the reduction of groundwater causes saltwater intrusion which is detrimental not only to people dependent on the aquifer as a water source, but also for the local fauna (Ringleb *et al.*, 2016). Climate change is also exacerbating groundwater depletion. Annual runoff continues to increase by 4% for every 1°C increase in global temperature (Labat *et al.*). Models have also predicted increased periods of droughts worldwide as well as more intense storms (Van Steenbergen and Tuinhof, 2010; Swain *et al.*, 2018). Less groundwater will replenish because of these storms (Bates *et al.*, 2008). Many committees have been formed to address and solve the problem of limited water such as the Intergovernmental Panel on Climate Change (IPCC) (Bates *et al.*, 2008) and the International Association of Hydrogeologists (IAH) (Van Steenbergen and Tuinhof, 2010). There are also many international directives and goals to increase water supply and quality such as the UN Millennium Goal for Water Supply (Dillon, 2005) and European Union Water Framework Directive (Casanova *et al.*, 2016).

Managed Aquifer Recharge (MAR) is one form of water resource management (Dillon, 2005). It is defined as the purposeful recharge of groundwater for recovery or environmental benefit (Dillon and Arshad, 2016). There are many forms of MAR which will be discussed in the next section. The implementation of these systems influences the biogeochemical cycling in the soil and has been shown to be a form of water treatment (Bates *et al.*, 2008). Soil microbes at the MAR sites can degrade pollutants that exist in the water such as nitrates (Qian, *et al.*, 2011), emerging organic contaminants (Rauch-Williams *et al.*, 2010), and change the movement of trace metals such as arsenic (Fakhreddine *et al.*, 2015). This review will focus on how MAR systems affect geochemical cycles and the microbes involved with the various processes.

Managed Aquifer Recharge

Managed Aquifer Recharge (MAR) is the intentional repurposing of surface water back to the ground. There are many types of managed aquifer recharge including bank filtration, aquifer storage and recovery, aquifer storage transfer and recovery, infiltration ponds, and underground dams to name a few (Dillon *et al.*, 2009). The International Groundwater Resource Assessment Centre classifies the MAR systems into five broad categories (Hannappel *et al.*, 2014):

1.) **Bank Filtration**- This type of MAR has a well that is set up near a lake or stream that induces surface water infiltration. The main purpose of this type of MAR is to improve water quality during transportation into the subsurface.

2.) **Rainwater Harvesting**- This type of MAR is made up of two primary forms- either using barriers and trenches to collect run-off and rainwater or rooftop

harvesting that collects and stores water in tanks and injects it back into the aquifer using an old well or borehole. Both forms can be utilized in an urbanized area (Dillon *et al.*, 2009).

3.) **In-channel modifications**- This MAR uses structures to slow down streams and allow for the water to seep back into the ground. It is common for this type to be used in areas with seasonal rain. Specific types of in-stream modification MARs are check dams and sand dams.

4.) **Well, shaft, dam, and borehole recharge**- This is the broadest range of MAR. Aquifers are recharged by gravity pulling water down through dug wells and pits or by injection of water into a well. Aquifer Storage and Recovery and Aquifer Storage Transfer and Recovery are two common forms of injection recharge(Dillon *et al.*, 2009). This type of recharge is usually built below ground level.

5.) **Spreading methods**- This method also uses gravitational forces to drive recharge, but it differs from the well, shaft, and borehole recharge because this type of MAR is constructed at or above ground level. Common forms of spreading methods are infiltration ponds and soil aquifer treatment, where water seeps through the soil to a vadose zone before hitting the saturated aquifer where the recharged water can be recovered.

All the different forms of MAR have pros and cons and the decision of what system should be used is highly dependent on the goal of the recharge and the geology of the area. The main limitations of MAR are due to the hydrogeological properties of an

aquifer and the ground above. In all systems, the aquifer must be able to store the excess water entering from the MAR (Dillon, 2005). For systems that rely on natural infiltration, the unsaturated zone must also have permeable soil (Casanova *et al.*, 2016). MAR systems are centered around the idea of maintaining water within the system, so evaporation while the water is at the surface is a major concern (Van Steenbergen and Tuinhof, 2010). The water quality of the recharge water is also a large concern – some countries, such as France, do not allow treated wastewater to be used for recharge due to concerns of aquifer contamination (Casanova *et al.*, 2016). Nitrogen, iron, sulfur, trace metals, and organic contaminants are common groundwater pollutants, and the chemical cycling of these compounds is commonly tracked as an indicator of water quality.

Nitrogen Cycling

Microbial-mediated nitrogen cycling is an important consideration for any water system that will be used for human consumption. Nitrogen is the fourth most common element in cellular biomass and makes up the majority of Earth's atmosphere (Stein and Klotz, 2016). Due to nitrogen's ability to exist in multiple oxidation states, the cycle is very complex. Most environmental scientists track the concentrations of nitrate (NO_3^-, oxidation state = +5), nitrite (NO_2^-, oxidation state = +3), ammonium (NH_4^+, oxidation state= -3), and ammonia (NH_3, oxidation state = -3) to gain a sense of how nitrogen is moving through a system (Shrimali and Singh, 2001). Due to the stability of many forms of nitrogen, transformations to different oxidation states are primarily dependent on microbes that can use the redox properties

to produce energy (Xia *et al.*, 2018). Microbes can reduce nitrate and nitrite to inert nitrogen gas (denitrification), oxidize ammonia to nitrate (nitrification), decompose biomass back into ammonia (ammonification), as well as fix nitrogen gas in the air to produce ammonium (nitrogen fixation) (Xia *et al.*, 2018).

In a MAR system, the presence of high nitrate in the recharge water, as well as the aquifer, is a health and environmental concern. Although plants primarily acquire nitrogen through the uptake of nitrate (López-Gutiérrez *et al.*, 2004), groundwater concentrations are very high in many areas of the world(Howarth *et al.*, 2002). The World Health Organization recommends drinking water to not exceed a NO_3-N concentration higher than 50 mg/L (Speijers, 2011), while the EPA suggests no greater than 10 mg/L (Wang and Chu, 2016). In the Jaipur district of India, 40% of the groundwater used by villages had NO_3-N concentrations greater than 20 mg/L (Joshi *et al.*, 1995), while in China 90% of the shallow groundwater is highly polluted with nitrate being one of the most common pollutants (Wei *et al.*, 2018). Australia, the United States, Japan, and the UK also have high levels of nitrate contamination in groundwater (Shrimali and Singh, 2001). This excess of nitrate is primarily due to the increased use of inorganic fertilizers starting in the 1950s and increasing by more than 200% between 1960 and 1990 (Howarth *et al.*, 2002). High levels of nitrate are an environmental concern due to the eutrophication that results in the loss of aquatic species diversity in surrounding water sources close to the MAR (Shrimali and Singh, 2001; Bates *et al.*, 2008). Nitrate, which is reduced to nitrite in the body and reacts with hemoglobin forming methemoglobin. Methemoglobin is unable to carry oxygen,

so it poses a major asphyxiation threat to infants who do not possess the enzyme to reverse the reaction (Speijers, 2011). Nitrites mixed with saliva also have been shown to form nitrosamines, which are a type of carcinogen (Han *et al.*, 2012). Because of the health and environmental issues, the nitrogen cycle should be a major consideration in the design of MAR sites.

MAR systems, especially those built near agricultural areas, are designed with an emphasis on the microbial denitrification process, or the removal of nitrate. In anoxic conditions, microbes can partially or fully reduce nitrate to nitrogen gas in the following reaction (Knowles, 1982):

$$NO_3^- \longrightarrow NO_2^- \longrightarrow NO \longrightarrow N_2O \longrightarrow N_2$$

Bacteria can also reduce nitrate using dissimilatory nitrate reduction to ammonium (DNRA). This pathway reduces using the following reaction (Kraft *et al.*, 2011):

$$NO_3^- \longrightarrow NO_2^- \longrightarrow NH_4^+$$

DNRA is thought to mostly occur when nitrate, rather than carbon is limiting (Cole and Brown, 1980). Denitrification is not tied with any particular carbon metabolism and is not a defining characteristic of a bacterium (Ward, 2007). Denitrification is not limited to a particular class and common denitrifying genera are common microbes that occupy soil systems (e.g., *Pseudomonas, Acidovorax, Bacillus*) (Lu *et al.*, 2014). The diversity of denitrifiers in a system is usually assessed by the nitrite reductase genes and 16S rRNA gene (Ward, 2007). There are two distinct nitrite reductase genes – *nirK* encodes a trimeric copper enzyme while *nirS* is a dimeric cytochrome cd_1 heme enzyme (Kraft *et al.*, 2011). The presence of n*osZ*, which encodes for a nitrous reductase, is another important gene that is considered due to nitrous oxide's

role as a greenhouse gas (Henry *et al.*, 2006; Ward, 2007). The abundance of DNRA bacteria can be assessed by the presence of the *nrfA* gene (Song *et al.*, 2014).

The rates of denitrification are not simple to calculate due to the large presence of N_2 in the atmosphere. If a direct increase in N_2 is being measured, then long incubations in a completely sealed chamber and a high-sensitivity mass spectrometer need to be used (Ward, 2007). Therefore, most studies quantify the loss of nitrate or the production of an intermediary instead. This can be done using tracer ^{15}N isotopes in experiments where the influent can have the isotope form of nitrate (Schmidt *et al.*, 2011). Nitrate can be detected colorimetrically using UV spectrophotometry (Qian, *et al.*, 2011) or indirectly using a reduction reaction(Grau-Martínez *et al.*, 2018). Nitrite can be calculated using the Griess reagent and spectrophotometry (Qian, *et al.*, 2011). The addition of acetylene can also give an idea of denitrification rates because it blocks nitrous oxide reductase. The accumulation of nitrous oxide can then be detected with electron capture gas chromatography(Ward, 2007).

To maximize denitrification rates in a MAR system that has an influent with high nitrate concentrations, an organic permeable reactive barrier (PRB) may be placed on top of the infiltration zone. Many different PRBs have been used around the world depending on the local availability of carbon sources. Cost feasibility is also a major concern when selecting a PRB. For example, polyhydroxyalkanoates (PHAs) were found to be an eco-friendly PRB that enhances denitrification rates. However, it was estimated that the nitrate removal cost of a PHA ends up being 21–

37 Euro kg^{-1} NO_3-N^{-1}, almost 10-fold more expensive than other materials (Hiraishi and Khan, 2003). In China, experiments have been set up that compare the use of a PRB made from reed-stalk and rice-stalk. The increase in carbon from both PRBs increased nitrate removal from 19% to 90% in 72 hours however the rice stalk had better denitrification rates (Qian, *et al.*, 2011).Other studies have looked into using palm leaves and composted material and found that even though nitrate levels were decreased, it is believed that the influx of carbon could be pushing bacteria towards DNRA as there was an accumulation of ammonium throughout the study (Grau-Martínez *et al.*, 2017). To date, there have been no studies on how the PRB surface could be influencing bacterial growth and metabolism by allowing the formation of biofilms, however, studies of wastewater treatment indicate this could be playing a factor (Wang and Chu, 2016).

Geological and chemical factors of a MAR site also play a role in the microbes' ability to denitrify the recharge water. The infiltration rate of the recharged water plays a large role in denitrification rates—when water flows quickly, the microbes are unable to use the dissolved oxygen quickly and the nitrate persists. The soil grain size as well as the aquifer's horizontal depth affect infiltration rate. One study found denitrification was undetectable when the infiltration rate exceeded 0.7 ± 0.2 m d^{-1} in a sandy soil aquifer (Schmidt *et al.*, 2011). In Europe, it was found that MAR sites on aquifers that had a large area for water to pass through horizontally were better at biochemical transformation (Hannappel *et al.*, 2014). Many different

modeling systems take in these factors while determining the best spot to implement a MAR (Ringleb *et al.*, 2016).

Trace Metal and Sulfur Cycling

MAR systems, as they become anoxic, move towards redox conditions favorable for metal reduction. After oxygen (Gibbs Free Energy= -78.5 kJ/electron) is depleted, nitrate is the next to be used as a terminal electron acceptor (-72.3 kJ/ electron) and is followed by manganese (-50.3 kJ/electron), iron (Fe (III)) (-4.6 kJ/electron) and sulfate (21.4 kJ/electron) (Rivett *et al.*, 2008). The common forms of iron, manganese, and sulfur are much more reactive than stable NO_3^- and N_2 so the cycling of these elements occurs abiotically and biotically (Devereux *et al.*, 2007; Emerson and Roden, 2007). However, in the right redox conditions, microbes, such as the genera *Geobacter* and *Shewanella* (Ko *et al.*, 2016; Lee and Lee, 2018) can reduce iron and manganese from Fe- or Mn- containing minerals which release the metals into the groundwater system (Fredrickson *et al.*, 1998; Jokela *et al.*, 2017). Released Fe (II) and Mn (II) change the pH and pore water chemistry of the aquifer, give the water a metallic taste, and mobilize arsenic (Ko *et al.*, 2016) therefore tracking this metal cycling is important when designing MAR systems.

Oxidation of iron and sulfur can also move metals through a system. Dissolved oxygen in the recharge water of a MAR can promote oxidation of Fe- and S-containing minerals in the soil which can then lead to mobilization of other metals. For example, a study at a MAR in the Netherlands showed that pyrite (iron disulfide mineral) oxidation leads to the mobilization of As, Co, Ni, and Zn (Stuyfzand, 1998). Pyrite oxidation can also contribute to aquifer acidification and change the redox

conditions to no longer favor the removal of micropollutants (Seibert *et al.*, 2017). Given the interrelatedness of Fe, Mn, and S cycling and metal mobilization, MAR models need to consider the complex geochemical effects an effluent might have on the quality of drinking water.

Arsenic contamination of groundwater is a major concern – it is on the World Health Organization's top ten list of chemicals of major public health concern (World Health Organization, 2017). In Bangladesh alone, it is estimated that 50 million people drink arsenic-contaminated water (Lièvremont *et al.*, 2009). Arsenic exists naturally in subsurface sediments, commonly in arsenic-sulfides or arsenic-iron-sulfides (Saltikov and Malasarn, 2007). Arsenic speciation helps to determine mobilization in groundwater. For example, the highly toxic arsenite (As (III)) has greater mobility through hydrological systems (Saltikov and Malasarn, 2007; Oremland *et al.*, 2009). The mobility and speciation of arsenic in a groundwater system are highly dependent on other chemicals present in the system. The presence of Ca^{2+} and Mg^{2+} cations in an aquifer system has been shown to decrease the mobilization of As by increasing absorption even when As is in a reduced form (Fakhreddine *et al.*, 2015). Oxidation of arsenite to arsenate is usually coupled with the reduction of another species (Saltikov and Malasarn, 2007). When this is coupled with nitrate reduction, it decreases mobility due to arsenate's affinity to be adsorbed to mineral surfaces (Saltikov and Malasarn, 2007). Conversely, when the oxidation is coupled with sulfate reduction, aqueous thioarsenate is created and arsenic mobility increases (Burton *et al.*, 2013). Sulfur reduction is dependent on sulfate-reducing

bacteria (SRBs). One study found that arsenic mobilization was correlated with sulfate reduction only in columns that contained SRBs and not in the abiotic controls (Burton *et al.*, 2013). This indicates that metal cycling is not only highly dependent on the other chemicals present in the soil but that the microbes play an important factor.

The microbes responsible for metal cycling are common soil microbes. SRBs are obligate anaerobes are represented by multiple genera such as *Desulfovibrio*, *Desulfotomaculum*, *Desulfobulbus,* and *Desulfomicrobium* and are also able to reduce Fe and Mn (Devereux *et al.*, 2007; Kushkevych *et al.*, 2018). Fe-reducing bacteria include *Pseudomonas, Propionibacterium, Lactobacillus,* and *Sphingomonas*. The microbial community and aquifer chemistry can also be influenced by surrounding conditions. For example, a study in South Korea found the microbial community in a suboxic saline aquifer shifted towards Fe-reducing *Citrobacter* species and high rates of Fe reduction but columns with the same soil but artificial water did not show the same microbial shift or iron reduction (Ko *et al.*, 2016). To gain a full picture of what is occurring in the aquifer, the water and soil chemistry as well as the microbial community must be analyzed.

Carbon Degradation

Up to this point, this review has focused primarily on the chemical reactions centered around microbial electron acceptors. This section will focus on the other half of metabolism—the electron donors. For the most part, the microbes previously discussed have been heterotrophs, organisms that derive nutrition from organic compounds (Devereux *et al.*, 2007; Emerson and Roden, 2007; Ward, 2007). In a

typical MAR system that uses stormwater or infiltration, the microbes will be able to grow using dissolved organic carbon (DOC) in the influent or particulate organic carbon as an electron donor (Grünheid *et al.*, 2005; Dillon *et al.*, 2009; Bayarsaikhan *et al.*, 2018). It is believed that organic permeable reactive barriers (PRBs) are adding carbon to the system which can be used by the microbes, thus improving rates of denitrification (Beganskas, *et al.*, 2018). However, organic compounds can also be pollutants.

The increase in urbanization has created emerging trace organic contaminants (EOC) such as pharmaceuticals, personal care products, and endocrine-disrupting chemicals (Valhondo *et al.*, 2014). Many factors such as "lithology, hydraulic and textural properties of the soil, temperature, physico-chemical properties of the specific compound, and microbial environment" (Barbieri *et al.*, 2011) play a role in determining degradation, however, the redox conditions are a vital determining factor. For example, in a microcosm experiment, it was found that redox conditions where sulfate was being actively reduced were the best conditions for degrading the drug atenolol (Barbieri *et al.*, 2011). Another study found that in a nutrient-rich aerobic infiltration zone, trace EOCs degraded better when biodegradable organic carbon (BDOC) was also present. This could indicate that microbes were using the BDOC as a co-substrate in the metabolic transformation of the EOCs (Rauch-Williams *et al.*, 2010). However, in the oligotrophic conditions, the opposite was true. It is hypothesized that the microbial communities in these conditions are specialized

in using hydrophilic refractory organic compounds as their carbon sources so they can also degrade the EOCs (Rauch-Williams *et al.*, 2010).

Like denitrification, the removal of carbon can be enhanced by the addition of a PRB. A PRB made of aquifer sand, vegetable compost, and clay covered with iron oxide dust improved degradation or had no effect on seven out of nine EOCs during an *in-situ* experiment. The other two EOCs, ibuprofen and paracetamol, are easily degraded under aerobic conditions and had reduced degradation with the use of the PRB (Valhondo *et al.*, 2014). Another study found that leaf litter also moved redox conditions to favor the degradation of EOPs (Bayarsaikhan *et al.*, 2018). PRBs can also be a sorption material, further reducing EOP contamination (Regnery *et al.*, 2017). These results indicate the need to further study how to best design a MAR depending on the pollutants present in the water at that site.

Conclusion

MAR is an incredibly useful tool to resupply aquifers as they are depleted by human use. It also has the potential to improve water quality by the degradation of pollutants such as nitrate and pharmaceuticals. Unfortunately, it also might increase the mobilization of metals such as arsenic. Many factors determine how materials are cycled through a MAR system. The redox conditions determine whether certain pollutants such as nitrate and sulfate are reduced. The reduction and oxidation of minerals in the soil promote or hinder the movement of metals such as arsenic and nickel into the groundwater. Water chemistry also plays a large factor in what will occur in a MAR system by changing the pH and influencing the microbial communities. The complexity and interrelatedness of the biogeochemical cycles

create a hard system to accurately model (Ringleb *et al.*, 2016). Therefore, it is important to continue to study how to optimize MAR systems to promote microbial communities that can degrade pollutants while also allowing for proper infiltration into the aquifer.

To understand the best way to promote microbial degradation of pollutants, a few key questions need to be understood. Given the experimental results that show increased degradation of nitrate and most EOCs with the addition of a PRB, understanding exactly how the PRB is influencing the community is necessary to improve MAR design. This includes understanding whether microbes are using the PRB as an attachment surface, how the influx of carbon is influencing the microbial community, and what is an optimal material to use. Another important aspect to consider is whether the microbial community is being changed by the recharge or if gene expression of the existing community is changing. Thirdly, considering how environmental factors such as infiltration rate, soil type, pH, and temperature influence the microbe's ability to degrade pollutants in the recharge water will give insights into what is important for a MAR system. Having a full picture of what is occurring at the microbial level will help guide the best way to implement MAR systems to be as efficient as possible at replenishing groundwater with high quality water.

References

Barbieri, M., Carrera, J., Sanchez-Vila, X., Ayora, C., Cama, J., Köck-Schulmeyer, M., et al. (2011) Microcosm experiments to control anaerobic redox conditions

when studying the fate of organic micropollutants in aquifer material. *Journal of Contaminant Hydrology* **126**: 330–345.

Bates, B.C., Z.W. Kundzewicz, and S. Wu and J.P. Palutikof, Eds. (2008) Climate Change and Water. Technical Paper of the Intergovernmental Panel on Climate Change, Geneva.

Bayarsaikhan, U., Filter, J., Gernert, U., Jekel, M., and Ruhl, A.S. (2018) Fate of leaf litter deposits and impacts on oxygen availability in bank filtration column studies. *Environmental Research* **164**: 495–500.

Beganskas, S., Gorski, G., Weathers, T., Fisher, A.T., Schmidt, C., Saltikov, C., et al. (2018) A horizontal permeable reactive barrier stimulates nitrate removal and shifts microbial ecology during rapid infiltration for managed recharge. *Water Research* **144**: 274–284.

Burton, E.D., Johnston, S.G., and Planer-Friedrich, B. (2013) Coupling of arsenic mobility to sulfur transformations during microbial sulfate reduction in the presence and absence of humic acid. *Chemical Geology* **343**: 12–24.

Casanova, J., Devau, N., and Pettenati, M. (2016) Managed Aquifer Recharge: An Overview of Issues and Options. In *Integrated Groundwater Management*. Cham: Springer International Publishing, pp. 413–434.

Cole, J.A. and Brown, C.M. (1980) Nitrite reduction to ammonia by fermentative bacteria: A short circuit in the biological nitrogen cycle. *FEMS Microbiology Letters* **7**: 65–72.

Devereux, R., Teske, A., Visscher, P.T., and Hines, M.E. (2007) Sulfur Cycling. *Manual of Environmental Microbiology, Third Edition*. American Society of Microbiology, pp. 497–510.

Dillon, P. (2005) Future management of aquifer recharge. *Hydrogeology Journal* **13**: 313–316.

Dillon, P. and Arshad, M. (2016) Managed Aquifer Recharge in Integrated Water Resource Management. In *Integrated Groundwater Management*. Cham: Springer International Publishing, pp. 435–452.

Dillon, P., Pavelic, P., Page, D., Beringen, H., and Ward, J. (2009) Managed aquifer recharge: An Introduction.

Emerson, D. and Roden, E.E. (2007) Microbial Metal Cycling in Aquatic Environments *. *Manual of Environmental Microbiology, Third Edition*. American Society of Microbiology, pp. 540–562.

Fakhreddine, S., Dittmar, J., Phipps, D., Dadakis, J., and Fendorf, S. (2015) Geochemical Triggers of Arsenic Mobilization during Managed Aquifer Recharge. *Environmental Science & Technology* **49**: 7802–7809.

Fredrickson, J.K., Zachara, J.M., Kennedy, D.W., Dong, H., Onstott, T.C., Hinman, N.W., and Li, S. (1998) Biogenic iron mineralization accompanying the dissimilatory reduction of hydrous ferric oxide by a groundwater bacterium. *Geochimica et Cosmochimica Acta* **62**: 3239–3257.

Gleeson, T., Wada, Y., Bierkens, M.F.P., and van Beek, L.P.H. (2012) Water balance of global aquifers revealed by groundwater foothe tprint. *Nature* **488**: 197–200.

Grau-Martínez, A., Folch, A., Torrentó, C., Valhondo, C., Barba, C., Domènech, C., et al. (2018) Monitoring induced denitrification during managed aquifer recharge in an infiltration pond. *Journal of Hydrology* **561**: 123–135.

Grau-Martínez, A., Torrentó, C., Carrey, R., Rodríguez-Escales, P., Domènech, C., Ghiglieri, G., et al. (2017) Feasibility of two low-cost organic substrates for inducing denitrification in artificial recharge ponds: Batch and flow-through experiments. *Journal of Contaminant Hydrology* **198**: 48–58.

Grünheid, S., Amy, G., and Jekel, M. (2005) Removal of bulk dissolved organic carbon (DOC) and trace organic compounds by bank filtration and artificial recharge. *Water Research* **39**: 3219–3228.

Han, J., Wang, Y., Sahin, O., Shen, Z., Guo, B., Shen, J., and Zhang, Q. (2012) A fluoroquinolone resistance associated mutation in gyrA Affects DNA supercoiling in Campylobacter jejuni. *Front Cell Infect Microbiol* **2**: 21.

Hannappel, S., Scheibler, F., Huber, A., and Sprenger, C. (2014) CHARACTERIZATION OF EUROPEAN MANAGED AQUIFER RECHARGE (MAR) SITES-ANALYSIS.

Henry, S., Bru, D., Stres, B., Hallet, S., and Philippot, L. (2006) Quantitative detection of the nosZ gene, encoding nitrous oxide reductase, and comparison of the abundances of 16S rRNA, narG, nirK, and nosZ genes in soils. *Appl Environ Microbiol* **72**: 5181–9.

Hiraishi, A. and Khan, S.T. (2003) Application of polyhydroxyalkanoates for denitrification in water and wastewater treatment. *Applied Microbiology and Biotechnology* **61**: 103–109.

Howarth, R.W., Sharpley, A., and Walker, D. (2002) Sources of Nutrient Pollution to Coastal Waters in the United States: Implications for Achieving Coastal Water Quality Goals.

Jokela, P., Eskola, T., Heinonen, T., Tanttu, U., Tyrväinen, J., and Artimo, A. (2017) Raw Water Quality and Pretreatment in Managed Aquifer Recharge for Drinking Water Production in Finland. *Water (Basel)* **9**: 138.

Joshi, V.A., Dhodapkar, R.S., Deshpande, L.S., and Nanoti, M.V. (1995) Nitrate in rural area of Nagpur. *IJJEP* **15**: 409–412.

Knowles, R. (1982) Denitrification. *Microbiological Reviews* **46**: 43–70.

Ko, M.-S., Cho, K., Jeong, D., and Lee, S. (2016) Identification of the microbes mediating Fe reduction in a deep saline aquifer and their influence during managed aquifer recharge. *Science of The Total Environment* **545–546**: 486–492.

Kraft, B., Strous, M., and Tegetmeyer, H.E. (2011) Microbial nitrate respiration – Genes, enzymes and environmental distribution. *Journal of Biotechnology* **155**: 104–117.

Kushkevych, I., Kováč, J., Vítězová, M., Vítěz, T., and Bartoš, M. (2018) The diversity of sulfate-reducing bacteria in the seven bioreactors. *Archives of Microbiology* **200**: 945–950.

Labat, D., Godd, Y., Luc, J., and Guyot, J.L. Evidence for global runoff increase related to climate warming.

Lee, J.-H. and Lee, B.-J. (2018) Microbial Reduction of Fe (III) and SO4 2− and Associated Microbial Communities in the Alluvial Aquifer Groundwater and Sediments. *Microbial Ecology* **76**: 182–191.

Lièvremont, D., Bertin, P.N., and Lett, M.-C. (2009) Arsenic in contaminated waters: Biogeochemical cycle, microbial metabolism and biotreatment processes. *Biochimie* **91**: 1229–1237.

López-Gutiérrez, J.C., Henry, S., Hallet, S., Martin-Laurent, F., Catroux, G., and Philippot, L. (2004) Quantification of a novel group of nitrate-reducing bacteria in the environment by real-time PCR. *Journal of Microbiological Methods* **57**: 399–407.

Lu, H., Chandran, K., and Stensel, D. (2014) Microbial ecology of denitrification in biological wastewater treatment. *Water Research* **64**: 237–254.

Oremland, R.S., Saltikov, C.W., Wolfe-Simon, F., and Stolz, J.F. (2009) Arsenic in the Evolution of Earth and Extraterrestrial Ecosystems. *Geomicrobiology Journal* **26**: 522–536.

Qian, J., Wang, Z., Jin, S., Liu, Y., Chen, T., and Fallgren, P.H. (2011) Nitrate removal from groundwater in columns packed with reed and rice stalks. *Environmental Technology* **32**: 1589–1595.

Rauch-Williams, T., Hoppe-Jones, C., and Drewes, J.E. (2010) The role of organic matter in the removal of emerging trace organic chemicals during managed aquifer recharge. *Water Research* **44**: 449–460.

Regnery, J., Gerba, C.P., Dickenson, E.R. V., and Drewes, J.E. (2017) The importance of key attenuation factors for microbial and chemical contaminants during managed aquifer recharge: A review. *Critical Reviews in Environmental Science and Technology* **47**: 1409–1452.

Ringleb, J., Sallwey, J., and Stefan, C. (2016) Assessment of Managed Aquifer Recharge through Modeling—A Review. *Water (Basel)* **8**: 579.

Rivett, M.O., Buss, S.R., Morgan, P., Smith, J.W.N., and Bemment, C.D. (2008) Nitrate attenuation in groundwater: A review of biogeochemical controlling processes. *Water Research* **42**: 4215–4232.

Saltikov, C.W. and Malasarn, D. (2007) Arsenate-Respiring Bacteria. In *Manual of Environmental Microbiology, Third Edition*. American Society of Microbiology, pp. 1214–1222.

Schmidt, C.M., Fisher, A.T., Racz, A.J., Lockwood, B.S., and Huertos, M.L. (2011) Linking Denitrification and Infiltration Rates during Managed Groundwater Recharge. *Environmental Science & Technology* **45**: 9634–9640.

Seibert, S., Descourvieres, C., Skrzypek, G., Deng, H., and Prommer, H. (2017) Model-based analysis of δ34S signatures to trace sedimentary pyrite oxidation during managed aquifer recharge in a heterogeneous aquifer. *Journal of Hydrology* **548**: 368–381.

Shrimali, M. and Singh, K.P. (2001) New methods of nitrate removal from water. *Environmental Pollution* **112**: 351–359.

Song, B., Lisa, J.A., and Tobias, C.R. (2014) Linking DNRA community structure and activity in a shallow lagoonal estuarine system. *Front Microbiol* **5**: 460.

Speijers, G.J.A. (2011) Nitrate and nitrite in drinking-water: Background document for development of WHO Guidelines for Drinking-water Quality.

Van Steenbergen, F. and Tuinhof, A. (2010) Managing the Water Buffer for Development and Climate Change Adaptation Groundwater Recharge, Retention, Reuse and Rainwater Storage, Michael van der Valk Grafisch Service Centrum Wageningen.

Stein, L.Y. and Klotz, M.G. (2016) The nitrogen cycle. *Current Biology* **26**: R94–R98.

Stuyfzand, P.J. (1998) Quality changes upon injection into anoxic aquifers in the Netherlands: Evaluation of 11 experiments.

Swain, D.L., Langenbrunner, B., Neelin, J.D., and Hall, A. (2018) Increasing precipitation volatility in twenty-first-century California. *Nature Climate Change* 1.

Valhondo, C., Carrera, J., Ayora, C., Barbieri, M., Nödler, K., Licha, T., and Huerta, M. (2014) Behavior of nine selected emerging trace organic contaminants in an artificial recharge system supplemented with a reactive barrier. *Environmental Science and Pollution Research* **21**: 11832–11843.

Wang, J. and Chu, L. (2016) Biological nitrate removal from water and wastewater by solid-phase denitrification process. *Biotechnology Advances* **34**: 1103–1112.

Ward, B.B. (2007) Nitrogen Cycling in Aquatic Environments. *Manual of Environmental Microbiology, Third Edition*. American Society of Microbiology, pp. 511–522.

Wei, A., Ma, J., Chen, J., Zhang, Y., Song, J., and Yu, X. (2018) Enhanced nitrate removal and high selectivity towards dinitrogen for groundwater remediation using biochar-supported nano zero-valent iron. *Chemical Engineering Journal* **353**: 595–605.

World Health Organization (2017) Arsenic Fact Sheet, World Health Organization.

Xia, X., Zhang, S., Li, S., Zhang, Liwei, Wang, G., Zhang, Ling, et al. (2018) Environmental Science Processes & Impacts The cycle of nitrogen in river systems: sources, transformation, and flux. **20**: 857–990.

Chapter 3: Soil characteristics and redox properties of infiltrating water are determinants of microbial communities at managed aquifer recharge sites

Abstract

In this study, we conducted a meta-analysis of microbial ecology in soils at three, pilot-scale field sites simulating shallow infiltration for managed aquifer recharge (MAR). We evaluated shifts in microbial ecology after infiltration across site locations, through different soils, with and without carbon-rich amendments added to test plots. We hypothesized infiltration and carbon amendments would lead to common changes in subsurface microbial communities at the field sites but found distinct differences instead. Sites with coarser soil had large changes in diversity and taxa abundance, while sites with finer soils had fewer significant changes in genera, despite having the greatest increase in nitrogen cycling. Below plots amended with a carbon-rich permeable reactive barrier, we observed more nitrate removal and a decrease in genera capable of nitrification. Multivariate statistics determined that the soil texture (a proxy for numerous soil characteristics) was the main determinant of whether the microbial community composition changed because of infiltration. These results suggest that microbial ecology in sandy soil with carbon-rich amendments is most impacted by infiltration. Soil composition is a critical parameter that links between microbial ecology and nutrient cycling during infiltration and could influence the citing and operation of MAR to benefit water quality and supply.

Introduction

Groundwater is the main water source for many populations worldwide. Aquifer overdraft occurs when more groundwater is extracted than is replenished

(Aeschbach-Hertig and Gleeson, 2012). Overdraft is often more severe during drought periods, which are predicted to increase 25-100% in the next fifty years (Swain *et al.*, 2018). Worldwide, some governments are responding by implementing programs aimed at improving water storage and conveyance (Dillon *et al.*, 2009; California Department of Water Resources, 2018). One such management practice is managed aquifer recharge (MAR), the purposeful routing of surface water into an underlying aquifer using a variety of methods. Recharge is the largest source of inflow to most aquifers–it helps mitigate negative outcomes from overdraft, including reduced storage, disconnection from surface water systems, and saltwater intrusion. Moreover, during extreme drought conditions, some of the recharged water can be recovered and used for irrigation, drinking water, or other purposes (Dillon *et al.*, 2009). Stormwater (Schmidt *et al.*, 2011) and treated wastewater (Fournier *et al.*, 2016) are increasingly considered sources of water input for MAR. The increasing reliance on non-traditional water sources has water-quality implications for MAR due to the variability of nutrients from these sources (Sheng, 2005; Fakhreddine et al., 2015)

MAR can result in improved water quality through several mechanisms (Hartog and Stuyfzand, 2017). Infiltrating water may dilute polluted aquifers to acceptable contaminant levels (Stuyfzand *et al.*, 2017). Infiltration can also help to reduce virus and pathogen loads (Hartog and Stuyfzand, 2017) and facilitate the degradation of contaminants like nitrate (Schmidt *et al.*, 2011) and emerging organic compounds (Rauch-Williams *et al.*, 2010). The fate of many pollutants is determined

by the pH, oxygen concentration, organic carbon availability, infiltration rate, microbial community, and the mineralogy of the soil in the subsurface during infiltration (Schmidt *et al.*, 2011; Casanova *et al.*, 2016; Gorski *et al.*, 2019). For example, adding dissolved organic carbon (DOC) to the input water can increase microbial attenuation of nitrate (Mariotti *et al.*, 1988; Starr and Gillham, 1993; Gorski *et al.*, 2019). Hence, a better understanding of water-soil-microbial interactions during infiltration has the potential to help protect groundwater resources, by influencing the selection of MAR sites, as well as the design and operation of associated systems.

Microbial metabolism, the primary driver of geochemical reactions occurring during surface water infiltration (Stein *et al.*, 2010), can improve or worsen the quality of the infiltrating water. Microbes in the subsurface preferentially oxidize organic carbon compounds and reduce the most energetically favorable electron acceptor to obtain energy. This can involve specialized microbial populations that can take advantage of the most favorable pathways and processes under ambient conditions. For example, complex organic contaminants are more likely to be biodegraded in aerobic conditions (Valhondo *et al.*, 2014). Once available oxygen is depleted, nitrate is the next most favorable electron acceptor, followed by metals such as manganese and iron. (Li *et al.*, 2012; Bayarsaikhan *et al.*, 2018). In these reducing conditions, metals such as arsenic can also be mobilized by desorption from soil minerals (Tufano *et al.*, 2008; Fakhreddine *et al.*, 2015). Understanding the microbial consortia present during infiltration will give insight into the potential geochemical cycling that can occur in the system.

Worldwide, nitrate (NO_3^-) is the most widespread non-point source groundwater contaminant (Spalding and Exner, 1993; Gurdak and Qi, 2012). The most well-studied nitrate removal pathway is denitrification, where nitrate is reduced to inert nitrogen gas (NO_3^- □ NO_2^- □ NO □ N_2O □ N_2). This process is carried out in soil systems primarily by facultative heterotrophs once dissolved oxygen is depleted (Starr and Gillham, 1993; Rivett *et al.*, 2008). Incomplete denitrification is also of environmental concern due to the potential for the production of nitrous oxide (N_2O), a greenhouse gas (Starr and Gillham, 1993; Henry *et al.*, 2006; Gurdak and Qi, 2012). Complete microbial denitrification is promoted in wastewater treatment bioreactors and denitrification beds by increasing dissolved organic carbon (DOC) concentrations (Lu *et al.*, 2014). Similarly, the addition of a carbon-rich permeable reactive barrier (e.g., woodchips, compost) to soils at a MAR site stimulates microbial removal of nitrate (Beganskas *et al.*, 2018; Grau-Martínez *et al.*, 2018; Gorski *et al.*, 2019). While microbial ecology is a fundamental parameter in these wastewater treatment reactors (Chu and Wang, 2013), few studies have explored microbial communities in operating MAR systems (Regnery et al., 2017). Barba, et al., 2019 used principal component analysis to determine statistical relationships between geochemical parameters and microbial community composition in the Llobregat MAR system (Spain), finding that certain genera correlated with carbon and nitrogen cycling. However, this study had limited resolution for taxa determination and only focused on one site. Next-generation sequencing methods allow for more precise identification of the microorganisms within MAR systems.

The overall goal of this study was to identify how the infiltration of water, which is simulating conditions during MAR, may influence microbial community composition and metabolism in soils, including soils augmented with a bio-available carbon source. We analyzed microbial communities and metabolisms from three sets of plot-scale field experiments in the Pajaro Valley groundwater basin in southern Santa Cruz County, CA (Beganskas *et al.*, 2018; Gorski *et al.*, 2019; Pensky *et al.*, 2022). The three field sites; Harkins Slough (HSP), Kelly Thompson Ranch (KTR), and Kitayama Ranch (KTYA); are active or planned locations of managed aquifer recharge. They are all located within a 15 km radius (Supplementary Information, Figure S-1). For each location, plots were dug (1m x 1m x 1m) and water was continuously applied to replicate infiltration and the shallow soil conditions of a saturated MAR (Beganskas *et al.*, 2018). Some of the experiments were amended with the addition of a carbon-rich, permeable reactive barrier (PRB) that released DOC into underlying soils to stimulate microbial activity and reduce nitrate concentration, while unamended plots were used as a control. Microbial community composition in native soils and below the PRBs, before and after infiltration, was determined with next-generation sequencing data of the 16S rRNA gene and the clade I nitrous oxide reductase gene, *nosZ* (reduces nitrous oxide to nitrogen gas) (Henry *et al.*, 2006). The 16S rRNA gene sequences from studies at these field sites have been published elsewhere. However, initial studies focused on the hydrologic properties and biogeochemical conditions and processes during shallow infiltration, with a limited assessment of site-specific microbiology. The present study links and

compares results from the three field sites, with the goal of understanding similarities and differences between soil microbial responses to (a) infiltration and (b) the addition of a carbon-rich PRB. This study also adds *nosZ* sequences to the inter-site comparison to take a more functional view of potential microbial metabolism and changes in rates of nitrogen cycling. We hypothesized that there would be common changes in soil microbial community compositions at the three sites induced by shallow infiltration, despite significant differences in soil characteristics. In addition, we expected that the introduction of bioavailable carbon from a woodchip PRB would result in consistent shifts towards the abundance of denitrifying microbes as associated conditions became more favorable.

Materials and Methods

This study combined datasets with sediment, DNA sequencing, and water chemistry datasets from Beganskas, *et al.,* 2018; Gorski, *et al.,* 2019; and Pensky, *et al.*, 2022.

Field Sites

Experimental plots were established at three field sites in the Pajaro Valley, central coastal California (SI, Figure S1), as described in earlier studies (Beganskas *et al.*, 2018; Gorski *et al.*, 2019; Pensky *et al.*, 2022). The details of each experiment, including water sources, test duration, and hydrologic analyses are described in earlier papers concerning tests at Harkins Slough (HSP, Beganskas et al., 2018), Kelly Thompson Ranch (KTR, Gorski. *et al.,* 2019), and Kitayama Ranch (KTYA, Pensky et al., 2022). Experiments at each site were conducted during the summer dry season (June-August); HSP in 2015, KTR in 2016, and KTYA in 2018. Field sites are

located adjacent to active agricultural fields and active or planned locations of managed aquifer recharge. Most freshwater demand in the Pajaro Valley is satisfied by extraction of groundwater, and groundwater in many locations has nitrate concentrations that are elevated relative to pre-development values, with some areas exceeding the federally mandated, maximum contaminant level of 10 mg/L NO_3-N (714 µmol/kg) (Pajaro Valley Water Management Agency Salt and Nutrient Management Plan, 2016).

Experimental plots were square in plain view (1 m x 1 m area), were hand excavated to 0.6 to 1 m depth, and were instrumented with thermal probes (to measure flow rates using heat as a tracer), piezometers (shallow, subsurface fluid samplers), and a continuous infiltration system. Fiberglass walls were inserted in the plots and backed with water-activated bentonite to limit lateral flow. As part of tests at each field site, 1-2 plots were established as "native sediment" controls, and one plot was modified with a 30-40 cm layer of redwood chips acquired from a local landscape supply as a source of bioavailable carbon (Beganskas *et al.*, 2018; Gorski *et al.*, 2019; Pensky *et al.*, 2022).

Fluid and Sediment Sampling

Infiltration tests lasted ~10-16 days, and fluid samples were collected from piezometers installed below the plots every 1-2 days. These samples were filtered and analyzed colorimetrically using a Lachat QuickChem to measure NO_3^-, NO_2^-, and NH_4^+ or a Shimadzu TOC Analyzer to measure DOC. A day before the plots were disassembled, samples from KTR and KTYA were filtered and sent to a professional water quality laboratory (Monterey Bay Analytical Services, MBAS) and subjected to

a drinking water panel, including analyses of NO_3^-, Mn, Fe, and DOC. MBAS data was used in the CCA plots. Values are listed in Supplementary Information Table 2.

Sediments were collected during plot construction and after experiments were complete, to determine conditions before and after infiltration. Sediments were collected by drilling into the plot using a hand auger and recovering samples at regular intervals from the auger bucket. Sampling occurred every 20 cm during the first study (HSP), whereas later studies collected samples every 10cm (KTR and KTYA). Importantly, sampling depth corresponds to the range within which conditions were fully saturated during the infiltration experiments, above the wetting front and inverted water table that formed during rapid infiltration (generally at 60-100 cm). Pre-infiltration samples were analyzed for grain size distribution using a Beckman Coulter LS 13320 Particle Size Analyzer. Total carbon and total nitrogen were analyzed using a Thermo Fisher Flash 2000. Sediment samples for DNA sequencing were collected before and after infiltration using sterile technique, transported in liquid nitrogen, and stored at -80°C. Samples are listed in Supplementary Information Figure Table 1.

DNA extraction and Processing

Soil DNA was extracted using Qiagen PowerSoil DNA Isolation Kit according to the manufacturer's instructions. For each sample, multiple replicates were extracted from the same soil sample from a core. The V4 and V5 regions of the 16S rRNA gene were amplified using 515F-Y and 926R primers that had an attached MiSeq adapter (Table 1)(Parada *et al.,* 2016). Each reaction had 0.2 mM dNTP (New England Biolabs), 5 µL 10X Titanium Taq buffer, 5 µL 10X MasterAmp PCR

enhancer (Illumina), 0.2 µM of each forward and reverse primer, 1µL Titanium Taq polymerase, 3 ng of DNA, and DEPC-treated water up to 50 µL. After the initial amplicons were produced, the Illumina MiSeq Platform Protocol was used as the pipeline for 16S rRNA samples (Illumina). The pooled 16S library was sequenced on the Illumina MiSeq (600 cycles v3 PE300 flow cell kit) at the University of California, Davis Genome Center. KTR and KTYA samples from 30 cm below the plot were sequenced for *nosZ* using the same 50 µL reactions using nosZ2-F and nosZ2-R (Henry *et al.*, 2006) as primers (Table 1). After an initial cleanup with AMPure XP beads, amplicons were sent to Genewiz to be sequenced. The HSP raw reads can be found in the National Center for Biotechnology Information (NCBI) Sequence Read Archive (accession number: SRP151895). The KTR reads are at accession number PRJNA523645, KTYA at PRJNA787642 and *nosZ* reads at PRJNA777280.

Sequenced reads were filtered to an average Q score of >30 and grouped into Amplicon Sequencing Variants (ASVs) using the Divisive Amplicon Denoising Algorithm (DADA2) (Callahan *et al.*, 2016) in R. 16S ASVs were assigned taxonomy using the SILVA reference database version 138 (Quast *et al.*, 2013), while *nosZ* taxonomy was based on a custom curated database created using sequences from Fungene (Fish *et al.*, 2013) and taxonomy from NCBI(National Center for Biotechnology Information, 2010). Sequenced reads from different field sites were combined and stored in a Phyloseq object (McMurdie and Holmes, 2013). A maximum likelihood tree for *nosZ* sequences was created using the phylogeny.fr

program from the Laboratoire d'Informatique, de Robotique et de Microélectronique de Montpellier (LIRMM) (Dereeper *et al.*, 2008). Data transformation and visualizations were conducted using R packages tidyverse (Wickham *et al.*, 2019), ggplot2(Wickham, 2016), tidytree (Yu *et al.*, 2021) ggtree (Yu, 2020), ggvegan (Simpson, 2019, ggpubr (Kassambara, 2020), and ggtext (Wilke, 2020).

Statistical Analysis

For all these analyses, there was no rarefaction. Non-metric multidimensional scaling, constrained correspondence analysis, Shannon-Weaver index, and analysis of variance were calculated using the *vegan* (v 2.5.7) package within R (Oksanen *et al.*, 2020). Environmental and taxa data were extracted from the Phyloseq object. For the Constrained Correspondence Analysis (CCA) plots, constraint formulas were calculated to increase the significance and reduce collinearity. The CCA of the initial communities used the formula Sand + Clay + Silt + C +N and was scaled to show relationships between samples and the constraints. The CCA formula using water chemistry data was DOC + NO3 + Mn + Fe and was scaled to show species' relationships to constraints. Before differential abundance was calculated, taxa were filtered so only reads representing 0.1% in a quarter of the samples were included. Differential analysis was conducted using Analysis of Composition of Microbiomes with Bias Correction (ANCOM-BC). ANCOM-BC was selected due to its design to correct uneven sampling biases (Lin and Peddada, 2020). Differential analysis was repeated when there was an uneven number of replicates to confirm the uneven sampling between treatments did not affect results.

Quantitative Polymerase Chain Reaction

Quantitative polymerase chain reaction (qPCR) was used to calculate the number of *nosZ* reads for KTR and KTYA samples from 30 cm below the plot, the depth where fluid collected fluid samples indicate the most active and consistent cycling. Table 1 shows the primers and cycling used for *nosZ* as well as 16S rRNA, the housekeeping gene. Each sample was done in triplicate and fluorescence was recorded during the annealing step. Each reaction had 10 µL of 2X SYBR Green Master Mix (QuantaBio), 3 ng of DNA, 0.5 µM forward and reverse primers, and water up to 20 µL. Changes in *nosZ* between pre- and post- infiltration were calculated using the Pfaffl method (Pfaffl, 2001). Significance was calculated using a two-tailed t-test.

Results

Summary of Field Sites Geochemistry

The three field sites, Harkins Slough (HSP), Kelly Thompson Ranch (KTR), and Kitayama Ranch (KTYA), were previously analyzed for geochemical parameters and soil properties(Beganskas *et al.*, 2018; Gorski *et al.*, 2019; Pensky *et al.*, 2022). Here we provide a comparative analysis across all three sites specifically comparing how infiltration impacted trends in nitrogen speciation in PRB and native soil field plots. The fraction of dissolved nitrogen species (NO_3^-, NO_2^-, and NH_4^+) was calculated by dividing the difference between the surface water and corresponding deepest piezometer concentrations by the total dissolved N of the surface water. While the dissolved N remained unchanged or increased in the native soil plots, the woodchip-amended plots show the removal of dissolved nitrogen (Figure 1). Overall, the addition of a PRB significantly increased the fraction N removed compared to the

native soil. KTR had the largest removal fraction, averaging around 40% removed in the PRB-amended plot, while at HSP and KTYA the PRB-amended plots removed up to 20% while the native soil plots usually had an addition of N.

We first assessed how the three field sites differed from each other with respect to soil physical-chemical properties that could influence how subsurface microbial communities respond to infiltration. Non-metric multidimensional scaling (NMDS) was used to visualize these differences. Total carbon (TC), total nitrogen (TN), sand, silt, and clay were used as inputs. NMDS analysis (Figure 2) shows that samples from the three sites are significantly grouped by location (Permutational multivariate analysis of variance (PERMANOVA) < 0.001), with Kelly-Thompson Ranch (KTR) samples being especially distinct from Kitayama Ranch (KTYA) and Harkins Slough (HSP) samples. HSP and KTYA samples were composed mainly of sand (93% and 88%, respectively) and were relatively uniform to ~110 cm below the plots, whereas KTR sediments averaged 46% sand, 36% silt, and 17% clay (Supplementary Information, Figure S-2). Conditions at the KTR site were also more heterogeneous; one plot was dominated by sandy layers near 30 and 60 cm depth, and silty layers at 10, 40, 80, and 90 cm depth. The other two KTR plots were a mixture of silt and clay. These physical properties should impact the microbial community makeup. KTR samples had significantly higher TC and TN than did samples from the other sites. TC and TN at KTR averaged 0.64% and 0.06% (by weight), compared to 0.04% and 0.004% at HSP and 0.09% and 0.01% at KTYA, respectively (Supplementary Information, Figure S-3). Additional insights into the hydrology can

be found at Beganskas, *et al.*, 2018 for HSP; Gorski, *et al.*, 2019 for KTR; and Pensky, *et al.*, 2022 for KTYA.

Correspondence of Initial Microbial Communities to Geochemical Data

We next assessed how much the microbial community composition at the three sites differed prior to initiating infiltration. We performed constrained correspondence analysis (CCA) to relate the initial ASVs of the field sites to the inputs used in the NMDS in Figure 1 (TC, TN, Percent Sand, Silt, and Clay). CCA is an ordination method that only displays the variance in population that can be explained by environmental inputs. The constrained axes of the model explain 31.2% of the variance among the community (Figure 3). Including the ASV data allowed for greater sample separation and grouping by location compared to environmental data alone (PERMANOVA(Location)=9.99×10^{-5}). The field locations themselves, as well as their initial microbial communities, are different from one another.

Microbial Community Characterization

To characterize microbial communities and their changes due to infiltration, ASVs were assigned taxonomy using the SILVA database. At least 90% of the reads per sample fell into 10 phyla: *Acidobacteriota*, *Actinobateriota*, *Bacteroidota*, *Crenarchaeota*, *Firmicutes*, *Myxococcota*, *Nitrospirota*, *Planctomycetota*, *Proteobacteria*, and *Verrucomicobiota* (Figure 4a). At all three locations regardless of treatment, there was an increase in *Proteobacteria* after infiltration compared to samples collected before infiltration, however, the change was only significant at HSP and KTYA ($p<0.001$). KTR did not have a significant change of any Phylum due to infiltration or between the PRB treated and native soil. *Proteobacteria* was the

most abundant phylum in all samples, making up on average 41.9% of the relative abundance among all samples. Shannon-Weaver indices were used to calculate sample diversity before and after infiltration (Figure 4b). At KTYA and HSP there was a significant decrease between before and after samples in diversity due to infiltration, whereas KTR showed no significant change. NMDS analysis of the microbial communities shows that samples from KTR and HSP are especially well grouped by location, whereas the KTYA samples encompass the two other groups (Figure 4c).

Impacts of Infiltration on Microbial Community

Infiltration through shallow soils resulted in measurable changes in hydrologic and geochemical conditions and consequent impacts on microbial communities. A PERMANOVA analysis showed that the microbial communities did not significantly separate into before and after infiltration groups ($p=0.05$). Therefore, we used the native soil samples from each location and compared after infiltration samples with before samples using Analysis of Composition of Microbiomes with Bias Correction (ANCOM-BC). To reduce the impact of low abundance species, taxa with less than 100 reads in 25% of the samples were removed. Differentially abundant taxa with adjusted *p* values greater than 0.05 were also removed. KTR only had one genus significantly increase between after infiltration and before, *Candidatus Nitrosotenuis*, which also significantly increased at HSP and KTYA (Figure 5). HSP had 40 genera that were significantly differentially abundant while KTYA had 35. More than half of the genera which had increased after infiltration were from the phylum *Proteobacteria* at both sites. Eight genera had similar changes at both HSP and

KTYA. *Nitrosomonas* and *Ensifer* had two of the largest increases at both HSP and KTYA and *Steroidobacter* and *Blastococcus* had similar decreases after infiltration. *Caenimonas* decreased more than 60-fold at HSP but increased more than 10-fold at KTYA. *Xylophilus* had a similar trend.

Impact of a Permeable Reactive Barrier on Microbial Communities

In this section, we focus on differences in microbial communities associated with the use or absence of a carbon-rich PRB. We expected that there would be differences in nitrogen cycling associated with the addition of a carbon-rich PRB (Figure 1), and this would also be expressed in the makeup of associated microbial communities. Post-infiltration samples were filtered to remove scarce ASVs, and ANCOM-BC analysis was performed to show which genera were significantly abundant across the experimental conditions. Genera that differed in abundance after infiltration with the woodchip PRB treatment compared to the after-infiltration samples through just native soil, but results were not the same for the three sites (Figure 6). KTR only had one genus with a significant ($p<0.05$) difference in abundance, *Polaromonas*, which also increased at HSP (but not at KTYA). Both HSP and KTYA had 41 genera with significant abundance differences, although HSP had 23 genera that had higher differential abundance in the PRB treated plot compared to 10 genera with larger abundance at KTYA. Three of the genera with the largest abundance difference at both HSP and KTYA (*Tropicimonas*, *Novosphingobium*, and *Sphingobium*) all belong to the *Proteobacteria* phylum. Some of the genera which had lower abundance in the PRB-treated plot at both HSP and KTYA are

Nitrosomonas, *Nitrospira*, *Nitrosomonadaceae*, and two archaea genera from the class *Nitrososphaeria*.

We used CCA and water chemistry data to infer which parameters were associated with these shifts in bacterial communities. For this part of the analysis, we focus on KTR and KTYA samples, because HSP lacked sufficient water chemistry data. Due to the increased nitrate removal in the plots with a PRB, we first looked at how the 20 most abundant genera related to redox-sensitive constituents in the infiltrating water (Figure 7). The CCA model was based on NO_3^-, Fe, Mn, and DOC concentrations. Nitrite was not included as its concentration was often below detection and sulfate was not included because it was collinear with nitrate. Overall, the constrained model explains 47.6% of the variance and was significant using PERMANOVA. *Nitrospira*, *Nitrosomondaceae MND1*, and *Candidatus Nitrososphaera* were found in samples that had high nitrate concentrations. *Pyrinomonadaceae RB41* and *Candidatus Nitrososphaera* were more likely to be found in samples with increased dissolved iron. Most *Proteobacteria* (e.g., *Sphingobium*, *Novosphingobium*, and *Pseudomonas*) correlated with lower concentrations of NO_3^-, Fe, Mn, and DOC. These correlations help to explain how individual environmental variables stimulate activity within specific microbial communities.

Metabolism of Microbial Communities

To further understand how the microbial ecology of denitrification was impacted by infiltration and the presence or absence of a carbon-rich PRB, we examined the relative abundance and diversity of the clade I nitrous oxide reductase

gene, *nosZ*. This gene encodes for the enzyme responsible for reducing nitrous oxide to nitrogen gas in the last step of denitrification. Soil samples were available for this analysis from KTR and KTYA, but not HSP. We performed quantitative PCR (qPCR) and analyzed fold-changes using the Pfaffl method (Pfaffl, 2001). The number of *nosZ* genes did not significantly change due to infiltration (Supplementary Information, Figure S-4). The addition of a carbon-rich PRB also did not change the number of *nosZ* genes.

We determined the sequence diversity of the *nosZ* gene as a proxy for which taxonomic group(s) are functionally active within each infiltration system. The partial *nosZ* sequencing reads were classified into 17 genera, all of which belonged to the *Proteobacteria* phylum. Most of the *nosZ* sequences are classified into one clade containing an unclassified *Alphaproteobacteria* (ASV3), an unclassified *Rhodobacteraceae* (ASV10), *Cereibacter* (ASV1), and *Ensifer* (ASV7) (Figure 8). *Cereibacter* was the most abundant, comprising on average 38% of the reads per sample. An unclassified ASV from the order *Hyphomicrobiales* (ASV4) was phyletically separate from the clade with the most abundant genera, but accounts for almost a tenth of the reads per sample. The phylogenetic tree shows that the taxonomy assigned to the ASVs are closely related to the taxonomy of the reference sequences. None of the genera at either site was significantly differentially abundant because of PRB treatment or infiltration (based on ANCOM-BC analysis).

Discussion

Differences in microbial community response in finer and coarser soils

In this study we related microbial communities with soil type and water chemistry. Grain size has been used as a constraint in predicting microbial communities in environments ranging from eutrophic lagoons (Highton *et al.*, 2016) to the Namib Desert (Gombeer *et al.*, 2015). It seems unlikely that microbes are solely impacted by the size of the soil particle. Rather, the nature of physical and geochemical conditions is likely to be impacted by soil texture, which influences the size and shape of pores as well as the surface area of a particular surface for a microbe to attach to (Santmire and Leff, 2015). Soil chemistry, including the presence of reactive surfaces and organic carbon (Horowitz and Elrick, 1987), is also correlated with soil texture (in which grain size distribution is one component). It makes sense that grain size can be used as an easily measured proxy for all the factors listed above.

The two field sites having coarser sediments rich in sand (Figure 2 and Supplemental Figure 2) (HSP and KTYA), had similar pre-infiltration microbial communities (Figure 3). In contrast, KTR samples are finer-grained, with a higher percentage of silt and clay, and had the most distinct initial community. KTR also had a more significant increase in the fraction of dissolved nitrogen removed (Figure 1) in woodchip-amended plots than did HSP or KTYA, and consequently lower N loads (g-N/m^2-day) (Pensky *et al.*, 2022). These observations thus connect soil texture, infiltration rate, nutrient cycling, and microbial ecology. The addition of initial microbial communities into the CCA model improved the statistical separation of samples by location. Even though the three sites were located less than 15 km from

one another, their soils are considerably different (particularly KTR compared to the other two) and they have distinct initial microbial communities.

Samples from HSP and KTYA both showed a decrease in Shannon-Weaver Index after infiltration (Figure 4b). An infrequent large disturbance, like the saturation of soil, promotes metabolically versatile populations and is likely to reduce diversity (Connell, 1978). Previous studies have also shown a loss of diversity due to MAR-induced infiltration (Barba, Folch, Sanchez-Vila, *et al.*, 2019; Fillinger *et al.*, 2021). In both HSP and KTYA, there is an increase in the differential abundance of *Proteobacteria* due to infiltration (Figure 4a), which is like the results found in the samples from the Llobregat MAR basin (Barba, et al., 2019). This likely means that during infiltration, *Proteobacteria* are less perturbed by the disturbance of water and can gain dominance.

In contrast, diversity indices at KTR differed little between pre-and post-infiltration (Figure 4b). This suggests that, although infiltration through a carbon-rich PRB during the KTR experiments did result in stimulation of microbially mediated nitrogen cycling (Gorski et al., 2019), it did so without a major shift in microbial ecology. It appears that pre-infiltration communities were poised to increase rates of nitrogen cycling when conditions became more favorable. A single genus showed an increase following infiltration during the KTR experiments *Candidatus Nitrosotenuis* (phylum *Crenarchaeota*) (Figure 5) and *Polaromonas* (phylum *Proteobacteria*) in soils below a carbon-rich PRB (Figure 6). The relative abundances of *Crenarchaeota* and *Proteobacteria* were little changed due to infiltration or the addition of a PRB

(Figure 4a). Understanding the nature of conditions that are beneficial to specific genera, or phyla, will require careful examination of environmental conditions that stimulate metabolism. For example, *Proteobacteria* preferentially colonize and form biofilms on larger grains (Santmire and Leff, 2015), so the dearth of particles larger than silt in KTR, compared to those seen at HSP and KTYA, may have limited opportunities for *Proteobacteria* to realize a trophic benefit to establish dominance during infiltration. Future work focused on soil composition, texture, and bioreactivity should elucidate microbial ecology during infiltration, with and without the addition of bioavailable carbon.

Infiltration impacted the relative abundance of specific microbial taxa at the sandy sites (Figure 5). We consider infiltration a large disturbance; with soil going from partially dry conditions to fully saturated within a day and concomitant changes in redox conditions. Infiltrating water delivers metabolites for microbes to consume (Ginige *et al.*, 2013). A previous study (Lennon *et al.*, 2012) found most Gram-negative bacteria preferred soil with higher moisture content and *Proteobacteria* preferred the wettest conditions out of all the phyla tested. This result is consistent with the findings at HSP and KTYA; more than half of the differentially more abundant taxa after infiltration were from the phylum *Proteobacteria*. Finer soils tend to have greater soil moisture retention and lower infiltration capacity (Childs, 1940); this may help to explain why the infiltration through the silt- and clay-rich KTR soils had less influence on microbial community composition. The only common taxa at all three sites to be impacted by infiltration was an increase in *Candidatus Nitrosotenuis*

(phylum *Crenarchaeota*). This phylum is known to oxidize ammonia and fix carbon and is found in many soil and marine settings (Hu *et al.*, 2011; Sun *et al.*, 2021). Many of the taxa which decreased at HSP and KTYA following infiltration were from the *Firmicutes* or *Actinobacteria* phylum. These Gram-negative taxa preferred dry soil conditions (Lennon et al., 2012). *Caenimonas* and *Xylophilus* are both from the family *Comamonadaceae* and showed an increase after infiltration at KTYA but a decrease at HSP. Taxa from this family have been used as complex-carbon degraders and denitrifiers in wastewater sludge (Khan *et al.*, 2002). It is possible that somewhat higher carbon contents in KTYA soils promoted *Comamonadaceae* growth, but both soils are relatively carbon poor. Additional factors resulting in different rates of nitrogen cycling at HSP and KTYA could include small differences in soil texture and composition and resulting infiltration rates (Pensky *et al.*, 2022).

Importance of dissolved organic carbon during infiltration

Earlier studies have shown that a carbon-rich PRB releases DOC (Qian *et al.*, 2011; Grau-Martínez *et al.*, 2017; Gorski *et al.*, 2019). The microbial nitrogen cycle is highly influenced by the C:N ratio; a large change in the ratio can favor microbes with different metabolisms (Kraft *et al.*, 2011). Furthermore, isotope analysis at KTR indicated nitrate removal under a PRB was primarily driven by microbes (Gorski *et al.*, 2019). Therefore, we expected that changes due to carbon influx by a PRB during infiltration could alter microbial community composition and ecophysiology. Interestingly, there were no common taxa among the three sites that significantly changed in abundance in response to treatment (e.g., PRB vs. no PRB). Instead at the

two sites with coarser soils (HSP and KTYA), we identified three differentially abundant genera (*Sphingobium*, *Novosphingobium*, and *Tropicimonas*) below PRB-treated plots. These genera are all known to be aerobic complex carbon degraders (White *et al.*, 1996; Harwati *et al.*, 2009; Wang *et al.*, 2018). One explanation for this is that the organic carbon leached from the woodchip PRB was degraded by these genera, where and when there was sufficient oxygen available, producing breakdown products that were subsequently used to fuel denitrification (Figure 6). These three genera also correspond to low nitrate and DOC concentrations in the CCA plot (Figure 7), which supports this hypothesis.

Another explanation could be that rapid infiltration at the sandier sites allowed for higher levels of oxygenation in the subsurface to drive complex carbon degradation that was not seen in the silty clay at KTR. The introduction of a PRB layer did not change the infiltration rate of the subsurface soil during any of these experiments, as PRB materials are much coarser and have larger pores (e.g., Beganskas *et al.*, 2018; Pensky *et al.*, 2022). As applied in this study, infiltration rates are intrinsic to the nature of ambient soil properties, but managed recharge systems could be engineered to target specific infiltration rates. Genera capable of aerobic ammonia oxidation (*Nitrospira, Nitrosomonas*, and strains from the *Nitrosomonadaceae* genus) (He *et al.*, 2018) exhibited the largest decrease in relative abundance below PRB-treated plots. During infiltration, these genera may have added nitrate to the system through ammonium and nitrite oxidation pathways but were less dominant in the environment under the PRB. We observed a close relationship

between aerobic ammonia-oxidizing genera and high nitrate concentration (Figure 7), further supporting their potential function towards nitrification. While anaerobic ammonia oxidizers (Anammox) from the phylum *Planctomycetes* existed in the plots, only *Pirellula* had a significant decrease between PRB treated and native soil plots. This decrease was only seen at KTYA where interestingly ammonium input was insignificant and the taxa represented less than 0.01% of the total reads (Pensky *et al.*, 2022). There were 19 taxa that had common differential abundance between PRB-treated and native soil plots at HSP and KTYA, which indicates that soil grain size also influences microbial community when other environmental factors, such as input DOC, are adjusted.

At all three sites, there was an increase in DOC down to the lowest depths sampled below the plots amended with a woodchip PRB (Beganskas *et al*., 2018, Gorski *et al.*, 2019, Pensky et al., 2022). Deeper levels were instrumented during these experiments, but piezometers cannot recover pore fluids when conditions are unsaturated, and reducing conditions are expected to be maintained mainly above the wetting front that forms below the infiltration plots (Gorski, *et al*., 2019). We expect that some of the elevated DOC was oxidized by the soil microbes. One study of four soil ecosystems found that two genera were responsible for nearly half of the carbon flow by respiration even though they comprised less than 20% of total sequencing reads (Stone *et al.*, 2021). Both genera identified in that study, *Bradyrhizobium* and *RB-41* (member of the *Pyrinomonadaceae* family), were highly abundant in the soil samples. However, *Bradyrhizobium* corresponded with lower DOC levels whereas

RB-41 was more associated with higher levels of DOC (Figure 7). *RB-41* is also known for its ability to hydrolyze polymers (Pascual *et al.*, 2018) and therefore could contribute to increasing DOC concentrations as a consequence of its metabolic activities.

While carbon can drive denitrification, DOC input may also influence metal cycling during infiltration. *Flavobacterium*, which oxides aqueous manganese(II) to manganese oxide precipitates (Akob *et al.*, 2014), corresponds to low Mn concentrations in the input water (Figure 7). Further investigation into the microbial Fe/Mn cycle could reveal important trends in how DOC could impact metal release during infiltration for MAR. In soil, there are numerous complex metabolisms interacting with one another. To better understand how the microbes are utilizing the carbon leached by the PRB material, techniques such as quantitative stable isotope probing would give an indication of what populations are increasing productivity with the addition of a PRB. Additionally, characterizing the carbon leached off the PRB could further aid in predicting the trajectory of a microbial community towards a certain eco-physiological outcome such as denitrification, nitrification, and/or metal release.

The potential role of the nitrous oxide reductase (*nosZ*) gene

In this study, we investigated clade I nitrous oxide reductase (*nosZ*) gene relative abundance and diversity to gain insights into changes in nitrogen cycling during infiltration. A study of denitrifying genes in agricultural soils found *nosZ* was stable in abundance and community makeup after irrigation with different water

sources while other nitrogen cycling genes had changes in response to input water (Zhou *et al.*, 2011). In the present study, only soils from KTR and KTYA were available for analysis of *nosZ*. Relative abundances and diversity of clade I *nosZ* were similar in both native soil plots and PRB plots, regardless of field site, treatment, or infiltration (Figure 8 and Supplementary Information, Figure S-4). The genera identified by the *nosZ* sequences were not among those taxa displaying significantly abundant 16S rRNA-gene classifications (Figure 5 and 6). The taxa associations of the *nosZ* sequences made up less than 1% of the total 16S rRNA sequencing reads. However, all the *nosZ* sequences belong to *Alpha-*, *Beta-*, and *Gammaproteobacteria*, which make up around half of the 16S rRNA reads. Previous studies also found that *nosZ* reads from sediments and soil are around 5% of the 16S reads (Mounler *et al.*, 2004; Zhou *et al.*, 2011; Bellini *et al.*, 2013). The primers we used are selective for clade I *nosZ* genes which are usually made up of *Alpha-*, *Beta-*, *and Gammaproteobacteria*. We only looked at clade I due to the high levels of 16S reads from those classes as well as clade I *nosZ* being >1000 times more abundant than clade II *nosZ* in coastal sediments and nitrate-rich bioreactors (Hallin *et al.*, 2018). However, we may have underestimated *nosZ* abundance and diversity by not including clade II *nosZ*. A metagenomic analysis will give a more comprehensive understanding of how microbial metabolism was affected by infiltration.

The use of meta-analysis to compare results from disparate infiltration sites

In this study, we used a meta-analysis approach to determine how microbial communities respond to infiltration and PRBs at geographically separated MAR

systems. Our initial expectation was that infiltration would result in common shifts among taxa, with particular increases in relative abundance towards specific taxa associated with carbon degradation. Instead, we saw major shifts mainly in the coarser soils, indicating that the nature of these soils (texture, pore size, and shape, carbon content, etc.) is the most important predictor for soil microbial communities during shallow infiltration. A single metric like median grain size could potentially serve as a useful proxy for more extensive differences in soil conditions, but it is important to take a process-based view of related sites. At the KTR field site where silt and clay-sized particles are more abundant, the microbial population showed the least perturbations as a result of either infiltration or the introduction of a carbon-rich PRB. In contrast, infiltration promoted the dominance of *Proteobacteria* in the sites with coarser soil (Lennon *et al.*, 2012; Tahon *et al.*, 2018). The addition of carbon-rich PRB reduced populations capable of nitrification and promoted populations known for complex carbon degradation in sandy soils, even though the field site with smaller grain size (KTR) had more complete denitrification compared to HSP and KTYA (Figure 1). Hence, our initial hypothesis was partially supported in this analysis: the addition of a carbon-rich PRB during shallow infiltration correlates with shifting taxa towards carbon degraders and nitrogen cyclers in sandy soils. We also analyzed *nosZ* sequences to address shifts in nitrate-reducing taxa. Although more nitrate was removed during infiltration in soils below a PRB, the quantity of the clade I nitrous oxide reductase gene did not change due to infiltration or the addition of a

PRB in either of the soil types tested. This suggests that other genes and pathways may play an important role in enhancing denitrification during infiltration for MAR.

While this meta-analysis has limitations due to constraints on available data sets from past field site studies, this study provides a useful framework for connecting the physical-chemical properties with site-specific metrics of microbial community diversity. This integrative analysis yielded insightful observations about the potential importance of soil properties and identified key genera that may help improve water quality as part of groundwater resource management and justifies more extensive and structured field and laboratory experiments, with a greater emphasis on experimental control, to resolve fundamental control on key processes. It is clear that a holistic assessment of physical-chemical and microbial data is needed to develop a predictive understanding of carbon and nutrient processing during infiltration for MAR, across a range of conditions.

Tables

Table 1: List of primers and PCR cycles used

Name	Sequence	Use	PCR cycle
515F-Y-MS	TCG TCG GCA GCG TCA GAT GTG TAT AAG AGA CAG GTG YCA GCM GCC GCG GTA A	16S rRNA sequences	95°C for 3 min, 25 cycles of: 95°C for 45 sec, 50°C for 45 sec, 68°C for 90 sec. Final extension 68°C for 5 min
926R-MS	GTC TCG TGG GCT CGG AGA TGT GTA TAA GAG ACA GCC GYC AAT TYM TTT RAG TTT		
nosZ2-F	CGC RAC GGC AAS AAG GTS MSS GT	*nosZ* sequences and qPCR	95°C for 5 min, 6 cycles of: 95°C for 15 sec, 65°C (-1°C /cycle) for 30 sec, 72°C for 30 sec. 40 cycles of: 95°C for 15 sec, 60°C for 15 sec, 72°C for 30 sec.
nosZ2-R	CAK RTG CAK SGC RTG GCA GAA		
515F-Y	GTG YCA GCM GCC GCG GTA A	16S qPCR	95°C for 3 min, 35 cycles of: 95°C for 45 sec, 55°C for 45 sec, 68°C for 45 sec
926R	CCG YCA AAT YMT TTR AGT TT		

Figures

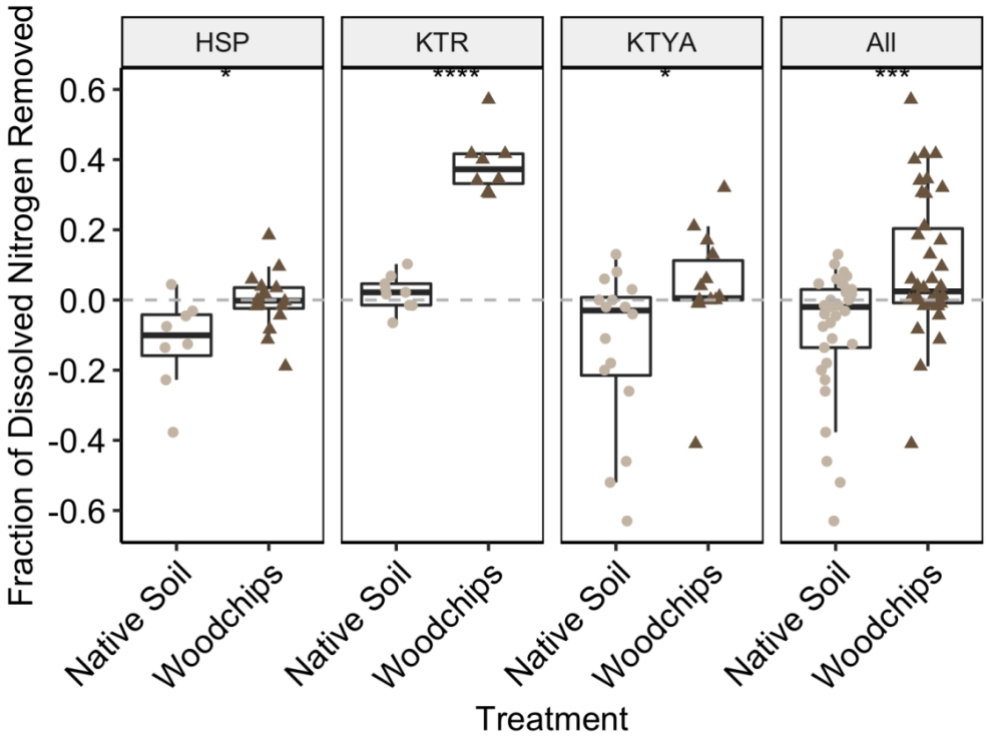

Figure 1: Fraction of dissolved nitrogen species (NO_3^-, NO_2^-, and NH_4^+) removed between input water and the deepest piezometer in the native soil (beige) and woodchip-amended plots (brown) at the three field sites (HSP= Harkins Slough, KTR= Kelly Thompson Ranch, KTYA= Kitayama Ranch). A positive fraction indicates that N was removed from the system while a negative fraction indicates addition of dissolved N species. The median is the bold line in the middle of the box, the upper and lower edges of the box represent the 25th and 75th percentiles. The whiskers extend to give the 90th percentile. Each point represents a chemical data from an infiltration day during the experiment. *=$p<0.01$ ***=$p<0.0001$, ****= $p<0.00001$.

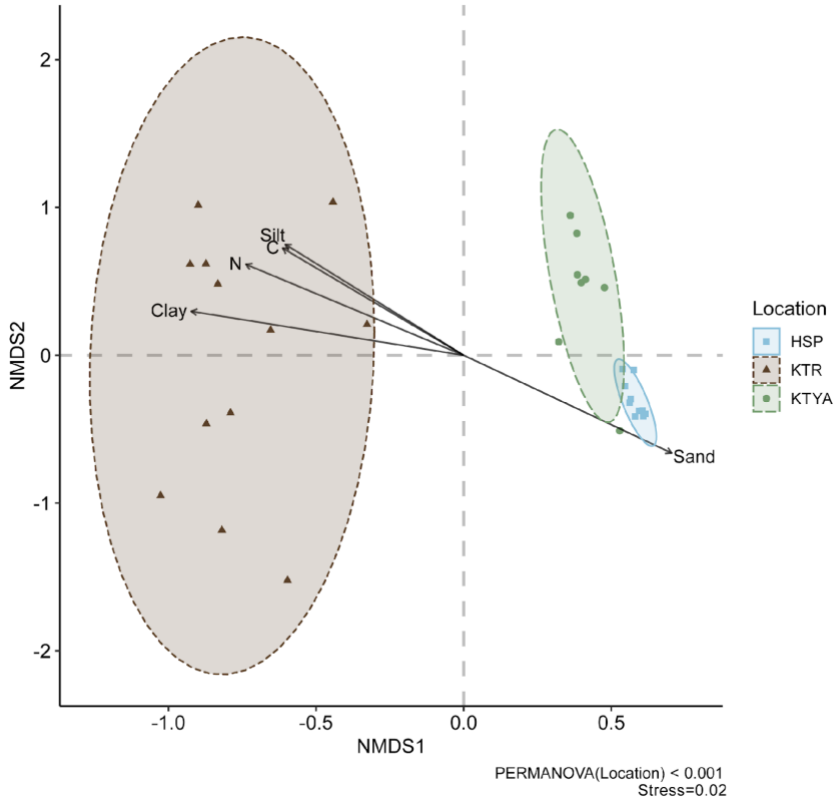

Figure 2: Non-metric multidimensional scales (NMDS) of the before infiltration samples (n=30, replicates were not included) from the different plots with Total Carbon, Total Nitrogen, and percent sand, silt, and clay as inputs. Samples from Harkins Slough (HSP) are blue squares (■), Kelly Thompson Ranch (KTR) are brown triangles (△), and Kitayama Ranch (KTYA) are green circles (●). The ellipses show the locations with a multivariate t-distribution of 95%.

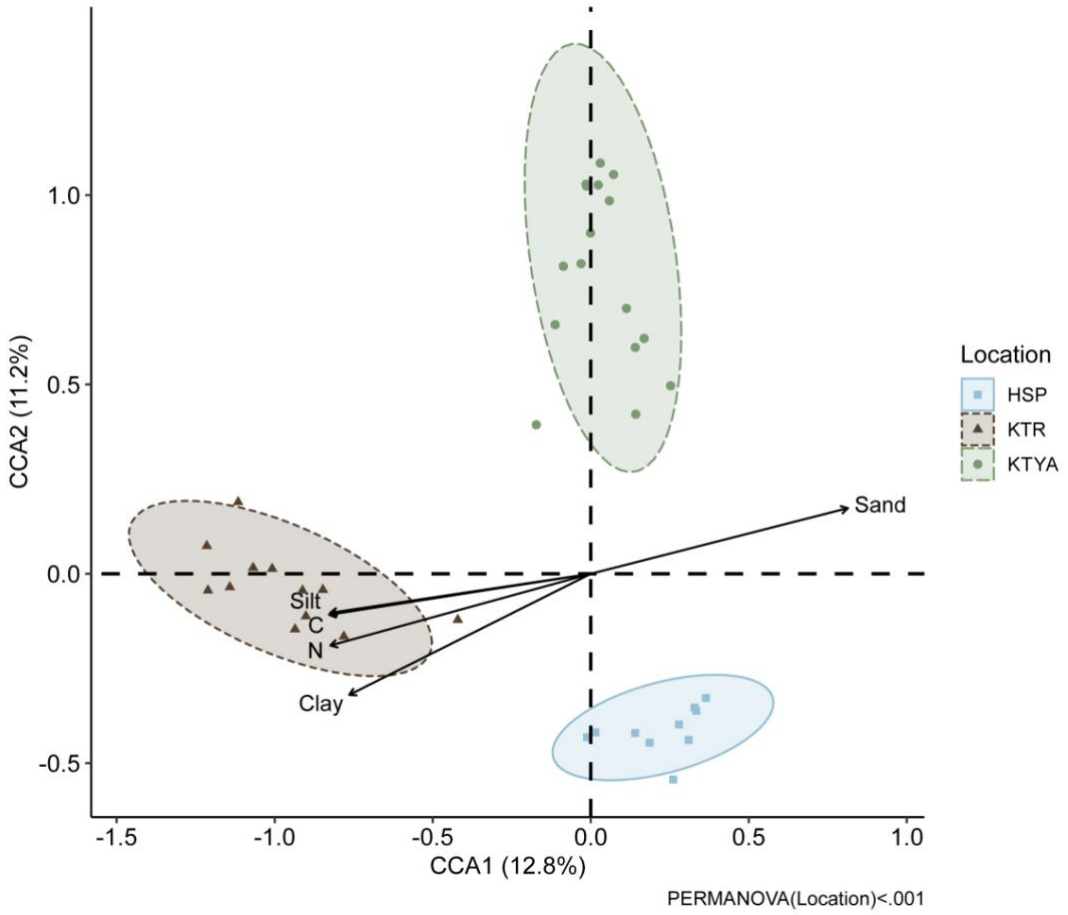

Figure 3: First two constrained axes (12.8% and 11.2% of variance respectively) of the Constrained Correspondence Analysis (CCA) of each initial sample's microbial community (n=38). The constraints were Total Carbon, Total Nitrogen, and percent sand, silt, and clay. Samples from Harkins Slough (HSP) are blue squares (■), Kelly Thompson Ranch (KTR) are brown triangles (△), and Kitayama Ranch (KTYA) are green circles (●). The ellipses show the locations with a multivariate t-distribution of 95%.

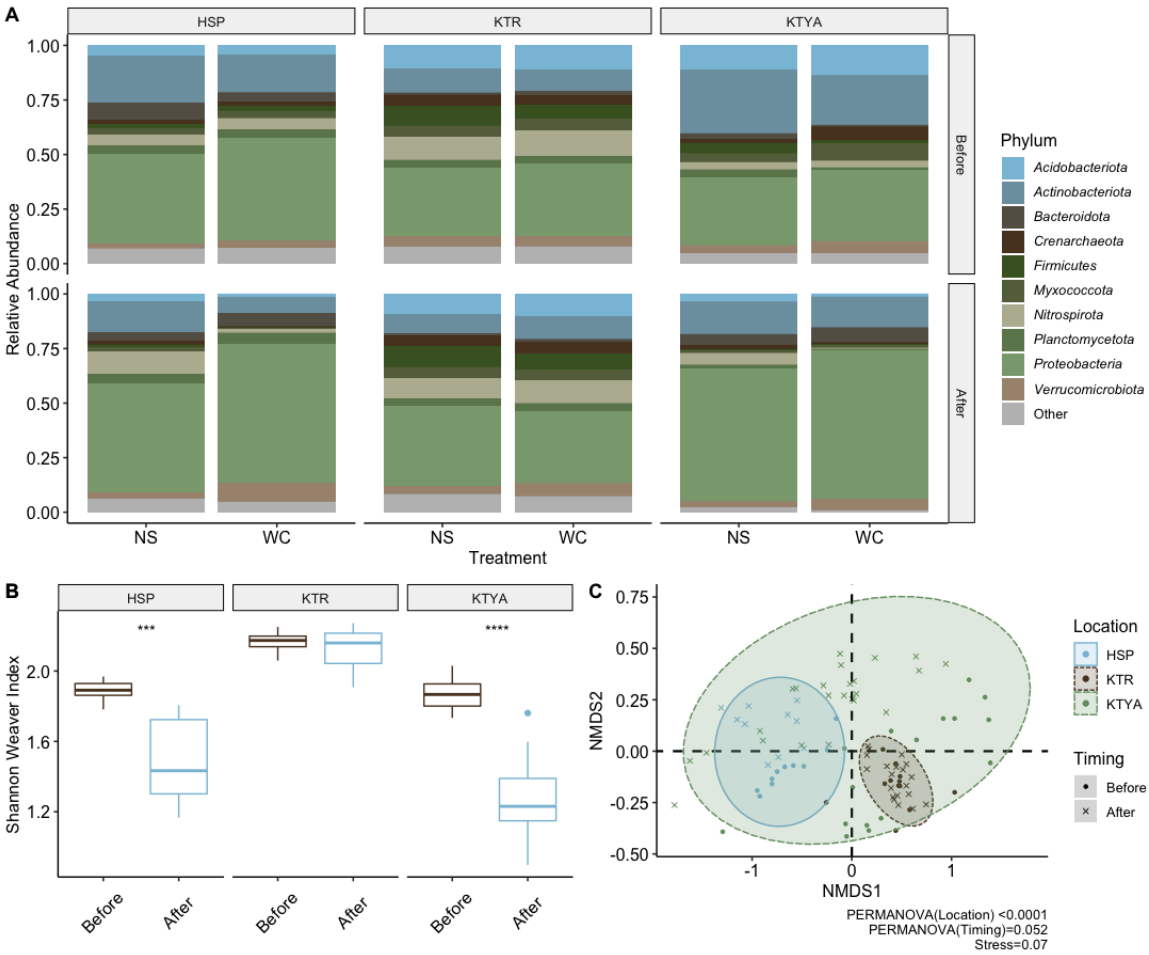

Figure 4: (a) Relative abundances of the top 10 phyla in soil samples (n=92) pooled by infiltration timing and treatment from Harkins Slough (HSP), Kelly Thompson Ranch (KTR), and Kitayama Ranch (KTYA). The top row shows before infiltration and the bottom shows after infiltration. Samples are split by treatment type: either native soil (NS) or a wood chip PRB (WC). (b) Shannon- Weaver diversity index for the samples at all three sites before and after infiltration. The median is the bold line in the middle of the box, the upper and lower edges of the box represent the 25th and 75th percentiles. The whiskers extend to give the 90th percentile. Data that extends outside the whiskers are represented as points. ***=p<0.0001, ****= p<0.00001. (c) Non-metric dimensional scaling (NMDS) of the microbial communities (Stress score=0.07). Each ● represents samples before infiltration (n=38) and each × (n=54) represents samples after infiltration. Colored ellipses show each location with a multivariate t-distribution of 95%.

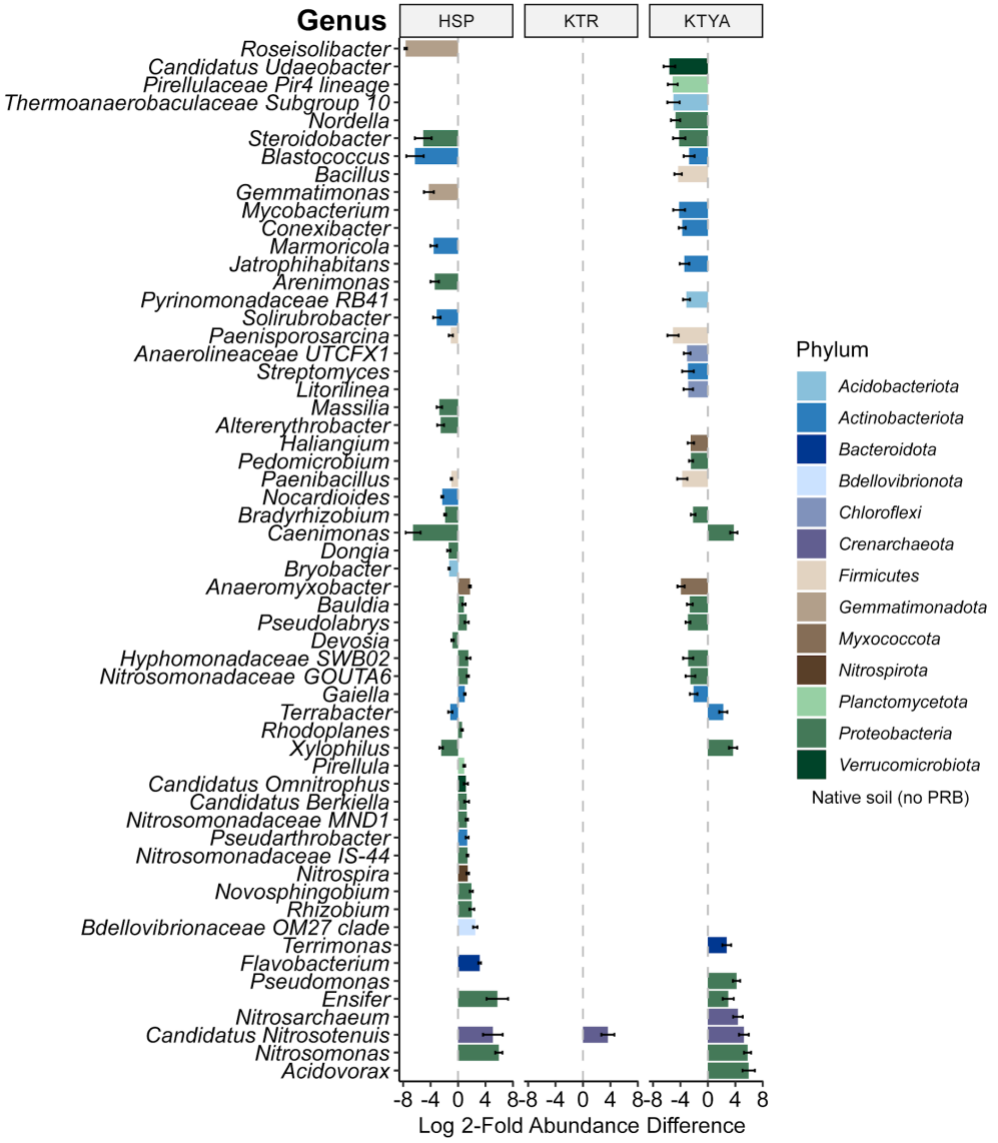

Figure 5: Significant ($p<0.05$) genera which had changes in differential abundance between before (n=17) and after (n=25) infiltration samples in native soil samples from Harkins Slough (HSP), Kelly Thompson Ranch (KTR), and Kitayama Ranch (KTYA). Analysis of Composition of Microbiomes with Bias Correction (ANCOM-BC) was used to calculate log 2-fold changes. A positive fold change indicates that abundance was high in post-infiltration samples. Error bars show standard errors. Color indicates the assigned Phylum of the sequence.

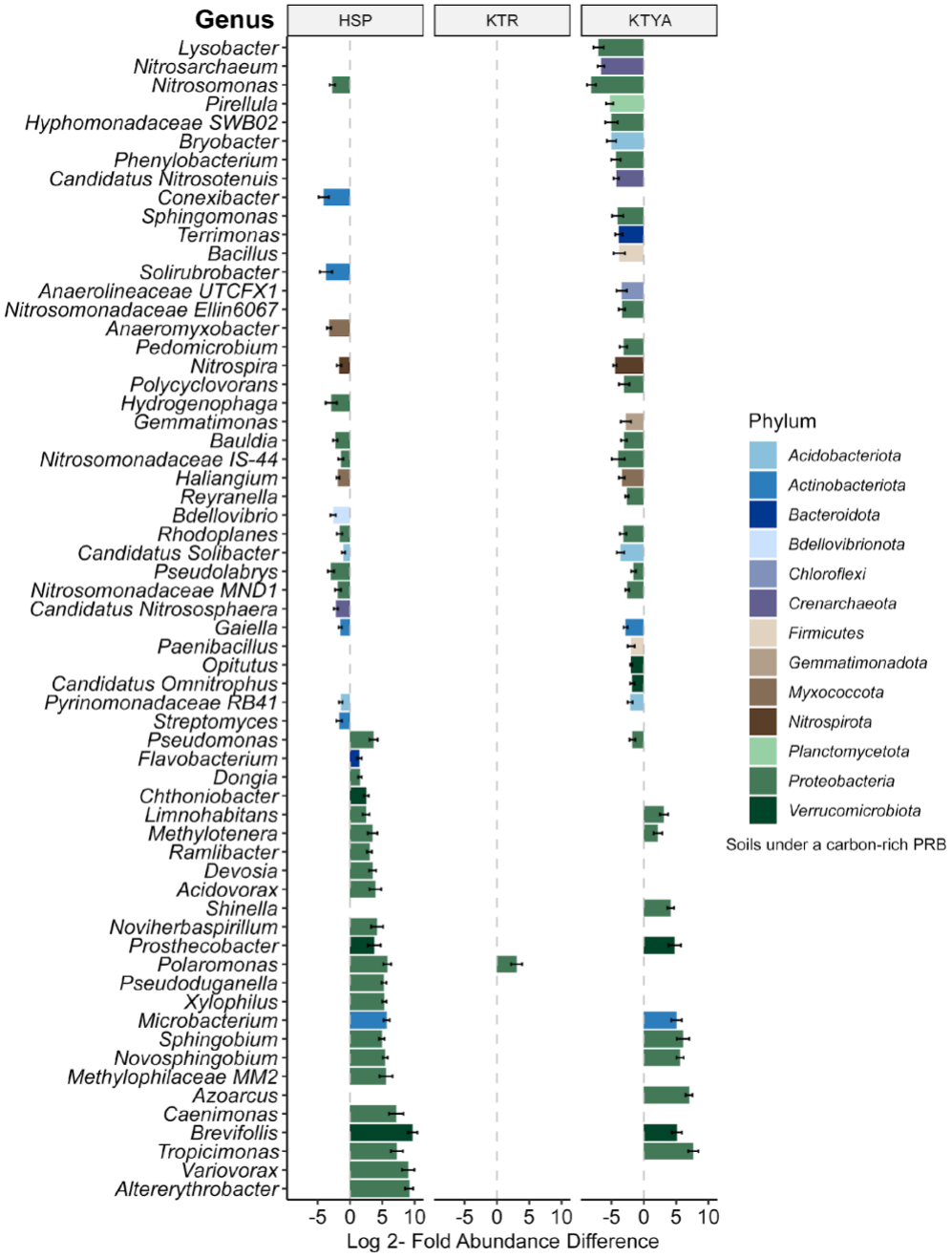

Figure 6: Significant ($p<0.05$) genera from Harkins Slough (HSP), Kelly Thompson Ranch (KTR), and Kitayama Ranch (KTYA) which had differential abundance between samples treated with a wood chip PRB (n=29) compared to samples with no treatment (n=25). Analysis of Composition of Microbiomes with Bias Correction (ANCOM-BC) was used to calculate log 2-fold changes. A positive fold change indicates that abundance was higher in treated samples. Error bars show standard errors. Color indicates the assigned Phylum of the sequence.

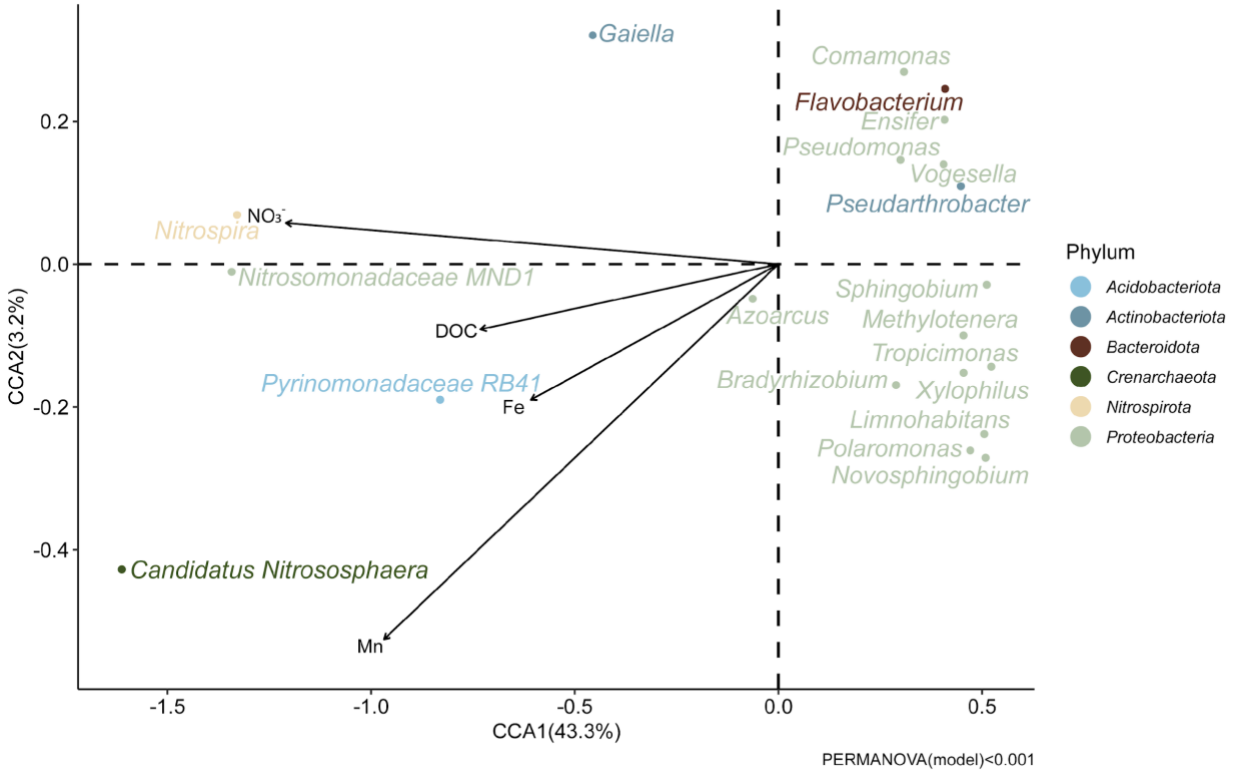

Figure 7: Constrained Correspondence Analysis (CCA) using NO_3^-. Mn, Fe, and DOC concentrations from the infiltrating water as constraints to explain the variance among the top 20 genera from the analyzed samples. Axis 1 explains 43.3% of the variance among species while axis 2 explains 3.2%. After infiltration samples (n=32) with profession water quality panel data were used for analysis.

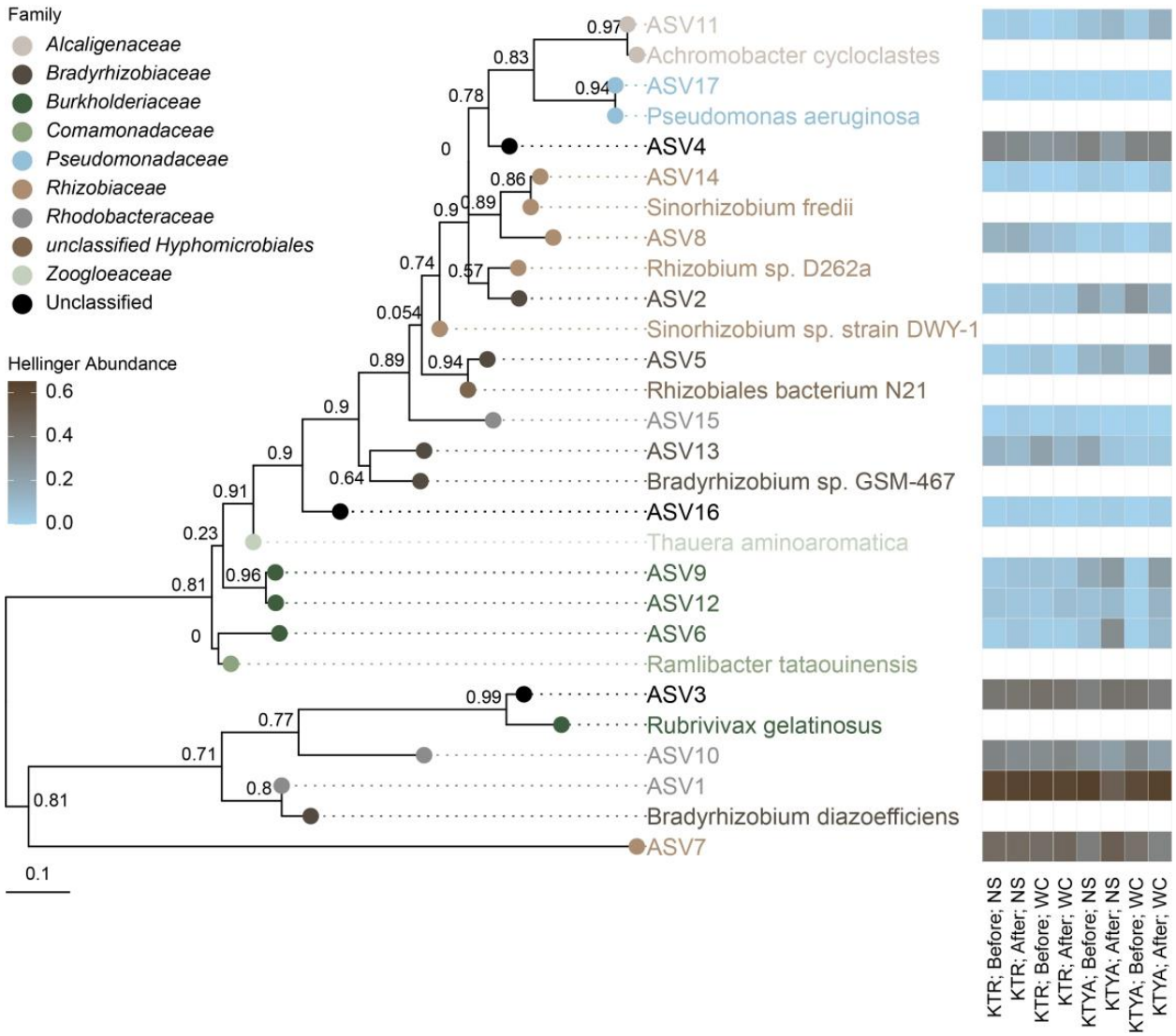

Figure 8: Phylogenetic tree of sequenced clade I *nosZ* reads with reference *nosZ* sequences and their relative abundance. Samples are from 30cm below the plot surface at either Kelly Thompson Ranch (KTR) or Kitayama Ranch (KTYA) before or after infiltration in native soil (NS) or wood chip (WC) amended plots. The tip points indicate the Family assigned to the sequences.

Funding and Acknowledgements

This work was supported by the Gordon and Betty Moore Foundation (grants #5595 and #9964), the USDA/NIFA (award #2021-67019-33595), the USDA/NRCS Resource Conservation Partnership Program (award #1726), and the Recharge Initiative (http://www.rechargeinitiative.org/). The authors declare that they have no conflicting interests.

We gratefully acknowledge the laboratory and field assistance of Kaitlyn Redford, Hannah Dailey, Tess Weathers, Araceli Serrano, Paige Borges, Sarah Faraola, and Sanjin Mehić. We thank the Pajaro Valley Water Management Agency and stakeholders at the managed aquifer recharge field sites for their collaboration and trust, including permission to access sites and facilities.

References

Aeschbach-Hertig, W. and Gleeson, T. (2012) Regional strategies for the accelerating global problem of groundwater depletion. Nature Geoscience 2012 5:12 5: 853–861.

Akob, D.M., Bohu, T., Beyer, A., Schäffner, F., Händel, M., Johnson, C.A., et al. (2014) Identification of Mn (II)-oxidizing bacteria from a Low-pH contaminated former uranium mine. Applied and Environmental Microbiology 80: 5086–5097.

Barba, C., Folch, A., Gaju, N., Sanchez-Vila, X., Carrasquilla, M., Grau-Martínez, A., and Martínez-Alonso, M. (2019) Microbial community changes induced

by Managed Aquifer Recharge activities: linking hydrogeological and biological processes. Hydrology and Earth System Sciences 23: 139–154.

Barba, C., Folch, A., Sanchez-Vila, X., Martínez-Alonso, M., and Gaju, N. (2019) Are dominant microbial sub-surface communities affected by water quality and soil characteristics? Journal of Environmental Management 237: 332–343.

Bayarsaikhan, U., Filter, J., Gernert, U., Jekel, M., and Ruhl, A.S. (2018) Fate of leaf litter deposits and impacts on oxygen availability in bank filtration column studies. Environmental Research 164: 495–500.

Beganskas, S., Gorski, G., Weathers, T., Fisher, A.T., Schmidt, C., Saltikov, C., et al. (2018) A horizontal permeable reactive barrier stimulates nitrate removal and shifts microbial ecology during rapid infiltration for managed recharge. Water Research 144: 274–284.

Bellini, M.I., Gutiérrez, L., Tarlera, S., and Scavino, A.F. (2013) Isolation and functional analysis of denitrifiers in an aquifer with high potential for denitrification. Systematic and Applied Microbiology 36: 505–516.

California Department of Water Resources (2018) California Water Plan Update 2018.

Callahan, B.J., McMurdie, P.J., Rosen, M.J., Han, A.W., Johnson, A.J.A., and Holmes, S.P. (2016) DADA2: High-resolution sample inference from Illumina amplicon data. Nature Methods 2016 13:7 13: 581–583.

Casanova, J., Devau, N., and Pettenati, M. (2016) Managed Aquifer Recharge: An Overview of Issues and Options. In Integrated Groundwater Management. Cham: Springer International Publishing, pp. 413–434.

Childs, E.C. (1940) THE USE OF SOIL MOISTURE CHARACTERISTICS IN SOIL STUDIES. Soil Science 50: 239–252.

Chu, L. and Wang, J. (2013) Denitrification performance and biofilm characteristics using biodegradable polymers PCL as carriers and carbon source. Chemosphere 91: 1310–1316.

Connell, J.H. (1978) Diversity in tropical rain forests and coral reefs. Science (1979) 199: 1302–1310.

Dereeper, A., Guignon, V., Blanc, G., Audic, S., Buffet, S., Chevenet, F., et al. (2008) Phylogeny.fr: robust phylogenetic analysis for the non-specialist. Nucleic Acids Res 36.

Dillon, P., Pavelic, P., Page, D., Beringen, H., and Ward, J. (2009) Managed aquifer recharge: An Introduction.

Fakhreddine, S., Dittmar, J., Phipps, D., Dadakis, J., and Fendorf, S. (2015) Geochemical Triggers of Arsenic Mobilization during Managed Aquifer Recharge. Environmental Science & Technology 49: 7802–7809.

Fillinger, L., Hug, K., and Griebler, C. (2021) Aquifer recharge viewed through the lens of microbial community ecology: Initial disturbance response, and impacts of species sorting versus mass effects on microbial community

assembly in groundwater during riverbank filtration. Water Research 189: 116631.

Fish, J.A., Chai, B., Wang, Q., Sun, Y., Brown, C.T., Tiedje, J.M., and Cole, J.R. (2013) FunGene: the functional gene pipeline and repository. Frontiers in Microbiology 0: 291.

Fournier, E., Keller, A., Geyer, R., and Frew, J. (2016) Investigating the Energy-Water Usage Efficiency of the Reuse of Treated Municipal Wastewater for Artificial Groundwater Recharge. Environ Sci Technol 50: 2044–2053.

Ginige, M.P., Kaksonen, A.H., Morris, C., Shackelton, M., and Patterson, B.M. (2013) Bacterial community and groundwater quality changes in an anaerobic aquifer during groundwater recharge with aerobic recycled water. FEMS Microbiology Ecology 85: 553–567.

Gombeer, S., Ramond, J.-B., Eckardt, F.D., Seely, M., and Cowan, D.A. (2015) The influence of surface soil physicochemistry on the edaphic bacterial communities in contrasting terrain types of the Central Namib Desert. Geobiology 13: 494–505.

Gorski, G., Fisher, A.T., Beganskas, S., Weir, W.B., Redford, K., Schmidt, C., and Saltikov, C. (2019) Field and Laboratory Studies Linking Hydrologic, Geochemical, and Microbiological Processes and Enhanced Denitrification during Infiltration for Managed Recharge. Environmental Science & Technology 53: 9491–9501.

Grau-Martínez, A., Folch, A., Torrentó, C., Valhondo, C., Barba, C., Domènech, C., et al. (2018) Monitoring induced denitrification during managed aquifer recharge in an infiltration pond. Journal of Hydrology 561: 123–135.

Grau-Martínez, A., Torrentó, C., Carrey, R., Rodríguez-Escales, P., Domènech, C., Ghiglieri, G., et al. (2017) Feasibility of two low-cost organic substrates for inducing denitrification in artificial recharge ponds: Batch and flow-through experiments. Journal of Contaminant Hydrology 198: 48–58.

Gurdak, J.J. and Qi, S.L. (2012) Vulnerability of Recently Recharged Groundwater in Principle Aquifers of the United States to Nitrate Contamination. Environmental Science and Technology 46: 6004–6012.

Hallin, S., Philippot, L., Löffler, F.E., Sanford, R.A., and Jones, C.M. (2018) Genomics and Ecology of Novel N2O-Reducing Microorganisms. Trends in Microbiology 26: 43–55.

Hartog, N. and Stuyfzand, P.J. (2017) Water Quality Considerations on the Rise as the Use of Managed Aquifer Recharge Systems Widens. Water 2017, Vol 9, Page 808 9: 808.

Harwati, T.U., Kasai, Y., Kodama, Y., Susilaningsih, D., and Watanabe, K. (2009) Tropicimonas isoalkanivorans gen. nov., sp. nov., a branched-alkane-degrading bacterium isolated from Semarang Port in Indonesia. International Journal of Systematic and Evolutionary Microbiology 59: 388–391.

He, H., Zhen, Y., Mi, T., Fu, L., and Yu, Z. (2018) Ammonia-Oxidizing Archaea and Bacteria Differentially Contribute to Ammonia Oxidation in Sediments from Adjacent Waters of Rushan Bay, China. Frontiers in Microbiology 0: 116.

Henry, S., Bru, D., Stres, B., Hallet, S., and Philippot, L. (2006) Quantitative detection of the nosZ gene, encoding nitrous oxide reductase, and comparison of the abundances of 16S rRNA, narG, nirK, and nosZ genes in soils. Appl Environ Microbiol 72: 5181–5189.

Highton, M.P., Roosa, S., Crawshaw, J., Schallenberg, M., and Morales, S.E. (2016) Physical Factors Correlate to Microbial Community Structure and Nitrogen Cycling Gene Abundance in a Nitrate Fed Eutrophic Lagoon. Frontiers in Microbiology 0: 1691.

Horowitz, A.J. and Elrick, K.A. (1987) The relation of stream sediment surface area, grain size and composition to trace element chemistry. Applied Geochemistry 2: 437–451.

Hu, A., Jiao, N., and Zhang, C.L. (2011) Community Structure and Function of Planktonic Crenarchaeota: Changes with Depth in the South China Sea. Microbial Ecology 2011 62:3 62: 549–563.

Huber, K.J. and Overmann, J. (2019) Vicinamibacter. Bergey's Manual of Systematics of Archaea and Bacteria 1–5.

Illumina 16S Metagenomic Sequencing Library Preparation.

Kassambara, A. (2020) ggpubr: "ggplot2" Based Publication Ready Plots.

Khan, S.T., Horiba, Y., Yamamoto, M., and Hiraishi, A. (2002) Members of the Family Comamonadaceae as Primary Poly(3-Hydroxybutyrate-co-3-Hydroxyvalerate)-Degrading Denitrifiers in Activated Sludge as Revealed by a Polyphasic Approach. Applied and Environmental Microbiology 68: 3206.

Kraft, B., Strous, M., and Tegetmeyer, H.E. (2011) Microbial nitrate respiration – Genes, enzymes and environmental distribution. Journal of Biotechnology 155: 104–117.

Lennon, J.T., Aanderud, Z.T., Lehmkuhl, B.K., and Schoolmaster, D.R. (2012) Mapping the niche space of soil microorganisms using taxonomy and traits. Ecology 93: 1867–1879.

Li, D., Sharp, J.O., Saikaly, P.E., Ali, S., Alidina, M., Alarawi, M.S., et al. (2012) Dissolved organic carbon influences microbial community composition and diversity in managed aquifer recharge systems. Applied and Environmental Microbiology 78: 6819–6828.

Lin, H. and Peddada, S. das (2020) Analysis of compositions of microbiomes with bias correction. Nature Communications 2020 11:1 11: 1–11.

Lu, H., Chandran, K., and Stensel, D. (2014) Microbial ecology of denitrification in biological wastewater treatment. Water Research 64: 237–254.

Mariotti, A., Landreau, A., and Simon, B. (1988) 15N isotope biogeochemistry and natural denitrification process in groundwater: Application to the chalk aquifer of northern France. Geochimica et Cosmochimica Acta 52: 1869–1878.

McMurdie, P.J. and Holmes, S. (2013) phyloseq: An R Package for Reproducible Interactive Analysis and Graphics of Microbiome Census Data. PLOS ONE 8: e61217.

Mounler, E., Hallet, S., Chèneby, D., Benizri, E., Gruet, Y., Nguyen, C., et al. (2004) Influence of maize mucilage on the diversity and activity of the denitrifying community. Environmental Microbiology 6: 301–312.

National Center for Biotechnology Information (2010) Entrez Programming Utilities Help.

Oksanen, J., Blanchet, F.G., Friendly, M., Kindt, R., Legendre, P., Mcglinn, D., et al. (2020) vegan: Community Ecology Package.

Pajaro Valley Water Management Agency Salt and Nutrient Management Plan (2016).

Parada, A.E., Needham, D.M., and Fuhrman, J.A. (2016) Every base matters: Assessing small subunit rRNA primers for marine microbiomes with mock communities, time series and global field samples. Environmental Microbiology 18: 1403–1414.

Pascual, J., Huber, K.J., and Overmann, J. (2018) Pyrinomonadaceae. Bergey's Manual of Systematics of Archaea and Bacteria 1–4.

Pensky, J., Fisher, A.T., Gorski, G., Schrad, N., Dailey, H., Beganskas, S., and Saltikov, C. (2022) Enhanced cycling of nitrogen and metals during rapid infiltration: Implications for managed recharge. Science of The Total Environment 838: 156439.

Pfaffl, M.W. (2001) A new mathematical model for relative quantification in real-time RT–PCR. Nucleic Acids Research 29: e45.

Qian, J., Wang, Z., Jin, S., Liu, Y., Chen, T., and Fallgren, P.H. (2011) Nitrate removal from groundwater in columns packed with reed and rice stalks. Environmental Technology 32: 1589–1595.

Quast, C., Pruesse, E., Yilmaz, P., Gerken, J., Schweer, T., Yarza, P., et al. (2013) The SILVA ribosomal RNA gene database project: improved data processing and web-based tools. Nucleic Acids Research 41: D590–D596.

Rauch-Williams, T., Hoppe-Jones, C., and Drewes, J.E. (2010) The role of organic matter in the removal of emerging trace organic chemicals during managed aquifer recharge. Water Research 44: 449–460.

Regnery, J., Gerba, C.P., Dickenson, E.R. V, and Drewes, J.E. (2017) The importance of key attenuation factors for microbial and chemical contaminants during managed aquifer recharge: A review. Critical Reviews in Environmental Science and Technology 47: 1409–1452.

Rivett, M.O., Buss, S.R., Morgan, P., Smith, J.W.N., and Bemment, C.D. (2008) Nitrate attenuation in groundwater: A review of biogeochemical controlling processes. Water Research 42: 4215–4232.

Santmire, J.A. and Leff, L.G. (2015) The effect of sediment grain size on bacterial communities in streams. Freshwater Science 26: 601–610.

Schmidt, C.M., Fisher, A.T., Racz, A.J., Lockwood, B.S., and Huertos, M.L. (2011) Linking Denitrification and Infiltration Rates during Managed Groundwater Recharge. Environmental Science & Technology 45: 9634–9640.

Sheng, Z. (2005) An aquifer storage and recovery system with reclaimed wastewater to preserve native groundwater resources in El Paso, Texas. Journal of Environmental Management 75: 367–377.

Simpson, G.L. (2019) ggvegan: "ggplot2" Plots for the "vegan" Package.

Spalding, R.F. and Exner, M.E. (1993) Occurrence of Nitrate in Groundwater—A Review. Journal of Environmental Quality 22: 392–402.

Starr, R.C. and Gillham, R.W. (1993) Denitrification and Organic Carbon Availability in Two Aquifers. Groundwater 31: 934–947.

Stein, H., Kellermann, C., Schmidt, S.I., Brielmann, H., Steube, C., Berkhoff, S.E., et al. (2010) The potential use of fauna and bacteria as ecological indicators for the assessment of groundwater quality. Journal of Environmental Monitoring 12: 242–254.

Stone, B.W., Li, J., Koch, B.J., Blazewicz, S.J., Dijkstra, P., Hayer, M., et al. (2021) Nutrients cause consolidation of soil carbon flux to small proportion of bacterial community. Nature Communications 2021 12:1 12: 1–9.

Stuyfzand, P.J., Smidt, E., Zuurbier, K.G., Hartog, N., and Dawoud, M.A. (2017) Observations and Prediction of Recovered Quality of Desalinated Seawater in the Strategic ASR Project in Liwa, Abu Dhabi. Water 2017, Vol 9, Page 177 9: 177.

Sun, Y., Sun, M., Chen, G., Chen, X., Li, B., and Wang, G. (2021) Aggregate sizes regulate the microbial community patterns in sandy soil profile. Soil Ecology Letters 2021 3:4 3: 313–327.

Swain, D.L., Langenbrunner, B., Neelin, J.D., and Hall, A. (2018) Increasing precipitation volatility in twenty-first-century California. Nature Climate Change 1.

Tahon, G., Tytgat, B., Lebbe, L., Carlier, A., and Willems, A. (2018) Abditibacterium utsteinense sp. nov., the first cultivated member of candidate phylum FBP, isolated from ice-free Antarctic soil samples. Systematic and Applied Microbiology 41: 279–290.

Tufano, K.J., Reyes, C., Saltikov, C.W., and Fendorf, S. (2008) Reductive processes controlling arsenic retention: Revealing the relative importance of iron and arsenic reduction. Environmental Science and Technology 42: 8283–8289.

Valhondo, C., Carrera, J., Ayora, C., Barbieri, M., Nödler, K., Licha, T., and Huerta, M. (2014) Behavior of nine selected emerging trace organic contaminants in an artificial recharge system supplemented with a reactive barrier. Environmental Science and Pollution Research 21: 11832–11843.

Wang, J., Wang, C., Li, J., Bai, P., Li, Q., Shen, M., et al. (2018) Comparative Genomics of Degradative Novosphingobium Strains with Special Reference to Microcystin-Degrading Novosphingobium sp. THN1. Frontiers in Microbiology 0: 2238.

White, D.C., Suttont, S.D., and Ringelberg, D.B. (1996) The genus Sphingomonas: physiology and ecology. Current Opinion in Biotechnology 7: 301–306.

Wickham, H. (2016) ggplot2: Elegant Graphics for Data Analysis, Springer-Verlag New York.

Wickham, H., Averick, M., Bryan, J., Chang, W., McGowan, L.D., François, R., et al. (2019) Welcome to the Tidyverse. Journal of Open Source Software 4: 1686.

Wilke, C.O. (2020) ggtext: Improved Text Rendering Support for "ggplot2."

Yu, G. (2020) Using ggtree to Visualize Data on Tree-Like Structures. Current Protocols in Bioinformatics 69: e96.

Yu, G., Jones, B., and Arendsee, Z. (2021) tidytree: A Tidy Tool for Phylogenetic Tree Data Manipulation.

Zhou, Z.F., Zheng, Y.M., Shen, J.P., Zhang, L.M., and He, J.Z. (2011) Response of denitrification genes nirS, nirK, and nosZ to irrigation water quality in a Chinese agricultural soil. Environmental Science and Pollution Research 18: 1644–1652.

Supplementary Information

Supplementary Table 1: List of samples and number of replicates

Field Site	Infiltration	Depths below plot (cm)	PRB	Number of Replicates	Read Count Distribution
HSP	Before	20, 50, 70	Native Soil	1	104,041-125,063
HSP	After	20, 50, 70	Native Soil	1	64,687-106,417
HSP	Before	10, 90	Woodchips	2	49,066-97,432
HSP	After	10, 90	Woodchips	2	54,496-156,364
HSP	Before	50, 70, 110	Woodchips	1	38,944-128,098
HSP	After	50, 70, 110	Woodchips	1	63,899-118,981
KTR	Before	40, 60, 80, 90	Native Soil	1	9,288-21,436
KTR	After	40, 60, 80, 90	Native Soil	1	17,325-23,557
KTR	Before	10, 30	Native Soil	1	20,936-57,733
KTR	After	10, 30	Native Soil	3	14,109-29,079
KTR	Before	40, 60, 80, 90	Woodchips	1	20,306-24,645
KTR	After	40, 60, 80, 90	Woodchips	1	17,846- 23,701
KTR	Before	10, 30	Woodchips	1	20,217-23,328
KTR	After	10, 30	Woodchips	3	18,279-30,865
KTYA	Before	10, 30, 60, 80	Native Soil	2	5,592-208,735
KTYA	After	10, 30, 60, 80	Native Soil	3	11,089-101,552
KTYA	Before	10, 30, 60, 80	Woodchips	2	5,572-39,311

KTYA	After	10, 30, 60, 80	Woodchips	3	7,838-328,074

Supplementary Table 2

Field Site	Depth below plot	PRB	DOC	NO_3^-	Mn	Fe
KTR	10	Native Soil	1.8	21.3	162	47
KTR	30	Native Soil	2.4	21.6	428	1168
KTR	60	Native Soil	2.4	21.4	141	568
KTR	10	Woodchips	2.8	26.2	152	0
KTR	30	Woodchips	8.4	24.6	171	0
KTR	60	Woodchips	11.1	14.9	410	92
KTYA	10	Native Soil	2.2	9.5	0	0
KTYA	30	Native Soil	2.1	9.7	0	0
KTYA	60	Native Soil	2.2	9.8	0	0
KTYA	10	Woodchips	1.6	4.8	0	0
KTYA	30	Woodchips	1.7	4.8	0	0
KTYA	60	Woodchips	1.7	4.8	25	0

Supplementary Figures

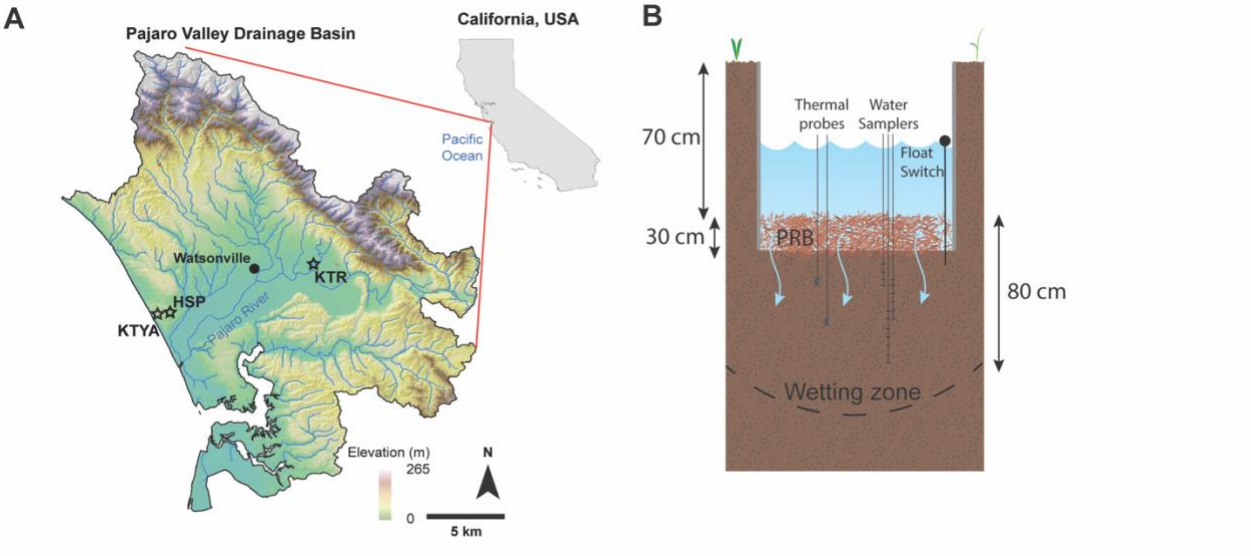

Supplementary Figure 1: Map showing (A) the locations of the three field sites where plot scale infiltration tests were conducted. Harkins Slough is notated by HSP, Kelly Thompson Ranch as KTR and Kitayama Ranch as KTYA (B) a typical plot set up with thermal probes, a float switch, and piezometers to sample water.

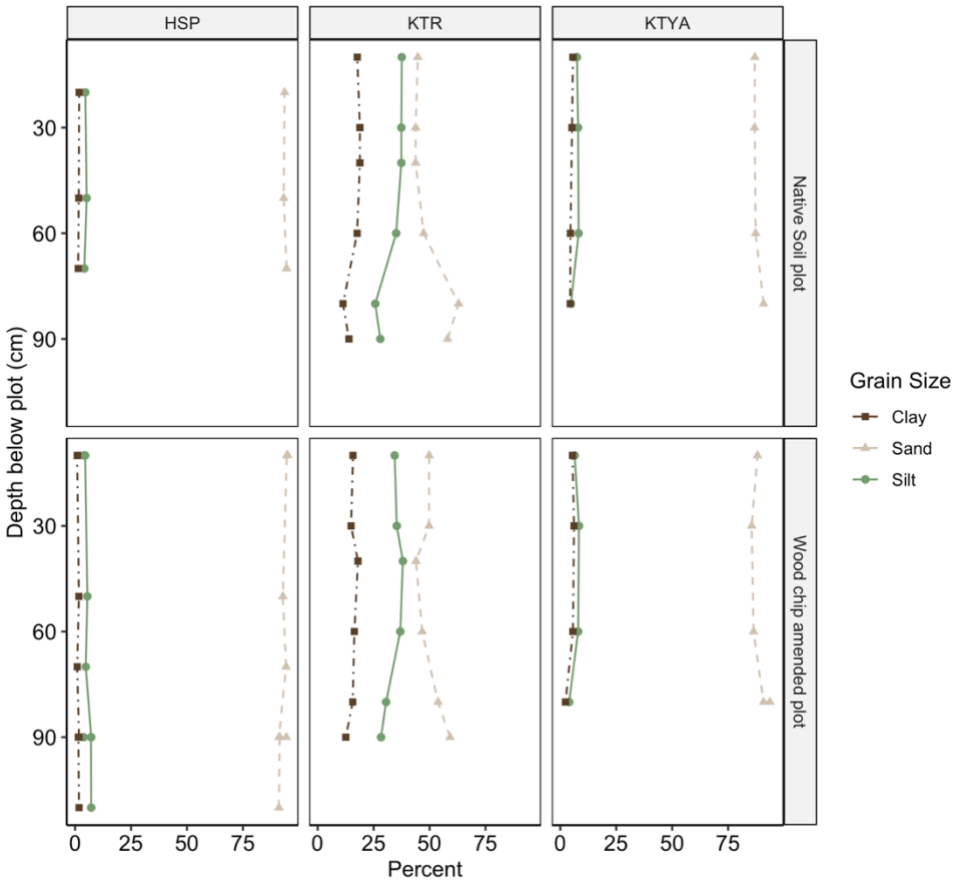

Supplementary Figure 2: Depth profile (cm below plot) of the soil grain size content at the three locations: Harkin Slough (HSP), Kelly Thompson Ranch (KTR), and Kitayama Ranch (KTYA) at native soil and wood chip amended plots. Percent clay is shown with a brown dot-dash line, percent silt is indicated with a solid green line, and percent sand is a sand-colored dashed line.

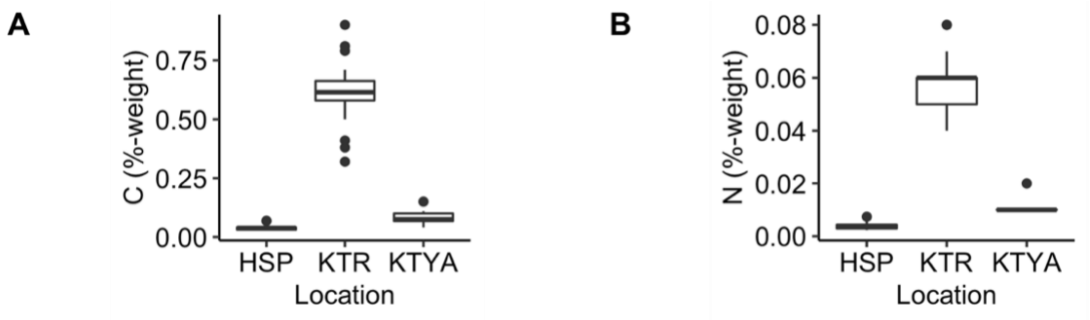

Supplementary Figure 3: Total C and total N of the soil by percent-weight at three field sites (HSP= Harkins Slough, KTR= Kelly Thompson Ranch, KTYA= Kitayama Ranch). The median is the bold line in the middle of the box, the upper and lower edges of the box represent the 25th and 75th percentiles. The whiskers extend to give the 90th percentile. Data that extends outside the whiskers are represented as points.

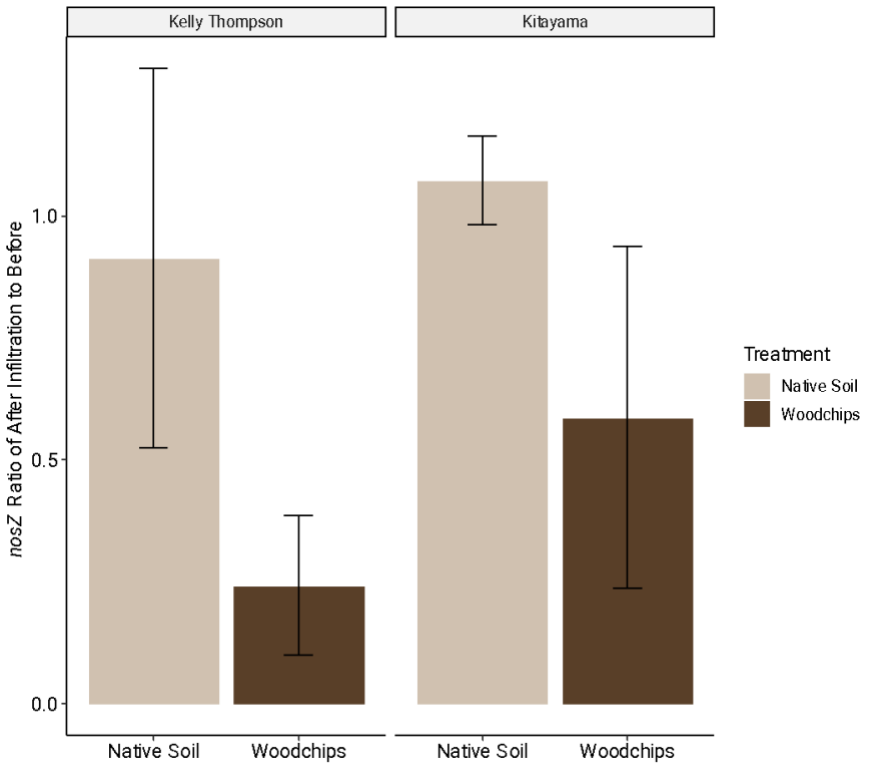

Supplementary Figure 4: Pfaffl ratio of *nosZ* reads at 30 cm below the plot depth at Kelly Thompson Ranch and Kitayama Ranch based on cycle threshold numbers (C_T) from quantitative PCR (qPCR). The ratio was calculated by the *nosZ* primer efficiency raised to the difference between before and after C_T number for *nosZ* samples divided by the 16S rRNA primer efficiency raised to the C_T difference of 16S samples.

Chapter 4: Metagenomic analysis and carbon characterization of anaerobic nitrate-reducing microcosms replicating saturated managed aquifer recharge basins

Abstract

In this study, we investigate how the carbon leached from two different carbon-rich permeable reactive barrier materials, almond shells and woodchips, can be used by soil microbes during managed aquifer recharge (MAR). Carbon-rich permeable reactive barriers are used to increase dissolved organic carbon concentrations to improve the removal of nitrates from the water. However, little is known about what carbon is being provided and how much can be consumed. Microbes are able to oxidize organic carbon while reducing nitrate and its byproducts to inert nitrogen gas as a form of metabolism in anoxic and suboxic conditions. We hypothesized that in microcosms simulating anoxic saturated conditions of a MAR basin, almond shell leachate would provide more easily digestible carbon and remove nitrate at faster rates. We also hypothesized that the metagenomics would shift toward more abundance of denitrifying genes. Using Illumina sequencing, we observed that the microbial community was primarily made up of bacteria and the overall distribution of metabolic genes did not change between the starting soil and post-incubation soil. However, we did observe that the leachate microcosms had more reads assigned to denitrification genes such as *nosZ* and *napA*. The almond shell leachate microcosm was able to remove nitrate faster than the woodchip leachate and provided more labile carbon. This study gives a framework for how permeable reactive barriers can be tested for efficiency.

Introduction

Aquifers provide the primary source of drinking water for about a quarter of the world's population (Gleeson *et al.*, 2012). However, reliance on groundwater has caused aquifer overdrafting where the water extracted from the aquifer exceeds the inputs (Galloway *et al.*, 1998). This creates many problems such as land sinkage, saltwater intrusion, and degradation of the groundwater quality (Galloway *et al.*, 1998; Casanova *et al.*, 2016; Levy *et al.*, 2021). Managed aquifer recharge (MAR) is the collection of tools and methods to purposefully collect surface water to replenish underground aquifers and combat over-drafting (Dillon *et al.*, 2009). One type of MAR is distributed stormwater collection (DSC-MAR), which uses gravity to direct hillslope runoff into a basin where it then percolates into the underground aquifer. This type is one of the most cost-effective options, is easy to maintain, and can infiltrate more than 100 acre-feet a year (Beganskas and Fisher, 2017).

In a DSC-MAR, the environmental conditions change due to infiltration in the basin. During rainy seasons the basin can fill up and the subsurface soil becomes fully saturated. In drought or extended dry periods, the soil loses its water content (Beganskas *et al.*, 2019). Along with water content, oxygen concentration varies with infiltration. During wetting cycles, oxygen concentrations in the subsurface soil (1 m) are depleted within hours but recover rapidly during drying periods (Dutta *et al.*, 2015). Oxic conditions can facilitate the degradation of complex emerging organic contaminants, such as ibuprofen and paracetamol (Valhondo *et al.*, 2014), while anoxic and suboxic conditions can promote the removal of nitrate (Starr and Gillham,

1993). To improve the water quality of the recharging water, the seasonality and current basin conditions need to be considered.

Permeable reactive barriers (PRBs) are a common technique used to improve water quality. PRBs are made from a variety of materials and help improve water quality by degrading organic materials, adsorbing heavy metals, or providing environmental conditions for microbial populations to degrade pollutants (Al-Hashimi *et al.*, 2021). In a MAR system, a PRB made of compost, clay, and iron oxide enhanced the removal of complex emerging trace organic chemicals and created nitrate-, iron-, and manganese-reducing conditions (Valhondo *et al.*, 2014). A carbon-rich PRB has been shown to increase the dissolved organic carbon (DOC) of the infiltrating water and promote microbial removal (Mariotti *et al.*, 1988; Starr and Gillham, 1993; Gorski *et al.*, 2019). Many factors determine the fate of pollutants including oxygen concentration, pH, carbon availability, infiltration rate, microbial community, and mineralogy of the soil (Valhondo *et al.*, 2014; Casanova *et al.*, 2016; Gorski *et al.*, 2020). Understanding how the introduction of a PRB affects those factors is an important point of consideration.

Nitrate (NO_3^-) is the most widespread non-point source pollutant of groundwater worldwide (Spalding and Exner, 1993). In MAR basins located near agricultural fields, it is of high concern given the high use of fertilizers (California Department of Water Resources, 2018). Microbes in the subsurface soil can respire nitrate in certain conditions. Generally, microbes will oxidize organic carbon compounds and generate energy by reducing a favorable molecule. Oxygen reduction

is the most energetically favorable, while nitrate is generally used once most of the oxygen is depleted (Rivett *et al.*, 2008). Full microbial denitrification will reduce nitrate to inert nitrogen gas, but incomplete denitrification could accumulate nitrous oxide (N_2O), a greenhouse gas (Starr and Gillham, 1993; Mcmahon *et al.*, 2000). In a MAR system, there are many different potential microbial nitrogen cycles, such as dissimilatory nitrate reduction to ammonia or anaerobic ammonium oxidation) that could lead to an accumulation of a certain N speciation. The addition of carbon into a saturated system increases the C:N ratio and promotes denitrification (Lu *et al.*, 2014; Beganskas and Fisher, 2017; Grau-Martínez *et al.*, 2017), thus carbon-rich PRBs can be used to promote the removal of nitrate in a MAR system.

Although carbon-rich PRBs promote the removal of some pollutants, it is important to consider what type of carbon is being introduced to the system and how that will affect the redox conditions in the soil. Introducing easily consumed carbon to the soil system promotes reducing conditions needed for denitrification (Starr and Gillham, 1993), but providing too much carbon can push reducing conditions that dissolve iron and manganese in the soils. Reduction of manganese from MnO_2 to aqueous Mn^{2+} and dissolution of ferric (hydr)oxides to Fe^{2+} also releases heavy metals, such as arsenic that adsorb to the minerals (Rivett *et al.*, 2008; Fendorf *et al.*, 2010). Thus, the carbon-rich PRB must provide enough carbon to promote denitrifying conditions but not too much, so metals are released into the water at high concentrations.

In this study, we aim to identify what type of PRB material provides the most benefit to the water quality of a MAR system. We tested how microbes respond to leached carbon from two low-cost carbon-rich PRB materials – redwood woodchips and almond shells. Previous analysis of woodchip leachate from a cottonwood tree found the DOC was high in high molecular weight and hydrophilic compounds like humic acids and aromatics (Abusallout and Hua, 2017). A study on the leachate from a redwood waste pile found an accumulation of tannin and lignin, which are more resistant to biodegradation (Tao *et al.*, 2005). Almond shell leachate is less characterized however, almond shells are made up of 20-38% cellulose, 18-30% sugar, and 7-29% lignin (Li *et al.*, 2018; Shaikhiev *et al.*, 2021). This suggests that almond shells are made of more easily broken-down materials.

In this study, we observe how woodchip and almond shell leachates impact microbial metabolism during anaerobic conditions simulating a saturated MAR basin. We used anaerobic microcosms to analyze nitrate removal as well as the impact of the leachate on the metagenomics of the soil microbial community. Then we characterized the carbon from the leachates using an Assimilable Organic Carbon (AOC) assay, a Biodegradable Organic Carbon (BDOC) assay, Nuclear Magnetic Resonance (NMR), Ultraviolet-visible spectroscopy (UV-Vis), and Specific Ultraviolet Absorbance (SUVA). We hypothesize that almond shells will promote a faster rate of nitrate removal and provide accessible carbon to the microbes. We also hypothesize that the metabolism of the microbes will shift towards a larger abundance of carbon consumption and anoxic respiration genes.

Materials and Methods

Sample Collection

Soil was collected in June 2020 from the untreated northern side of the Kelly Thompson Ranch MAR basin (36.920420, -121.697869). Sandy samples from depths 15 cm to 30 cm were sterilely collected into Whirl-Pak and kept on dry ice. Soil was stored in a -20°C freezer until use. Soil for the microcosms was homogenized through a 1mm sieve and left to dry overnight at 25°C before being used in the microcosms.

Media

Leachates from wood chips and almond shells were extracted by incubating 5 g of PRB material in 500 mL of autoclaved MilliQ water in an anaerobic chamber for 24 hours. For the NMR microcosm, 20 g of woodchips was incubated in 500 mL to increase the DOC to 100 mg/L. The incubations were then filtered through a 20 µm filter and DOC was measured using a Shimadzu TOC analyzer. Leachates were kept at 4°C until use.

An artificial stormwater media (Mohanty *et al.*, 2014) was modified to represent nitrate concentrations in the MAR basin for a final concentration of 0.75 mM $CaCl_2$, 0.075 mM $MgCl_2$, 0.33 mM Na_2SO_4, 1 mM $NaHCO_3$, 323 mM $NaNO_3$ (5 mg/ L NO_3-N), 0.072 mM NH_4Cl, and 0.016 mM Na_2HPO_4. The leachates were diluted and mixed with the artificial stormwater media to a final concentration of 5 mg/L DOC in the nitrate-reducing microcosm and biodegradable carbon assays, 1 mg/L for the AOC assay, and 100 mg/L for the NMR microcosm.

Glassware preparation

All glassware was washed with detergent then rinsed three times with water then three times with deionized water. It was then soaked in a 5% nitric acid bath for at least 24 hours and washed with deionized water. Glassware was then capped with foil and put in the oven at 400°C for 6 hours. Caps were prepared similarly but were autoclaved instead of being put in the oven.

Nitrate-reducing Microcosm

In an anaerobic chamber, 100 mL of artificial stormwater leachate and 5 g of dried soil were added to a 115 mL autoclaved serum bottle. The bottles were capped with a rubber stopper, removed from the anaerobic chamber, and kept in the dark at 25°C. Experiments were held in triplicate for almond shell leachate, wood chip leachate, glucose (+), and artificial stormwater with no added carbon (-). Bottles were regularly sampled using the Hungate method and analyzed for nitrate, nitrite, and ammonium. Starting and ending fluids were analyzed for Mg, Fe, and As.

DNA extraction, library prep, and sequencing

Starting and ending soils from the nitrate-reducing microcosms were kept frozen at -20°C until extraction with a PowerSoil (Qiagen), PowerSoil Max (Qiagen), or PowerSoil Pro kit (Qiagen). DNA concentration was calculated using a Qubit 4 Fluorometer (Thermo Fisher). Low yield extractions were concentrated using a Microcon 30kDa centrifugal filter (Millipore). 16S rRNA libraries were prepared in duplicate using the 16S barcoding kit SQK-16S024 (Nanopore) and run on a Minion Mk1B Sequencing device (Nanopore). DNA samples for metagenomic analysis were sent to Novogene for Illumina NovaSeq 6000 150 bp paired-end reads.

Metagenomic analysis

Paired-end reads were received from Novogene ranging from 47 million to 60 million reads per sample and a Q30 average of 93%. Reads were uploaded to the MG-RAST server (mg-rast.org) (Meyer *et al.*, 2008). Post processing, there were 2,794,166 sequences for the beginning soil sample; 3,611,729 from the microcosm with almond shell leachate; 3,407,621 from the microcosm with woodchip leachate; and 2,955,094 from the native soil microcosm. Taxonomic assignment was performed using the RefSeq database and metabolic assignments were done using the Subsystems, KEGG, and eggNOG databases. Figures were created using the KEGG annotation. For both types of assignments, we employed a maximum e-value of 10^{-5}, a minimum identity of 60%, and a maximum alignment length of 15 bp. The uploaded samples can be found on MG-RAST under the project ID mgp103791. Rarefication curves show samples reached an appropriate taxonomic depth (Supplementary Figure 1).

Biodegradable Organic Carbon Assay

Microcosms were set up according to the fixed sand method in Volk et al., 1994 with a few adaptations. The dried soil was washed 10 times with distilled water until DOC did not change. Washed soil (5 g) was added to 100 mL of artificial stormwater (containing 5 mg /L NO_3-N) in 115 mL serum bottles and sealed with a butyl stopper and aluminum crimp. Microcosms were set up in an anaerobic chamber (Coy) so the headspace of the microcosms consisted of nitrogen gas. The experiment was done in triplicate with a washed soil negative control. Serum bottles were kept in

the dark at 25°C for 28 days and were regularly sampled for DOC using the Hungate method.

Assimilable Organic Carbon Assay

Pseudomonas fluorescens P-17 ATCC 49642 and *Spirillum* sp. strain NOX ATCC 49643 were acquired from ATCC. The assimilable organic carbon assay was conducted according to the protocol in Standard Methods for Water and Wastewater (American Public Health Association *et al.*, 2017) and Volk et al., 1994, except for the diluted leachates (~ 1 mg/ L) and stormwater mixture were used instead of tap water and the mineral salts solution. The media was still pasteurized in a 70°C water bath for 30 minutes and vials were kept at 15 °C (±2°C) throughout the experiment. Bacteria were plated on R2A agar (Difco) on days 8, 9, and 10 and counted 3 days later. Empirical Yield values were calculated from growth in bottles with either 1 mg/L acetate-C or 1 mg/L oxalate-C and are 3.9×10^7 CFU-P17/ µg acetate-C, 9.1×10^6 CFU-NOX/µg acetate-C, and 3.2×10^7 CFU-NOX/µg oxalate-C. Percent assimilable organic carbon was calculated as follows: [(mean P-17 CFU/mL) (1/yield) + (mean NOX CFU/mL) (1/yield)] (1000 mL/L) (mg/1000µg) (1/DOC mg/L). Experiments were conducted in triplicate with each replicate being plated twice.

NMR microcosms

For each microcosm, 100 mg/L DOC of leachate-artificial stormwater was added to 10 g of soil anaerobically into 115 mL serum bottles. Almond shell leachate and woodchip leachate were both tested in triplicate along with a negative soil-only

control. Leachate-artificial stormwater was also inoculated with 500 CFU/ mL of both *Pseudomonas fluorescens* P-17 and *Spirillum* sp. strain NOX in aerobic serum bottles as a positive control. The microcosms were kept at 25°C in the dark for 28 days. The starting and ending liquid was filtered and analyzed for NMR, UV-Vis, and DOC.

NMR Analysis

Filtered samples were aliquoted into NMR tubes along with 10% deuterium oxide (vol/vol). ^{1}H NMR spectra were acquired using a Bruker 800 MHz NMR Instrument (UCSC). The water and deuterium signals were suppressed and the spectra was acquired with 64 scans of 1.3 s. Spectra were processed and analyzed using MNova v12 (Mestrelab Research). The spectra were integrated under five regions based on assignments (Santos *et al.*, 2016): aliphatic structures (0.0-1.9 ppm), functionalized aliphatic (1.9-3.1 ppm), oxygenated (3.1- 4.3 ppm), vinylic (5.3-7.0 ppm), and aromatic functional groups (7.0-10.0 ppm).

UV-Vis and SUVA

UV absorbance for wavelengths 250, 350, 365, 440, 465, and 665 nm were taken using a 96-well UV-Transparent microplate (Corning) and a SpectraMax 190 Microplate reader with PathCheck (Molecular Devices). Absorbance at 254 nm was taken using AquaMate 7100 - Vis Spectrophotometer (Thermo Fisher) and a 1 cm pathlength cuvette. Ultrapure water was used as a blank for both assays. SUVA was calculated by dividing absorbance with DOC concentration. SUVA was used as a proxy for aromaticity in the DOC. The ratio of absorption at 250 nm to 365 nm

(E2:E3) inferred molecular size and the ratio of 465 nm to 665 nm (E4: E6) inferred humification (Ly *et al.*, 2021).

Nutrient Analysis (DOC, N-speciation, metals)

All fluid samples collected were filtered through a 20 µm filter and kept at 4°C. Nitrate was reduced using vanadium (III) and nitrite concentrations were calculated using the Griess method in a microplate (Miranda *et al.*, 2001). Ammonium was calculated using a colorimetric microplate analysis adapted from Baethgen and Alley, 2008. DOC was quantified on the Shimadzu TOC analyzer. Samples quantified for metal concentrations (arsenic, manganese, and iron) were preserved with 2 % HNO_3 prior to analysis. Metal samples were analyzed using a Thermo ElementXR High Resolution Inductively Coupled Mass Spectrometer.

Data Transformation analysis and Visualization

Data transformation, analysis, and visualizations were conducted using R packages: Divisive Amplicon Denoising Algorithm (DADA2) (Callahan *et al.*, 2016), ANCOM-BC (Lin and Peddada, 2020), *vegan* (v 2.5.7) (Oksanen *et al.*, 2020), tidyverse (Wickham *et al.*, 2019), ggplot2 (Wickham, 2016), ggvegan (Simpson, 2019), ggpubr (Kassambara, 2020), and ggtext (Wilke, 2020).

Results and Discussion

Almond shells promoted nitrate reduction rates

We first observed how the leachates affect nutrient cycling in anaerobic microcosms. All the microcosms showed a reduction of nitrate and nitrite (Figure 1). The microcosm amended with almond shell leachate and the positive control with lactate had the fastest removal. Nitrate was completely depleted after two days for

both conditions, while almond shells took three days for the nitrite signal to be removed compared to the two days in the lactate microcosms. Nitrite reduction rates are more affected by the input carbon source because many microbes can grow using nitrate reduction while only denitrifying bacteria use nitrite as an electron acceptor (Wilderer *et al.*, 1987). Woodchip leachate microcosms had no detectable nitrate or nitrite by day 3. Nitrate was removed in the negative control of native soil by day 4, but nitrite persisted for 11 days. Ammonium concentration remained relatively the same throughout the incubation for all treatments (Supplementary Figure 2). These results are consistent with rates of nitrate removal from studies using woodchip PRBs for wastewater treatment (Wang and Chu, 2016), as well as similar to rates of nitrate removal of cut-up palm tree leaves and organic compost in an active MAR basin (Grau-Martínez *et al.*, 2017).

In both of the leachate microcosms, there was an increase in arsenic and manganese, but the difference between the leachates was not significant (Figure 1c). Dissolved iron decreased after incubation with almond shell leachates. The almond shell leachate had a starting concentration of 0.08 mg dissolved Fe / L, almost four times as much as the woodchip leachate, but post-microcosm, dissolved iron had a similar concentration as the woodchip leachate microcosm. Iron oxidation has been linked to denitrification by particular chemoautotrophic bacteria but usually, this occurs in low C environments (Wang *et al.*, 2017). However, it is unknown why the almond shell leachate would have such high levels of dissolved Fe. Almond shells have been shown to function as a Fe adsorption material in water with high dissolved

iron concentrations (Anusha and Murgadoss, 2014), so the almond shells used in this experiment may have been previously exposed to high Fe levels. The increase in dissolved As and Mn aligns with the reducing anaerobic metabolism after the nitrogen was consumed. However, the differences between metal release were not significant between the leachates which could mean neither leachate pushed conditions too far toward reducing conditions. It could also mean that was the maximum amount of Mn or As that could be released. Sampling more for metals would give a better picture of when certain electron acceptors become the dominant metabolism.

Metagenomes show bacteria-dominated populations experience similar changes after incubation regardless of leachate

Previous analysis of 16S rRNA amplicons from field sites replicating MAR infiltration through the subsurface found infiltration shifted the population towards predominately *Proteobacteria* in coarse soil profiles (Chapter 3). In this experiment (also conducted with coarse sandy soils), we saw a similar shift in microbial community (Figure 2). The beginning soil had 47% of the reads assigned to *Actinobacteria* and 30% to *Proteobacteria*, but all of the post-incubation samples had over 64% *Proteobacteria* reads. The beginning soil, the woodchip leachate, and negative microcosms had over 1% of reads from *Planctomycetes*, a phylum known for its ability to oxidize ammonium to nitrite anaerobically (Kuenen, 2008), but was not as abundant in the almond shell leachate microcosm. The hydrazine oxidoreductase gene known for anaerobic oxidation of ammonia (anammox)

(Harhangi *et al.*, 2012) was not annotated as part of the metagenomic analysis. *Gemmatimondetes* made up over 1% of the reads in the negative control post-incubation but were less than 1% of the reads in other samples. A principal coordinate analysis shows a distinction between before and after samples along the primary axis and separation by treatment on the secondary axis (Supplementary Figure 3). Previous studies from MAR experimental sites had focused on bacterial communities as only the 16S rRNA gene (present in bacteria and archaea) was sequenced to gain a sense of the community (Beganskas *et al.*, 2018; Gorski *et al.*, 2019; Pensky *et al.*, 2022). We expected we were missing populations of fungal communities that could thrive in the saturated MAR conditions. However, less than 1% of the reads were assigned to fungal communities. One reason for this might be the strict anaerobic environment of the microcosm could have stunted fungal growth. Anaerobic fungi exist but are not well characterized (Hess *et al.*, 2020) so our reads may have not been mapped to the limited genomes provided.

The overall metabolism of the microcosms and starting soil did not differ very much (Figure 3). About 20% of the reads from each sample were assigned to the amino acid metabolism. The beginning soil had 1-2% more reads dedicated to amino acid metabolism than the post-incubation soils, which is probably a result of dependence on the breakdown of amino acids for maintenance in nutrient-limited conditions. The negative control had 0.5% fewer reads assigned to carbohydrate metabolism, while the beginning soil had fewer reads assigned to glycan biosynthesis and energy metabolism. Included in the energy metabolism level are genes that carry

out nitrogen metabolism, oxidative phosphorylation, carbon fixation, sulfur metabolism, photosynthesis, and methane metabolism. Overall, the general trends of the metabolism are similar to a study of anaerobic digestion of rice straw, with the primary metabolic pathway being amino acid metabolism (Chen *et al.*, 2020). Analysis using annotations from the other databases mimicked the KEGG results shown in the figure.

Given the overarching goal of this study was to observe how different carbon-rich PRB materials can power denitrification, we observed the changes in the relative abundance of reads assigned to the nitrogen cycle (Figure 4). The largest differences in nitrogen cycling genes were seen between the beginning soil and post-incubation soils. The beginning soil lacked detectable reads for multiple nitrogen cycling pathways. For example, nitrogenases that fix nitrogen gas into ammonia were present in both the leachate microcosms but did not exist in the beginning soil. One important gene that had more reads in the leachate microcosms compared to the beginning soil or the negative control was *nosZ*, the nitrous oxide reductase. Nitrous oxide is an important greenhouse gas, and its reduction is the last step of denitrification (Henry *et al.*, 2006). The *nosZ* reads were primarily related to *Proteobacteria* and to a lesser extent *Bacteroidetes* (Figure 4b). The most abundant genera in the post-incubation samples included *Dyadobacter* (*Bacteroidetes*) and *Thiobacillus* (*Betaproteobacteria*). These results suggest diversity among the *nosZ* reads as both clades were present, abundant, and identified (Chee-Sanford, *et al*., 2020). *Dyadobacter* has a clade II *nosZ* and is a genus that does not contain other

denitrifying genes but is a main contributor to nitrous oxide consumption in soils (Domeignoz-Horta *et al.*, 2016). On the other hand, *Thiobacillus* is a genus that contains the clade I *nosZ* gene and has the ability to complete full denitrification in soils (Beller *et al.*, 2006). Ensuring that our denitrifying MAR systems have the gene capable of reducing this greenhouse gas to inert N_2 is an important environmental concern in designing a functional MAR site.

The gene with the most reads from the leachate microcosms was *napA*, a periplasmic nitrate reductase. The enzyme encoded by this gene is used in dissimilatory nitrate reduction and its enzyme activity is largely dependent on the availability of a reduced carbon substrate in the absence of oxygen (Sears *et al.*, 1997). Majority of the reads assigned to *napA* were *Betaproteobacteria* with *Azoarcus* being the genus with the most reads (Figure 4c). *Azoarcus* is a genus capable of anaerobic aromatic degradation (Fernandez, *et al*., 2014). The PRB leachates could potentially have provided reduced aromatic substrates to power denitrification in this genus.

Almond shells provide more labile carbon that is degraded by the soil microbial communities

To elucidate how much carbon was being provided to the soil microbial community, we performed two different assays – a biodegradable organic carbon assay and an assimilable carbon assay. The biodegradable organic carbon (BDOC) assay utilizes the native soil population and is calculated by taking starting DOC-ending DOC after the DOC concentration starts stalling (Volk *et al.*, 1994). It gives

an estimate of how much carbon is being provided to the microbes that exist in the system being studied. Alternatively, the assimilable carbon (AOC) assay is a well-developed water quality protocol that uses two known carbon degraders (*Pseudomonas fluorescens* P17 and *Spirillum* str. NOX) to approximate what fraction of carbon is most readily available for bacteria (Haddix *et al.*, 2004).

The almond shell leachate had a higher fraction of BDOC and AOC than the woodchip leachate (Figure 5). Over 74% of the DOC in the almond shell leachate microcosm was consumed during the 28-day BDOC incubation with native flora compared to 64.5% of DOC in the woodchip leachate. In the AOC assay, the almond shell leachate also had a higher fraction of available carbon than the woodchip leachate – 9.2% compared to 3.6%. Almond shells dry-weight can be made up of up to 37% water-soluble fermentable sugars such as sucrose and fructose (Holtman *et al.*, 2015), while woodchips primarily leach hydrophobic and high molecular weight compounds (Abusallout and Hua, 2017). The simple sugars of the almond shell leachate provided more available carbon to the microbes. The anaerobic conditions studied in this experiment also favor simple, fermentable carbon, as complex DOC rates are dependent on oxygen concentration (Hulthe *et al.*, 1998). The AOC fractions were significantly lower than the BDOC fractions, but the plating method we used can underestimate AOC (Tang *et al.*, 2018). AOC being much lower than BDOC is also common; AOC is considered to only be carbon (e.g. sugars, carboxylic and dicarboxylic acids) that is available for microbes to grow and under aerobic conditions, while BDOC is carbon that can be metabolized for maintenance as well as

growth (Escobar and Randall, 2001). We further constrained the BDOC analysis by conducting the experiment in anaerobic conditions with added nitrate concentrations similar to those found in the basin. From a thermodynamic perspective, reduction of oxygen to water or nitrate to N_2 yield similar reduction potentials, +0.816 mV and +0.75 mV, respectively (Rivett, *et al.*, 2008). However, nitrate reduction to N_2 requires greater transfer of electrons per molecule of N_2 produced. Hence more carbon is likely needed for complete denitrification relative to aerobic respiration. The anaerobic conditions in the microcosms gives us an idea of how much carbon is available for the microbes in the most metabolically limited conditions seen in a MAR basin.

Characteristics of the carbon from the leachates changed after incubation

In order to see how incubation with native soil microbes and *Pseudomonas fluorescens* P17 and *Spirillum* sp. NOX affected the characterization of carbon; we used proton NMR to gain insights into the functional groups and UV-Vis spectrophotometry as a proxy for other characteristics. To avoid potential artifacts introduced by sample lyophilization or other DOC concentrating methods, we conducted these microcoms at higher DOC (100 mg DOC L^{-1}), which yielded greater natural ^1H and clearer spectra. The majority of both leachates at the start of the microcosm contained carbon with oxygenated C resonances (Figure 6, Table 1), but woodchips were also 41.9% aliphatic structures. Aliphatic protons included protons on saturated carbon chains as well as protons on allylic carbons. After 28 days of incubation with soil, 97.8% of the oxygenated C resonances from almond shell

leachate were metabolized and there was an accumulation of aliphatic resonances. This was also seen by the incubation with AOC bacteria but to a lesser degree. The woodchip leachate spectra changed less dramatically than the almond shell leachate, but still showed a decrease in oxygenated resonances from 48% of the peaks to 23% and an increase in functionalized aliphatic resonances from 8% to 23% after incubation with the soil microbes. The AOC bacteria incubated with woodchip leachate also had an increase in functionalized aliphatic structure but a loss of basic aliphatic structures. Interestingly, the woodchip leachate did not have a large proportion of dissolved aromatic structures. This may be due to anaerobic conditions. Aromatic degradation is primarily done with enzymes dependent on oxygen (Seo *et al.*, 2009). The shift towards the right of the post-incubation samples is indicative of degradation into simpler molecules and microbial-derived C (Hertkorn *et al.*, 2013; Santos *et al.*, 2016). It is also important to note that ^{1}H spectra show peaks for all hydrogens not just those attached to carbons (inorganic H are usually in the 1.6-3.2 ppm range) (Matilainen *et al.*, 2011), therefore the post-incubation may have some peaks from compounds from the artificial stormwater. The starting leachate material was the PRB material soaked in distilled water, so all of the peaks are solely from the leachate.

SUVA (UV-adsorption A_{254nm}(1cm)/mg C L^{-1}) is a commonly used proxy of aromatic content per DOC unit – values greater than four indicate highly aromatic and hydrophobic carbon; between two and four indicates mixtures of aquatic humics and both hydrophilic and hydrophobic compounds; and less than two is indicative of

primarily low-molecular weight, hydrophilic compounds (Edzwald and Tobiason, 1999). When comparing the SUVA values for the soil NMR microcosms, we see that only woodchips have values greater than 2 (Figure 7a). This confirms our previous results that suggest the woodchip leachate has more complex, and therefore less labile, carbon compounds. In all three treatments, we see a significant increase in SUVA values. We believe as the microbes consumed or respired the labile carbon of the leachate, the relative percentage of large molecular weight, hydrophobic, and/or aromatic compounds in the leachate increased. The NMR spectra do not give us any idea about the molecular weight of the compounds, but the increase of aliphatic protons in the spectra after incubation could indicate the post-incubation DOC had high molecular weight, hydrophobic molecules.

The ratio of UV absorbance at 250 nm compared to 365 nm (E_2:E_3) is inversely related to the average molecular weight of the DOC while the ratio of 465 nm to 665 nm (E_4:E_6) is positively correlated to the humification of the carbon i.e., O:C ratio, C:N ratio, carboxylic content, and total acidity (Helms *et al.*, 2008). The leachates started with similar E_2:E_3 values however, the almond shells decreased after the 28-day incubation and woodchips increased (Figure 7b). The starting unamended microcosms had very little to no carbon at the start but after incubation had a large increase in the E_2:E_3 value, indicating that the soil provided dissolved concentrations of smaller molecular weight compounds. The E_2:E_3 value for the negative control was uncharacteristically high compared to other soils (Heckman *et al.*, 2011; Santos *et al.*, 2016). This may be due to the abrupt change to anaerobic and saturated conditions,

which caused growth and metabolism activation of *Proteobacteria* (Figure 2) . The E_4:E_6 ratio decreased significantly in the almond shell microcosm (Figure 7c). The woodchip microcosm also decreased, albeit with less confidence that that change was due to incubation ($p = .06$). The negative control microcosm did not have a change. In the woodchip microcosm, ~50% of the DOC was consumed and removed from the system, while ~83% was removed in the almond shell leachate. These results indicate that in the almond shell microcosms, consumption of readily available carbon occurred leaving high molecular weight compounds that were more aromatic and less humic. In the woodchip microcosms, there was also increased aromaticity of the DOC, but a reduction in humic acids and a decrease in overall molecular weight. Given the differences in the starting leachate composition, almond shells were able to provide more readily available carbon and were left with high molecular weight compounds with more aromaticity. Woodchips started more aromatic and the consumption of humic acids helped to decrease the average molecular weight giving us an increase in SUVA, an increase in E_2:E_3, and a decrease in E_4:E_6 post-incubation. Humic acids tend to have large peaks around 2.5-4 ppm in ^{1}H spectra, so the reduction of humic acids can also be seen on the NMR spectra (Figure 6). The combination of ^{1}H NMR, SUVA, E_2:E_3, and E_4:E_6 can be used to approximate how the carbon in the microcosm is changing, but separation columns, FTIR-MS, ^{13}C NMR could also be used to further resolve potential metabolites being introduced into the system (Matilainen *et al.*, 2011).

Conclusions and Future Directions

In this study, we observed the differences in two leachates from a carbon-rich permeable reactive barrier in terms of nutrient cycling, impact on the microbial community, accessibility of using the carbon for metabolism, and changes to the carbon characteristics through incubation. We found that the almond shell leachate provides more labile carbon that powers faster nitrate removal compared to woodchip leachate. The introduction of saturated conditions does not change the overall metabolism patterns in the soil, but it does shift the microbial community towards *Proteobacteria* dominance. Through incubation with native soil microbes, the dissolved compounds shifted from primarily oxygenated resonances to aliphatic resonances.

One limitation of this research is we are only looking at one set of conditions experienced in a MAR basin. Full anaerobic saturation does occur when the basin is full and infiltration is slow, but the soil is also exposed to dry-wet cycling which reintroduces oxygen. To gain a better picture of the full carbon cycling that is occurring in the basin, the seasonality's impact should be observed. We believe this study provides critical insights into how carbon is driving geochemical cycling in the subsurface during MAR.

Tables

Table 1: Relative proportion (%) of major functional groups assigned for ^{1}H spectra

	Aromatic	Unsaturated HC=	Oxygenated HCO	Functionalized Aliphatic HCCO	Aliphatic HCCC
Woodchip Microcosm End (P17 and NOX)	0.01	1.65	42.35	21.39	34.6
Woodchip Microcosm End (soil)	0.21	0.27	23.62	24.32	51.58
Woodchip Leachate	1.38	0	48.39	8.34	41.9
Almond Shell Microcosm End (P17 and NOX)	0	0	75.01	10.14	14.85
Almond Shell Microcosm End (soil)	2.49	2.17	7.96	13.46	73.91
Almond Shell Leachate	0.25	1.06	86.07	6.98	5.64

Figures

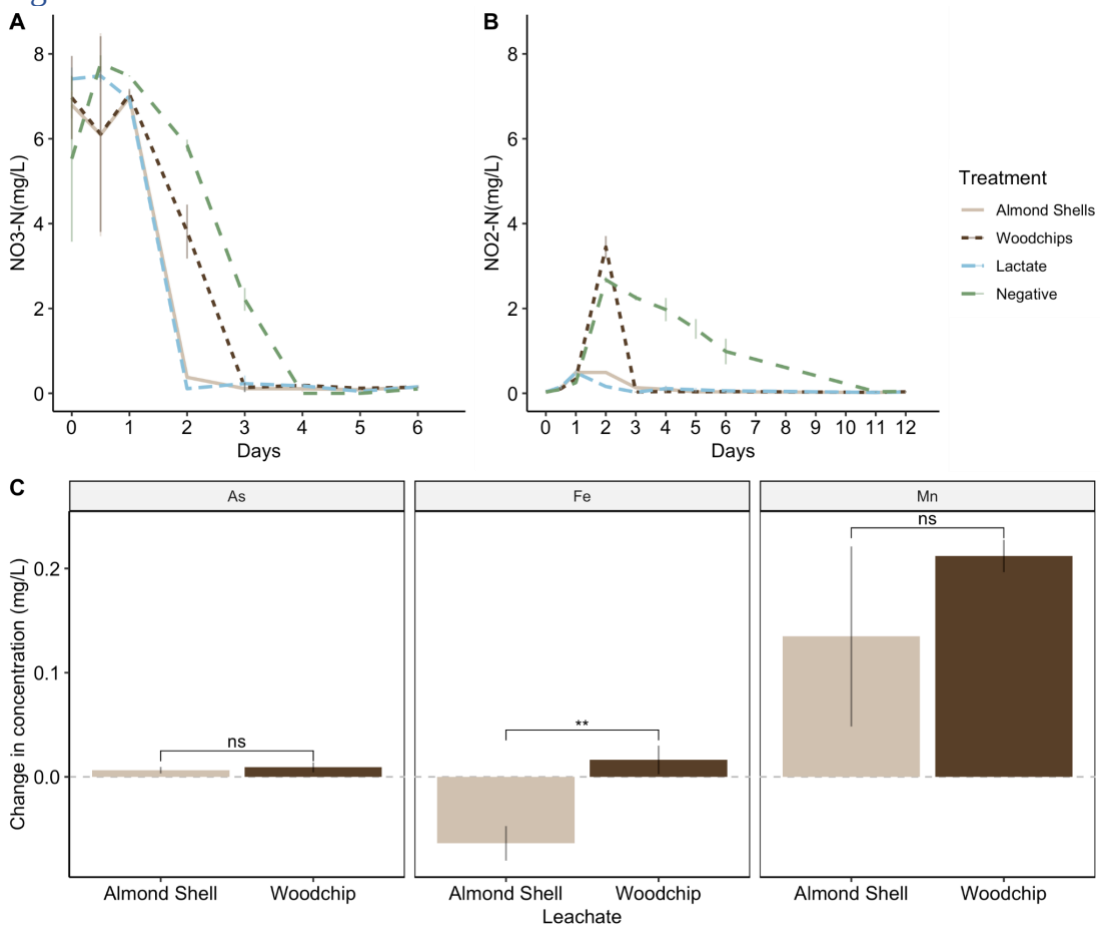

Figure 1: Concentrations of nitrate as nitrogen (a) and nitrite as nitrogen (b) over time in four different microcosm conditions: Almond shell leachate (beige), woodchip leachate(brown), lactate amended (blue, positive control), and an unamended negative control (green). (c) Change between the ending and starting concentration of arsenic (As), iron (Fe), and Manganese (Mn) between almond shells (beige) and woodchips (brown) Significance is notated as ns= not significant, **=p<0.01. Error bars show the standard deviation between replicates.

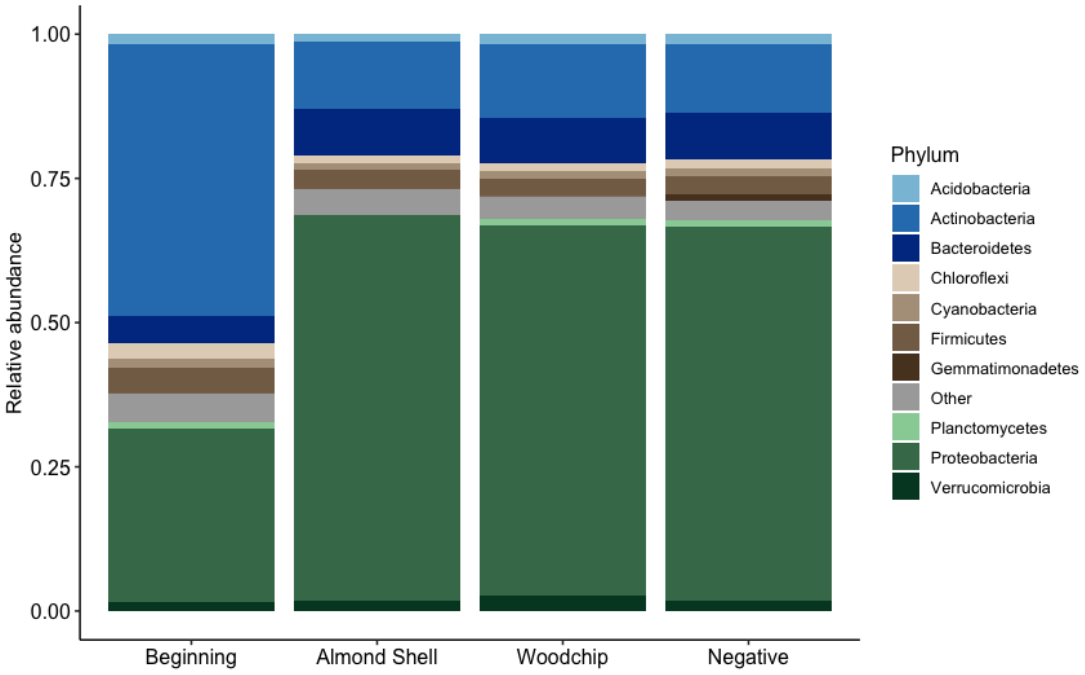

Figure 2: Relative abundances of the phyla making up more than 1% of reads in soil samples from the beginning soil, and the end of a microcosm treated with almond shell leachate, woodchip leachate, or unamended native soil as a negative control.

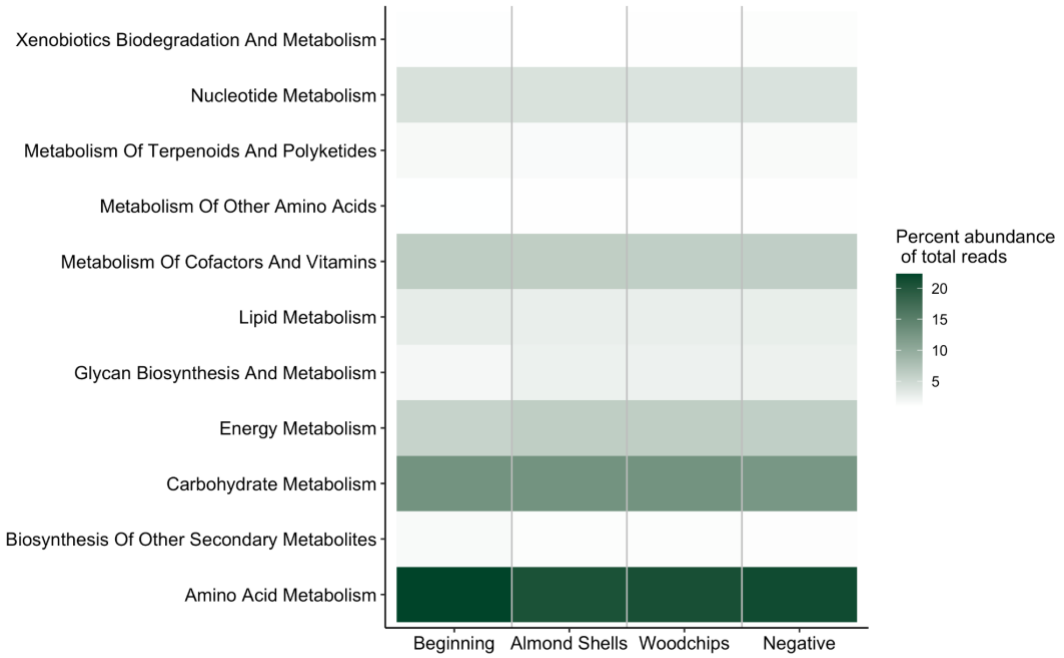

Figure 3: Percent of the total reads assigned per sample assigned to a KO level 1 function. Abundant reads are shown in light blue while less abundant are in navy. The four samples are beginning soil, almond shell leachate, woodchip leachate, and an unamended negative control.

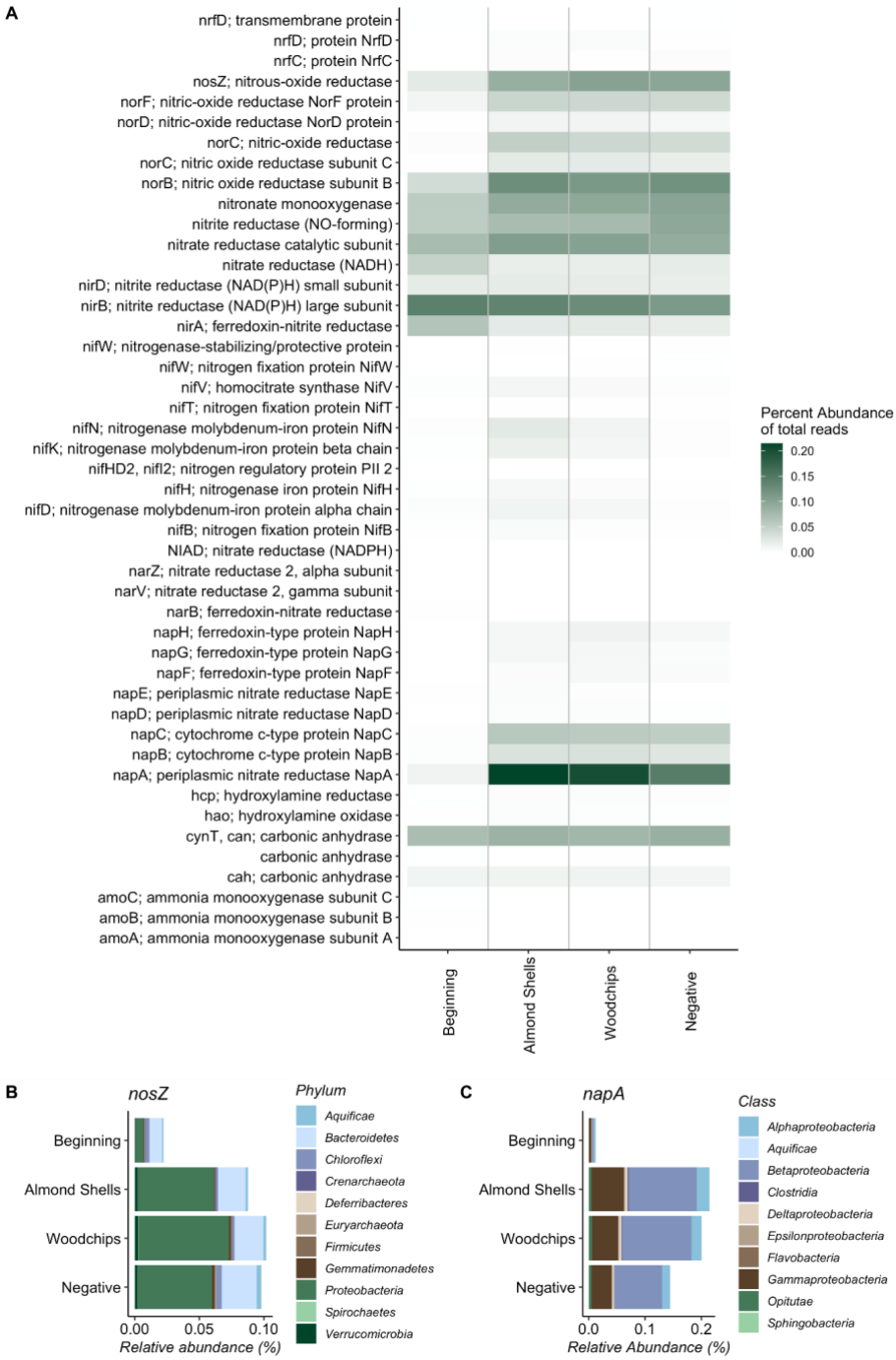

Figure 4: (a) Relative abundance of reads assigned to particular nitrogen cycling genes using the KEGG database from four samples – the beginning soil, and post-incubation with either almond shells, woodchips, or unamended native soil as a negative control. Light blue shows a high abundance of reads while navy indicates low levels of reads. Relative abundance of reads assigned to (b) *nosZ* by phylum or (c) *napA* by class

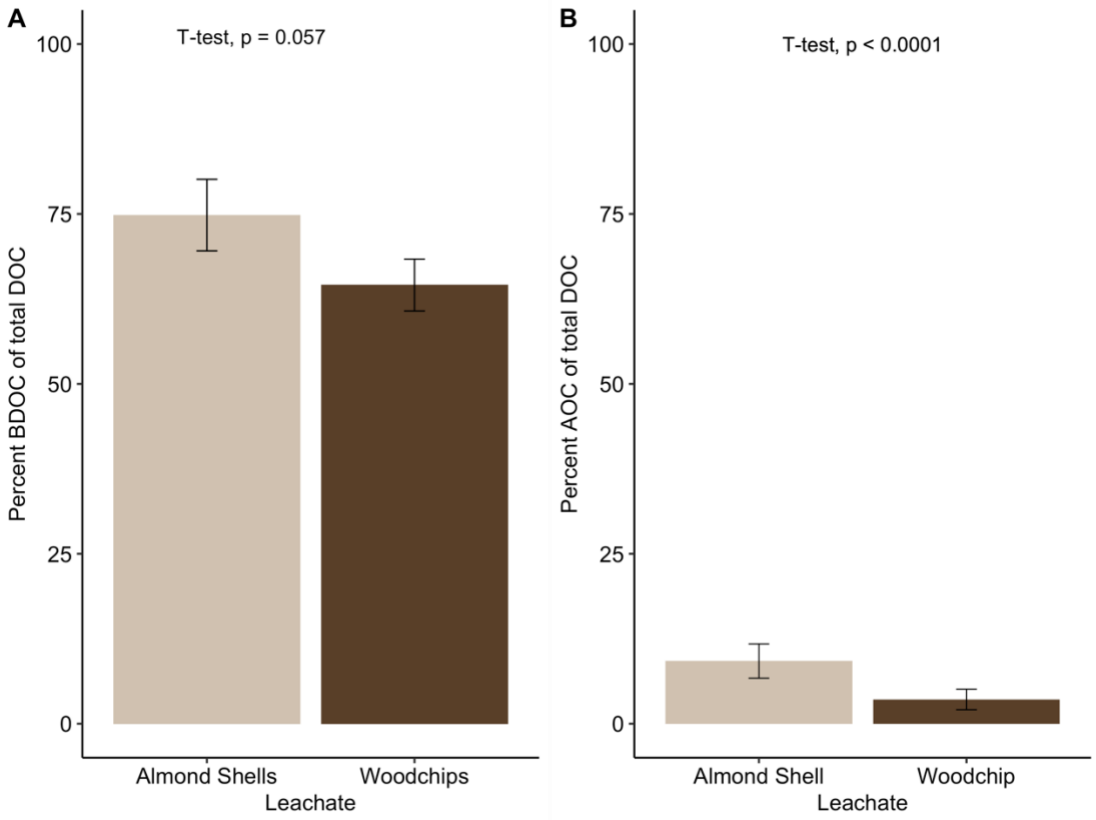

Figure 5: (a) Average percent biodegradable organic carbon (BDOC) of the total dissolved organic carbon (~5 mg C /L from leachate) in anaerobic microcosms supplemented with almond shell leachate (beige) or woodchip leachate (brown). (b) Average percent assimilable organic carbon (AOC) of the total dissolved organic carbon in anaerobic microcosms supplemented with almond shell leachate (beige) or woodchip leachate (brown). Error bars indicate standard deviation among replications.

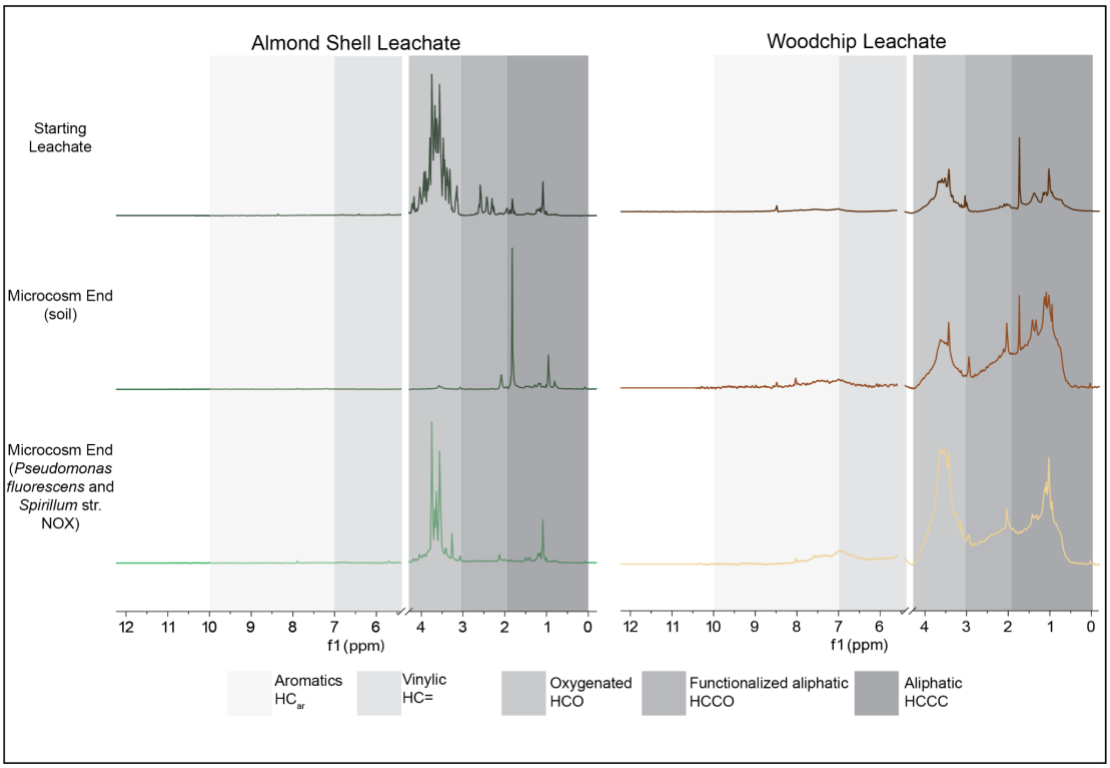

Figure 6: ^{1}H Nuclear Magnetic Resonance spectra from the anaerobic leachates of almond shells (dark green) or woodchips (dark brown). Spectra from leachates post incubation with native soil flora is shown in green (almond shells) and brown (woodchips), as well as post aerobic incubation with *Pseudomonas fluorescens* P17 and *Spirillum* str. NOX. Functional groups are shown in boxes going light to dark: aromatics, vinylic HC=, Oxygenated HCO, Functionalized aliphatic HCCO, and aliphatic HCCC resonances.

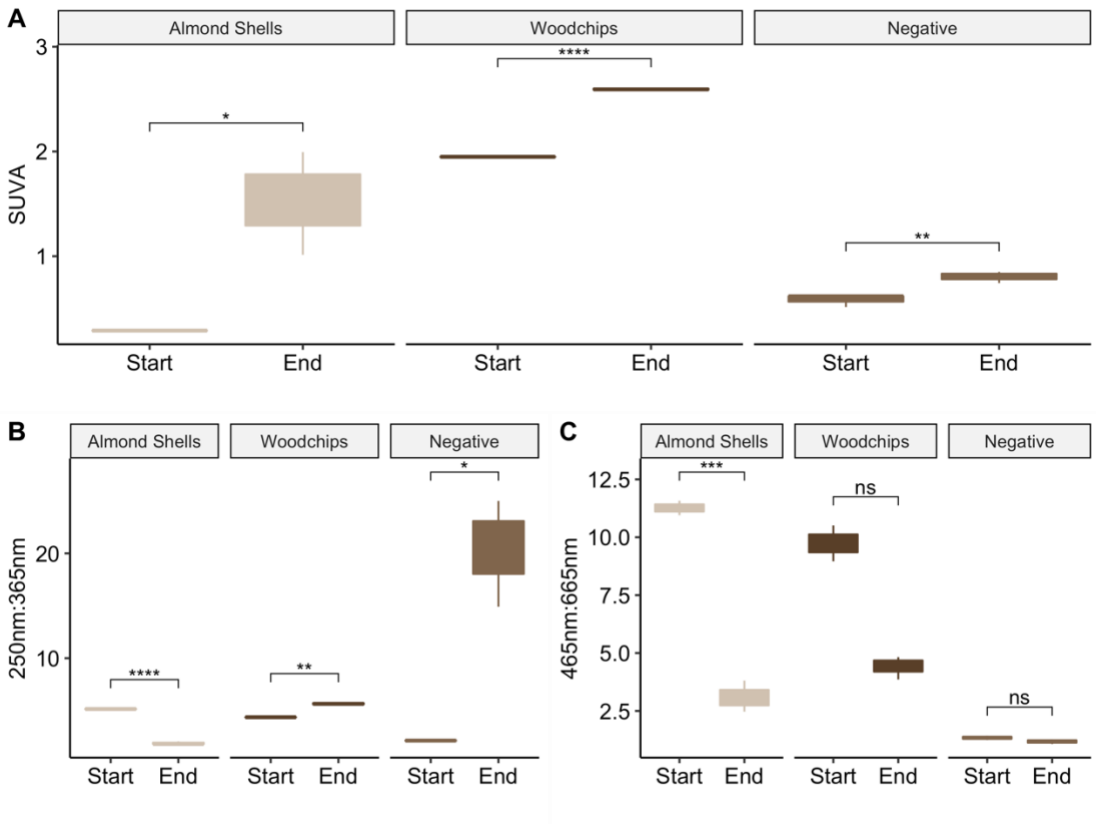

Figure 7: (a) Specific Ultraviolet Absorbance at 254 nm (SUVA) (UV-adsorption A_{254nm}(1cm)/mg C L^{-1}) for NMR microcosms (Figure 6) at the start and end of a 28-day incubation. Microcosms were supplemented with almond shell leachate (beige), woodchip leachate (dark brown), or an unamended negative control (brown). (b) the ratio of 250 nm to 365 nm absorbance was used as a proxy for average molecular weight. (c) the ratio of 465 nm to 665 nm was used as a proxy for the fraction of humic compounds. The median is the bold line in the middle of the box, and the upper and lower edges of the box represent the 25th and 75th percentiles. The whiskers extend to give the 90th percentile. Each point represents a chemical data from an infiltration day during the experiment. ns= not significant, *= $p<0.05$, **=$p<0.01$ ***=$p<0.0001$, ****= $p<0.00001$.

References

Abusallout, I. and Hua, G. (2017) Characterization of dissolved organic carbon leached from a woodchip bioreactor. Chemosphere 183: 36–43.

Al-Hashimi, O., Hashim, K., Loffill, E., Marolt Čebašek, T., Nakouti, I., Faisal, A.A.H., and Al-Ansari, N. (2021) A Comprehensive Review for Groundwater Contamination and Remediation: Occurrence, Migration and Adsorption Modelling. Molecules 26:.

American Public Health Association, American Water Works Association, and Water Environment Federation (2017) Assimilable Organic Carbon Assay. In Standard Methods for the Examination of Water and Wastewater. Baird, R.B., Eaton, A.D., and Rice, E.W. (eds). Washington D.C.: Standard Methods.

Anusha, G. and Murgadoss, J.R. (2014) Adsorption Of Iron From Aqueous Solution Using Almond Shell As Adsorbent, IJSR - International Journal of Scientific Research(IJSR), IJSR | World Wide Journals. International Journal of Scientific Research 3:.

Baethgen, W.E. and Alley, M.M. (2008) A manual colorimetric procedure for measuring ammonium nitrogen in soil and plant Kjeldahl digests. http://dx.doi.org/101080/00103628909368129 20: 961–969.

Beller, H.R., Letain, T.E., Chakicherla, A., Kane, S.R., Legler, T.C., and Coleman, M.A. (2006) Whole-genome transcriptional analysis of chemolithoautotrophic thiosulfate oxidation by *Thiobacillus denitrificans* under aerobic versus denitrifying conditions. *Journal of Bacteriology* **188**: 7005–7015.

Beganskas, S. and Fisher, A.T. (2017) Coupling distributed stormwater collection and managed aquifer recharge: Field application and implications. Journal of Environmental Management 200: 366–379.

Beganskas, S., Gorski, G., Weathers, T., Fisher, A.T., Schmidt, C., Saltikov, C., et al. (2018) A horizontal permeable reactive barrier stimulates nitrate removal and shifts microbial ecology during rapid infiltration for managed recharge. Water Research 144: 274–284.

Beganskas, S., Young, K.S., Fisher, A.T., Harmon, R., and Lozano, S. (2019) Runoff Modeling of a Coastal Basin to Assess Variations in Response to Shifting Climate and Land Use: Implications for Managed Recharge. Water Resources Management 33: 1683–1698.

California Department of Water Resources (2018) California Water Plan Update 2018.

Callahan, B.J., McMurdie, P.J., Rosen, M.J., Han, A.W., Johnson, A.J.A., and Holmes, S.P. (2016) DADA2: High-resolution sample inference from Illumina amplicon data. Nature Methods 2016 13:7 13: 581–583.

Casanova, J., Devau, N., and Pettenati, M. (2016) Managed Aquifer Recharge: An Overview of Issues and Options. In Integrated Groundwater Management. Cham: Springer International Publishing, pp. 413–434.

Chee-Sanford, J.C., Connor, L., Krichels, A., Yang, W.H., and Sanford, R.A. (2020) Hierarchical detection of diverse Clade II (atypical) nosZ genes using

new primer sets for classical- and multiplex PCR array applications. *Journal of Microbiological Methods* **172**: 105908.

Chen, D., Zuo, X., Li, J., Wang, X., and Liu, J. (2020) Carbon migration and metagenomic characteristics during anaerobic digestion of rice straw. Biotechnology for Biofuels 13: 1–13.

Dillon, P., Pavelic, P., Page, D., Beringen, H., and Ward, J. (2009) Managed aquifer recharge: An Introduction.

Domeignoz-Horta, L.A., Putz, M., Spor, A., Bru, D., Breuil, M.C., Hallin, S., and Philippot, L. (2016) Non-denitrifying nitrous oxide-reducing bacteria - An effective N2O sink in soil. *Soil Biology and Biochemistry* **103**: 376–379.

Dutta, T., Carles-Brangarí, A., Fernàndez-Garcia, D., Rubol, S., Tirado-Conde, J., and Sanchez-Vila, X. (2015) Vadose zone oxygen (O2) dynamics during drying and wetting cycles: An artificial recharge laboratory experiment. Journal of Hydrology 527: 151–159.

Edzwald, J.K. and Tobiason, J.E. (1999) Enhanced coagulation: US requirements and a broader view. Water Science and Technology 40: 63–70.

Escobar, I.C. and Randall, A.A. (2001) Assimilable organic carbon (AOC) and biodegradable dissolved organic carbon (BDOC):: complementary measurements. Water Research 35: 4444–4454.

Fendorf, S., Nico, P.S., Kocar, B.D., Masue, Y., and Tufano, K.J. (2010) Arsenic chemistry in soils and sediments. Developments in Soil Science 34: 357–378.

Fernández, H., Prandoni, N., Fernández-Pascual, M., Fajardo, S., Morcillo, C., Díaz, E., and Carmona, M. (2014) Azoarcus sp. CIB, an Anaerobic Biodegrader of Aromatic Compounds Shows an Endophytic Lifestyle. *PLoS ONE* **9**.

Galloway, D.L., Hudnut, K.W., Ingebritsen, S.E., Phillips, S.P., Peltzer, G., Rogez, F., and Rosen, P.A. (1998) Detection of aquifer system compaction and land subsidence using interferometric synthetic aperture radar, Antelope Valley, Mojave Desert, California. Water Resources Research 34: 2573–2585.

Gleeson, T., Wada, Y., Bierkens, M.F.P., and van Beek, L.P.H. (2012) Water balance of global aquifers revealed by groundwater footprint. Nature 488: 197–200.

Gorski, G., Dailey, H., Fisher, A.T., Schrad, N., and Saltikov, C. (2020) Denitrification during infiltration for managed aquifer recharge: Infiltration rate controls and microbial response. Science of The Total Environment 727: 138642.

Gorski, G., Fisher, A.T., Beganskas, S., Weir, W.B., Redford, K., Schmidt, C., and Saltikov, C. (2019) Field and Laboratory Studies Linking Hydrologic, Geochemical, and Microbiological Processes and Enhanced Denitrification during Infiltration for Managed Recharge. Environmental Science & Technology 53: 9491–9501.

Grau-Martínez, A., Torrentó, C., Carrey, R., Rodríguez-Escales, P., Domènech, C., Ghiglieri, G., et al. (2017) Feasibility of two low-cost organic substrates for inducing denitrification in artificial recharge ponds: Batch and flow-through experiments. Journal of Contaminant Hydrology 198: 48–58.

Haddix, P.L., Shaw, N.J., and LeChevallier, M.W. (2004) Characterization of Bioluminescent Derivatives of Assimilable Organic Carbon Test Bacteria. Applied and Environmental Microbiology 70: 850–854.

Harhangi, H.R., le Roy, M., van Alen, T., Hu, B.-L., Groen, J., Kartal, B., et al. (2012) Hydrazine synthase, a unique phylomarker with which to study the presence and biodiversity of anammox bacteria. Appl Environ Microbiol 78: 752–758.

Heckman, K., Vazquez-Ortega, A., Gao, X., Chorover, J., and Rasmussen, C. (2011) Changes in water extractable organic matter during incubation of forest floor material in the presence of quartz, goethite and gibbsite surfaces.

Helms, J.R., Stubbins, A., Ritchie, J.D., Minor, E.C., Kieber, D.J., and Mopper, K. (2008) Absorption spectral slopes and slope ratios as indicators of molecular weight, source, and photobleaching of chromophoric dissolved organic matter. Limnology and Oceanography 53: 955–969.

Henry, S., Bru, D., Stres, B., Hallet, S., and Philippot, L. (2006) Quantitative detection of the nosZ gene, encoding nitrous oxide reductase, and comparison of the abundances of 16S rRNA, narG, nirK, and nosZ genes in soils. Appl Environ Microbiol 72: 5181–5189.

Hertkorn, N., Harir, M., Koch, B.P., Michalke, B., and Schmitt-Kopplin, P. (2013) High-field NMR spectroscopy and FTICR mass spectrometry: Powerful discovery tools for the molecular level characterization of marine dissolved organic matter. Biogeosciences 10: 1583–1624.

Hess, M., Paul, S.S., Puniya, A.K., van der Giezen, M., Shaw, C., Edwards, J.E., and Fliegerová, K. (2020) Anaerobic Fungi: Past, Present, and Future. Frontiers in Microbiology 11: 2621.

Holtman, K.M., Offeman, R.D., Franqui-Villanueva, D., Bayati, A.K., and Orts, W.J. (2015) Countercurrent extraction of soluble sugars from almond hulls and assessment of the bioenergy potential. Journal of Agricultural and Food Chemistry 63: 2490–2498.

Hulthe, G., Hulth, S., and Hall, P.O.J. (1998) Effect of oxygen on degradation rate of refractory and labile organic matter in continental margin sediments. Geochimica et Cosmochimica Acta 62: 1319–1328.

Kassambara, A. (2020) ggpubr: "ggplot2" Based Publication Ready Plots.

Kuenen, J.G. (2008) Anammox bacteria: from discovery to application. Nature Reviews Microbiology 2008 6:4 6: 320–326.

Levy, Z.F., Jurgens, B.C., Burow, K.R., Voss, S.A., Faulkner, K.E., Arroyo-Lopez, J.A., and Fram, M.S. (2021) Critical Aquifer Overdraft Accelerates Degradation of Groundwater Quality in California's Central Valley During Drought. Geophysical Research Letters 48: e2021GL094398.

Li, X., Liu, Y., Hao, J., and Wang, W. (2018) Study of Almond Shell Characteristics. Materials 11:.

Lin, H. and Peddada, S. das (2020) Analysis of compositions of microbiomes with bias correction. Nature Communications 2020 11:1 11: 1–11.

Lu, H., Chandran, K., and Stensel, D. (2014) Microbial ecology of denitrification in biological wastewater treatment. Water Research 64: 237–254.

Ly, Q.V., Maqbool, T., Zhang, Z., van Le, Q., An, X., Hu, Y., et al. (2021) Characterization of dissolved organic matter for understanding the adsorption on nanomaterials in aquatic environment: A review. Chemosphere 269: 128690.

Mariotti, A., Landreau, A., and Simon, B. (1988) 15N isotope biogeochemistry and natural denitrification process in groundwater: Application to the chalk aquifer of northern France. Geochimica et Cosmochimica Acta 52: 1869–1878.

Matilainen, A., Gjessing, E.T., Lahtinen, T., Hed, L., Bhatnagar, A., and Sillanpää, M. (2011) An overview of the methods used in the characterisation of natural organic matter (NOM) in relation to drinking water treatment. Chemosphere 83: 1431–1442.

Mcmahon, P.B., Bruch, B.W., Becker, M.F., Pope, L.M., and Dennehy, K.F. (2000) Occurrence of nitrous oxide in the central High Plains aquifer, 1999. Environmental Science and Technology 34: 4873–4877.

Meyer, F., Paarmann, D., D'Souza, M., Olson, R., Glass, E.M., Kubal, M., et al. (2008) The metagenomics RAST server - A public resource for the automatic phylogenetic and functional analysis of metagenomes. BMC Bioinformatics 9: 1–8.

Miranda, K.M., Espey, M.G., and Wink, D.A. (2001) A Rapid, Simple Spectrophotometric Method for Simultaneous Detection of Nitrate and Nitrite. Nitric Oxide 5: 62–71.

Mohanty, S.K., Cantrell, K.B., Nelson, K.L., and Boehm, A.B. (2014) Efficacy of biochar to remove Escherichia coli from stormwater under steady and intermittent flow. Water Research 61: 288–296.

Oksanen, J., Blanchet, F.G., Friendly, M., Kindt, R., Legendre, P., Mcglinn, D., et al. (2020) vegan: Community Ecology Package.

Pensky, J., Fisher, A.T., Gorski, G., Schrad, N., Dailey, H., Beganskas, S., and Saltikov, C. (2022) Enhanced cycling of nitrogen and metals during rapid infiltration: Implications for managed recharge. Science of The Total Environment 838: 156439.

Rivett, M.O., Buss, S.R., Morgan, P., Smith, J.W.N., and Bemment, C.D. (2008) Nitrate attenuation in groundwater: A review of biogeochemical controlling processes. Water Research 42: 4215–4232.

Santos, F., Russell, D., and Berhe, A.A. (2016) Thermal alteration of water extractable organic matter in climosequence soils from the Sierra Nevada, California. Journal of Geophysical Research: Biogeosciences 121: 2877–2885.

Sears, H.J., Spiro, S., and Richardson, D.J. (1997) Effect of carbon substrate and aeration on nitrate reduction and expression of the periplasmic and membrane-

bound nitrate reductases in carbon-limited continuous cultures of Paracoccus denitrificans Pd1222. Microbiology (N Y) 143: 3767–3774.

Seo, J.S., Keum, Y.S., and Li, Q.X. (2009) Bacterial Degradation of Aromatic Compounds. International Journal of Environmental Research and Public Health 6: 278.

Shaikhiev, I.G., Kraysman, N. v, and Sverguzova, S. v (2021) Review of Almond (Prunus Dulcis) Shell Use to Remove Pollutants from Aquatic Environments. 11: 14866–14880.

Simpson, G.L. (2019) ggvegan: "ggplot2" Plots for the "vegan" Package.

Spalding, R.F. and Exner, M.E. (1993) Occurrence of Nitrate in Groundwater—A Review. Journal of Environmental Quality 22: 392–402.

Starr, R.C. and Gillham, R.W. (1993) Denitrification and Organic Carbon Availability in Two Aquifers. Groundwater 31: 934–947.

Tang, P., Wu, J., Liu, H., Liu, Y., and Zhou, X. (2018) Assimilable organic carbon (AOC) determination using GFP-tagged Pseudomonas fluorescens P-17 in water by flow cytometry. PLoS ONE 13:.

Tao, W., Hall, K.J., Masbough, A., Frankowski, K., and Duff, S.J.B. (2005) Characterization of Leachate from a Woodwaste Pile. Water Quality Research Journal 40: 476–483.

Valhondo, C., Carrera, J., Ayora, C., Barbieri, M., Nödler, K., Licha, T., and Huerta, M. (2014) Behavior of nine selected emerging trace organic contaminants in

an artificial recharge system supplemented with a reactive barrier. Environmental Science and Pollution Research 21: 11832–11843.

Volk, C., Renner, C., Robert, C., and Joret, J.C. (1994) Comparison of two techniques for measuring biodegradable dissolved organic carbon in water. Environmental Technology 15: 545–556.

Wang, J. and Chu, L. (2016) Biological nitrate removal from water and wastewater by solid-phase denitrification process. *Biotechnology Advances* **34**: 1103–1112.

Wang, R., Yang, C., Zhang, M., Xu, S.Y., Dai, C.L., Liang, L.Y., et al. (2017) Chemoautotrophic denitrification based on ferrous iron oxidation: Reactor performance and sludge characteristics. Chemical Engineering Journal 313: 693–701.

Wickham, H. (2016) ggplot2: Elegant Graphics for Data Analysis, Springer-Verlag New York.

Wickham, H., Averick, M., Bryan, J., Chang, W., McGowan, L.D., François, R., et al. (2019) Welcome to the Tidyverse. Journal of Open Source Software 4: 1686.

Wilderer, P.A., Jones, W.L., and Daub, U. (1987) COMPETITION IN DENITRIFICATION SYSTEMS AFFECTING REDUCTION RATE AND ACCUMULATION OF NITRITE. War Res 21: 239–245.

Wilke, C.O. (2020) ggtext: Improved Text Rendering Support for “ggplot2.”

Supplementary Information

Supplemental Figures

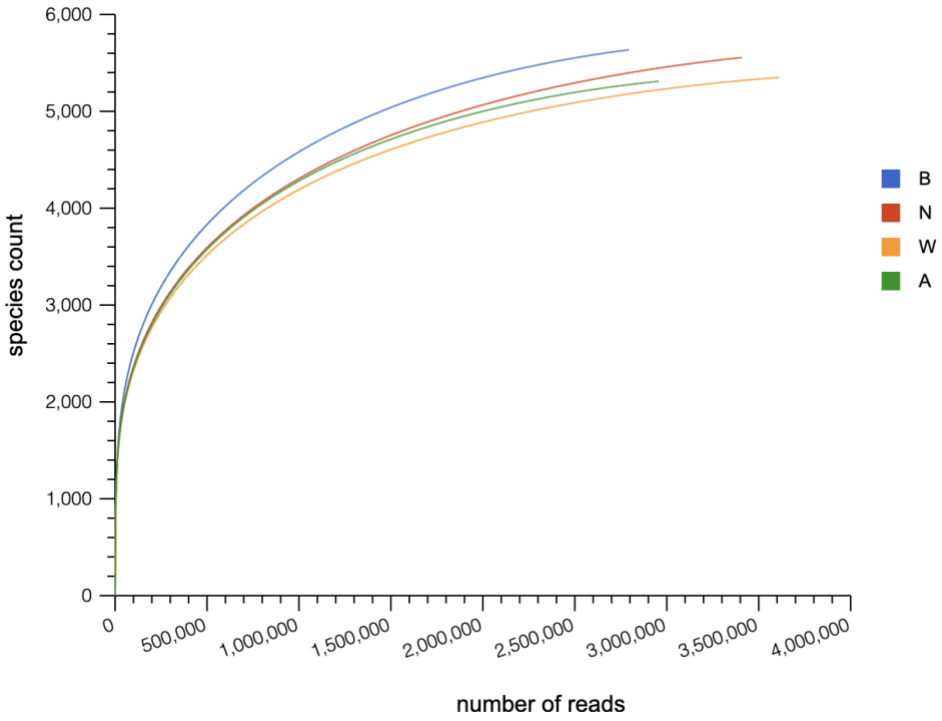

Supplemental Figure 1: Rarefaction curves of Illumina shotgun metagenomic sequences with the number of reads to species count. Blue (B) indicates the beginning soil, red (N) shows post-incubation negative microcosm, yellow (W) indicates post-incubation woodchip leachate microcosm, and green (A) indicates the post-incubation almond shell leachate.

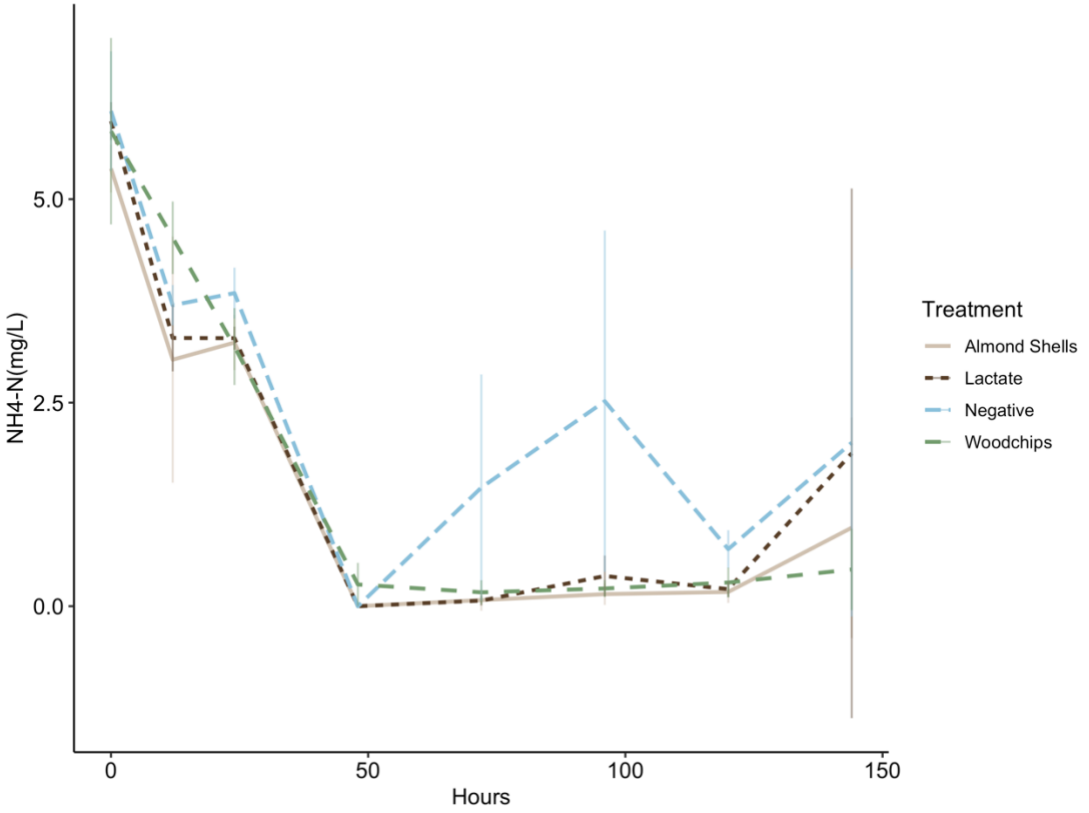

Supplemental Figure 2: Ammonium as nitrogen concentrations (mg/L) over time for microcosms with almond shell leachate, woodchip leachate, lactate (positive control), and unamended (negative control). Error bars show the standard deviation of the replicates

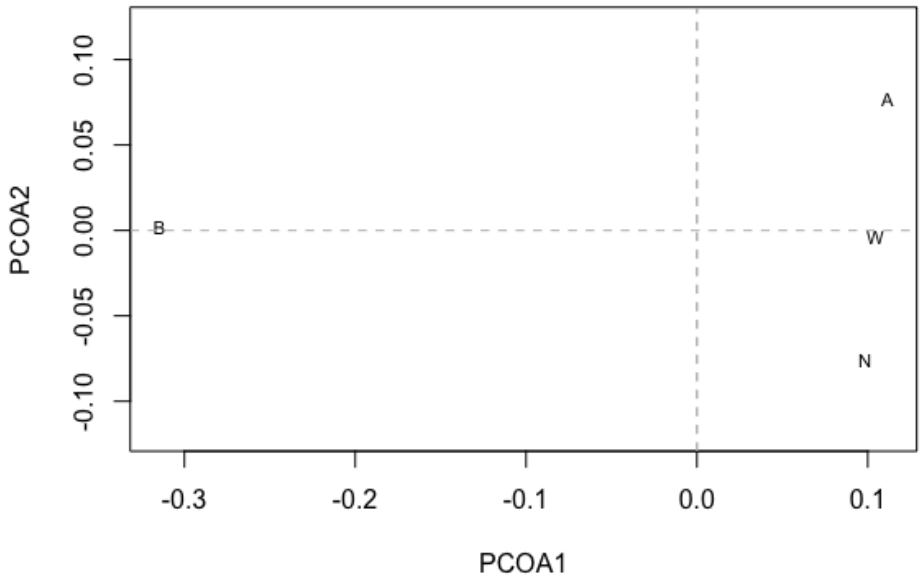

Supplemental Figure 3: Principal coordinate analysis to show differences in taxonomy assigned to B- beginning soil, A-post-incubation almond shell leachate, W-post-incubation woodchip leachate, and N- post-incubation negative control.

Chapter 5: Conclusions and Future Directions

Conclusions

Overarching goals

The aim of this research was to provide insights into the changes in microbial community composition and metabolism during MAR infiltration. Through statistical analysis of metadata, microcosms, carbon characterization and assays, and metagenomics, I have uncovered some of the complexities of the micro-ecosystem's impact on geochemical cycling during MAR infiltration.

Meta-analysis of microbial community changes MAR

Through the analyses presented in chapter 3, we disproved our hypothesis that (a) infiltration and (b) the introduction of a carbon-rich PRB would promote common changes in microbial community composition regardless of the field site. Instead, we found that common changes were only seen in sites with similar soil characteristics (e.g., grain size profile, total C, total N, surface area, etc.). HSP and KTYA, the two sites with coarser grain size (primarily sand), had lower rates of nitrate removal but exhibited common changes in the microbial community composition. At both sites, there was a reduction in alpha diversity and promotion of genera from the *Proteobacteria* phylum after infiltration through the native subsurface. The microbial community at the site with finer grain size (primarily silt and clay) did not show significant changes through infiltration nor the addition of a carbon-rich PRB. At the sandier sites, the addition of a carbon-rich PRB caused an increase in differential abundance of genera capable of complex carbon degraders and a decrease in genera

capable of nitrification. Interestingly enough, analysis of the nitrous oxide reductase gene did not find differences between either quantity or taxonomy between different soil characteristics nor the addition of a carbon-rich PRB. Overall, this research concludes that soil grain size could be used as a proxy for microbial community composition in predictive models.

Metabolic analysis and carbon characterization of different PRB leachates

In Chapter 4, we mimicked the anaerobic conditions of a fully saturated MAR basin to observe how leachates drove denitrification. We observed that microcosms with almond shell leachate removed nitrate at the same rate as the positive control of lactate. Woodchip leachate also improved nitrate removal compared to unamended soil, but at a slower rate than almond shell leachate. There was an increase in manganese and arsenic at the end of both experiments indicating that the microcosm was likely in reducing conditions that favored the reduction of metals once the nitrate was removed. Metagenomic analysis indicated that the majority of the sequenced reads came from bacteria rather than archaea or eukaryotes. There were no large differences in gene abundance between the almond shell leachate, woodchip leachate, and unamended microcosms. However, the end microbial community differed greatly from the starting microbial – both in taxonomy as well as metabolic pathways. The post-microcosm communities majorly consisted of *Proteobacteria*, with increased genes for nitrogen metabolism. The starting community had more *Actinobacteria*. Overall, the metabolism stayed consistent among the samples. However, on the gene

level, there were marked differences between the samples indicating they have the potential for different metabolisms.

The nitrate reduction microcosms caused us to hypothesize that the almond shells were providing more carbon to the soil microbial community so we also characterized the carbon using an assimilable organic carbon assay, a biodegradable organic carbon assay, and NMR. As predicted by our hypothesis, the almond shell leachate had a higher percentage of assimilable organic carbon and biodegradable organic carbon than the woodchip leachate. The almond shell leachate provided more labile carbon that was degraded from primarily oxygenated carbonate compounds into simpler aliphatic compounds. The woodchip leachate was also primarily oxygenated carbonate compounds with some aromatic and aliphatic compounds that were not degraded as much at the end of the microcosm. The complexity and aromaticity of the woodchip leachate was also supported by the UV-Vis results. These results lead to the conclusion that almond shells provide more labile carbon that can power denitrification but could also push MAR conditions to reducing conditions that could release heavy metals into the water.

Future Directions

As the climate changes, the Earth is going to experience more extreme weather patterns – multi-year long droughts (i.e. “mega-droughts”) followed by massive rainfall events (Swain, *et al.*, 2018). This highlights the need for tools, such as MAR, that help to save our limited water. Designing low-cost, easy-to-implement MAR basins has the ability to replenish more than 100 acre-feet of water per year, which is enough water for 200 families of four (Beganskas and Fisher, 2017).

However, this also highlights the importance of having parameters that can be quickly measured to ensure the MAR is functioning in the right way. Understanding the microbial community and what factors impact it, will help improve predictive models regarding nutrient cycling during infiltration.

In this research, we built the foundation for understanding soil-microbe-water interactions, but there is still much to learn. Given that soil characteristics played such an important role in influencing microbial community composition, future studies should look at the spatial layout and biofilm formation of the subsurface microbial community. Coarser sands have high rates of infiltration and could potentially replenish more water. However, the faster rates of infiltration reduce the rate of nitrates removed from the water (Gorski, *et al.*, 2020). If we could understand what soil properties are important for denitrifying taxa to gain a trophic benefit, we could improve the design. We could also employ techniques such as stable isotope probing to understand which taxa are the primary contributors to metabolism.

Through this research, we also established an understanding of how the carbon from different PRB material leachates are degraded in fully saturated, anaerobic conditions. Yet, MAR basins go through a wetting and drying cycle which presents the subsurface microbes with a lot of rapid changes. To fully understand the carbon cycling and nutrient metabolism in a MAR system, the other conditions need to be explored from a microbiological standpoint. This could be accomplished with column studies and exposing microcosms to varying oxygen levels. Observing leachate degradation in microcosms with various soil characteristics in the

experiments would also help to improve our understanding of the impact a PRB has on the ecology of a MAR basin. We could improve the accuracy of metabolism changes by using meta-transcriptomic analysis.

Managed aquifer recharge provides a solution to an eminent environmental threat. As more basins are being implemented worldwide, it is important to consider the microbes that are responsible for most of the nutrient cycling. As more predictive models are made and important taxa are identified, it also opens up the opportunity for synthetic biology and applying microbes to the MAR basin. Continuing this work will improve the design of new MAR systems.

References

Beganskas, S. and Fisher, A.T. (2017) Coupling distributed stormwater collection and managed aquifer recharge: Field application and implications. *Journal of Environmental Management* **200**: 366–379.

Gorski, G., Dailey, H., Fisher, A.T., Schrad, N., and Saltikov, C. (2020) Denitrification during infiltration for managed aquifer recharge: Infiltration rate controls and microbial response. *Science of The Total Environment* **727**: 138642.

Swain, D.L., Langenbrunner, B., Neelin, J.D., and Hall, A. (2018) Increasing precipitation volatility in twenty-first-century California. *Nature Climate Change*.